

UCSF

UC San Francisco Electronic Theses and Dissertations

Title

The Molecular Basis of Recognition and Targeting of Misfolded Proteins by Endoplasmic Reticulum-Associated Degradation

Permalink

<https://escholarship.org/uc/item/0dw3j5jn>

Author

Toyama, Erin Quan

Publication Date

2009

Peer reviewed|Thesis/dissertation

**The Molecular Basis of Recognition and Targeting of Misfolded Proteins by
Endoplasmic Reticulum-Associated Degradation**

by

Erin Quan Toyama

DISSERTATION

Submitted in partial satisfaction of the requirements for the degree of

DOCTOR OF PHILOSOPHY

in

Biochemistry

in the

GRADUATE DIVISION

of the

UNIVERSITY OF CALIFORNIA, SAN FRANCISCO

Copyright (2009)
By
Erin Quan Toyama

for my family
and Brandon

AWKNOWLEDGEMENTS

There is a long list of people that I wish to thank for making graduate school a great experience and making this work possible:

I'd like to thank Jonathan for letting me join his always too full lab, insisting that I work on ERAD, and for all his valuable guidance. I really appreciate being able to learn critical thinking from someone who is brilliant at so many aspects of science from the big picture to detailed problem solving, and importantly (to me), is a really nice person. I am grateful for the opportunities and experiences that I know would not have existed elsewhere.

Vladimir Denic (aka my reluctant mentor). I spent my first year in the Weissman lab afraid and intimidated by his intelligence and sarcasm (closely followed by his wish to work in an empty room and his hipster wardrobe). I'm glad that eventually I grew a thick enough skin to be able to take advantage of his brilliant mind and celebrate with him at my wedding. I am grateful that he was willing to work on ERAD with me instead of leaving me to get stomped over by the competition. I am thankful for his valuable training, advice, input on my project and helpful discussion throughout our overlapping time.

David Breslow (aka my lab twin). As much as he does not want to admit it, Dave and I share many personality quirks (let's say, inquisitiveness, thoroughness, and an excitement for science that leads to talking about our projects all the time) that has led me to learn a lot about myself and Brandon to swear he has many conversations twice -- once with me and once with Dave. I also want to thank Harvard because Dave has done a lot

of key editing of my writing. I have really enjoyed our banter, our scientific exchanges and admire his talent -- hopefully there will be “another Dave” at my postdoc.

Clement Chu. Clement has been a tremendous source of support. I am grateful that from rotation day 1 to the end he has always been generous with his time whether it be imparting biochemistry advice, technical support or a sympathetic ear. Also thanks to Dave and Clement, I’ve had some of my best (and most efficient) times in lab at night. They help make it possible by through a combination of Subway relief, a tremendous amount of fast food, and a lot of camaraderie. Hopefully Dave can find a new person to “halvsie” meals with and “mooch” food off of. There will always be half a meal for Dave and double portion for Clement if they come to visit.

Katherine Verges and Claire Rowe. As my classmates, apartmentmates and in Katie’s case, also my labmate, I am grateful for their friendship and their willingness to be sympathetic listeners without making me feel bad because I always knew that the favor will be reciprocated. I’m surely going to feel a bit lost without them.

Cat Foo. Lots of thanks to Cat for making my life more exciting and fun inside lab and out -- a much needed addition. Hanging out with Cat has guaranteed yummy food and great company. I very much admire her honesty and tenacity when things aren’t going her way.

Kim Tipton. Kim was my excellent rotation advisor who, even though I ended working in a different scientific area of the lab, has really looked out for me at a couple key points in my graduate career. I have always felt that she played a pivotal role with my acceptance to the lab when Jonathan was faced with choosing three students out the six who wanted join in one year and for that I am extremely grateful.

Arunashree Bhamdipati. I am so thankful that Aruna discovered Yos9p in the lab and (accidently) enabled me to grow so much my first year through a crash course in putting together a paper under pressure. The Yos9p project has proved to be continually interesting, exciting, frustrating, and an overall remarkable experience.

Edwin Rodriguez. Thanks to Edwin for letting practice my mentoring skills on him and for not holding it against me that the Yos9p purification ended up being rather difficult (as evidenced by his Yos9-stained pants).

The Weissman lab. When I joined the lab, I had my doubts about how much interaction I would see Jonathan but in the end I decided it didn't matter because I thought that the graduate students and postdocs were awesome. And they haven't let me down. I am still am amazed that such a diverse set of people can be nice, smart and get along so well. Thanks especially to Mona Kulp, Julie Hollien, Mike Bassik and Gloria Ann Brar for support and encouragement and to Nick Ingolia for fielding a lot of my toughest questions because of my total faith and trust in his insight and textbook-like knowledge of yeast genetics.

I would like to thank Joachim Li for helping me to decide to come to UCSF; Sue, Danny, Alice, Manny and Lily for keeping everything running smoothly; my classmates especially Tetsuya Matsuguchi, Kevin Jones and Monica Rodrigo-Brenni, for their continued support, help with classes, reagent generosity and sharing their expertise; my thesis committee, Dave Morgan and Peter Walter for their scientific insight and their encouragement that I should graduate and keep going, and to Jeremy Reiter, David Toczyski, Davide Ruggero and Holly Ingraham for assisting me in where to go next.

I am grateful to my childhood circle of friends, Connie, Lynn, and Keri, for always being there for me even after I left home and for helping me survive the worst things about graduate school with their support, wisdom, and wit.

Importantly, I thank my parents, sister and extended family for their continued encouragement, love, and support. And Brandon. I have so much to thank him for -- there are days when I think I couldn't have done it without him. I look forward to seeing where our new adventures take us.

The Molecular Basis of Recognition and Targeting of Misfolded Proteins by Endoplasmic Reticulum-Associated Degradation

Erin Quan Toyama

ABSTRACT

This work focuses on how the endoplasmic reticulum-associated degradation (ERAD) quality control machinery is able to distinguish terminally misfolded glycoproteins from folding intermediates and target these potentially toxic forms across the ER membrane for degradation. For luminal, glycosylated proteins, this discrimination depends both on the protein's folding status and on its glycosylation state, but much is still unknown about the mechanism.

My research centers on Yos9p, a recently identified protein that is essential for luminal ERAD in *Saccharomyces cerevisiae*. I demonstrated that Yos9p's predicted glycan-binding domain is necessary for ERAD and together with data showing that Yos9p interacts with ERAD substrates, these results implicated Yos9p as a critical sensor of the glycan-based degradation signal on misfolded substrates. Thus two important questions arose: how does Yos9p participate with the rest of the ERAD machinery to target substrates for degradation, and what is the glycan destruction signal that Yos9p recognizes? By affinity purifying Yos9p, I found that Yos9p, its binding partner, Hrd3p, and the chaperone Kar2p form the luminal components of a multi-protein complex that organizes key ERAD factors including the transmembrane ubiquitin ligase Hrd1p and cytosolic AAA ATPase Cdc48p. My characterization of this complex complemented the

observation that Yos9p and Hrd3p each form a complex specifically with misfolded substrates independently of substrate glycosylation. My studies further suggested that Yos9p and Hrd3p act as gatekeepers that ensure that only legitimate substrates are degraded. Together, these findings indicate that Yos9p forms a luminal surveillance complex with Hrd3p to recruit misfolded proteins to the core ERAD complex and that Yos9p assists in a distinct sugar-dependent step necessary for degradation of correct substrates.

To characterize Yos9p's glycan specificity, I developed a protocol to make functional Yos9p from *E. coli* by refolding the protein *in vitro*. Frontal affinity chromatography determined that Yos9p recognizes N-linked glycans containing a terminal α 1,6-linked mannose. My *in vivo* studies then showed that this glycan signal is necessary for degradation. I also provide evidence that another ERAD factor, Htm1p, generates this specific glycan for recognition by Yos9p, adding another step to potentially increase the specificity of the recognition process.

CONTRIBUTIONS

Portions of the text and figures presented in this thesis are reproduced with permission from material published previously. Chapter 2 “Exploration of the Topological Requirements of ERAD Identifies Yos9p as a Lectin Sensor of Misfolded Glycoproteins in the ER Lumen” was published in September 2005 in *Molecular Cell*, Vol. 19, pp. 741-751. This work was initiated by Dr. Arunashree Bhamidipati who performed the experiments showing the effects of fusing DHFR to CPY*, identification that Yos9p is an important factor for ERAD-L (analyzed by EMQ), and the crosslinking of CPY*/CPY*0000 to Yos9p/R200A Yos9p. Vladimir Denic performed the experiments showing that Yos9p and the Yos9p MRH mutants interact with misfolded proteins independent of substrate glycosylation.

Chapter 3 “A Luminal Surveillance Complex that Selects Misfolded Glycoproteins for ER-Associated Degradation” was published in July 26 in *Cell*, Vol. 126, pp. 349-359 as a result of a close collaboration with Vladimir Denic. Vladimir Denic performed co-immunoprecipitation experiments showing that the Yos9p/Kar2p interaction is substrate independent and Usa1p interacts with CPY*0000, confirmation that Yos9 R200A complexes with Ubx2p and Yos9p complexes with Hrd1p, and characterization of Yos9p/Hrd3p interaction with each other and with CPY*/CPY^{wt}/CPY*0000 in various ERAD deletion backgrounds. Sharleen Zhou, Arnie Falick and David King from the HHMI Mass Spectrometry Laboratory carried out the mass spectrometry analysis.

Chapter 4, “Defining the Glycan Destruction Signal for Endoplasmic Reticulum-Associated Degradation” was published in December 2008 in *Molecular Cell*, Vol. 32, pp. 870-877. Daiki Kamiya and Dr. Yukiko Kamiya performed the CD spectroscopy of Yos9p/R200A Yos9p and the frontal affinity chromatography of Yos9p/R200A under the supervision of Dr. Koichi Kato. Vladimir Denic provided input in to the writing process, and project direction and Jimena Weibezahn provided biochemistry advice.

With the exception of those items listed above, the work presented in this thesis was performed by its author, Erin Quan Toyama, under the supervision of Dr. Jonathan S. Weissman.

**ELSEVIER LICENSE
TERMS AND CONDITIONS**

Aug 30, 2009

This is a License Agreement between Erin M Quan ("You") and Elsevier ("Elsevier") provided by Copyright Clearance Center ("CCC"). The license consists of your order details, the terms and conditions provided by Elsevier, and the payment terms and conditions.

All payments must be made in full to CCC. For payment instructions, please see information listed at the bottom of this form.

Supplier	Elsevier Limited The Boulevard, Langford Lane Kidlington, Oxford, OX5 1GB, UK
Registered Company Number	1982084
Customer name	Erin M Quan
Customer address	1700 4th St San Francisco, CA 94158
License Number	2239660017481
License date	Jul 31, 2009
Licensed content publisher	Elsevier
Licensed content publication	Molecular Cell
Licensed content title	Exploration of the Topological Requirements of ERAD Identifies Yos9p as a Lectin Sensor of Misfolded Glycoproteins in the ER Lumen
Licensed content author	Arunashree Bhamidipati, Vladimir Denic, Erin M. Quan and Jonathan S. Weissman
Licensed content date	16 September 2005
Volume number	19
Issue number	6
Pages	11
Type of Use	Thesis / Dissertation
Portion	Full article
Format	Both print and electronic
You are an author of the Elsevier article	Yes
Are you translating?	No

Order Reference Number	
Expected publication date	Sep 2009
Elsevier VAT number	GB 494 6272 12
Permissions price	0.00 USD
Value added tax 0.0%	0.00 USD
Total	0.00 USD
Terms and Conditions	

INTRODUCTION

1. The publisher for this copyrighted material is Elsevier. By clicking "accept" in connection with completing this licensing transaction, you agree that the following terms and conditions apply to this transaction (along with the Billing and Payment terms and conditions established by Copyright Clearance Center, Inc. ("CCC"), at the time that you opened your Rightslink account and that are available at any time at <http://myaccount.copyright.com>).

GENERAL TERMS

2. Elsevier hereby grants you permission to reproduce the aforementioned material subject to the terms and conditions indicated.

3. Acknowledgement: If any part of the material to be used (for example, figures) has appeared in our publication with credit or acknowledgement to another source, permission must also be sought from that source. If such permission is not obtained then that material may not be included in your publication/copies. Suitable acknowledgement to the source must be made, either as a footnote or in a reference list at the end of your publication, as follows:

"Reprinted from Publication title, Vol /edition number, Author(s), Title of article / title of chapter, Pages No., Copyright (Year), with permission from Elsevier [OR APPLICABLE SOCIETY COPYRIGHT OWNER]." Also Lancet special credit - "Reprinted from The Lancet, Vol. number, Author(s), Title of article, Pages No., Copyright (Year), with permission from Elsevier."

4. Reproduction of this material is confined to the purpose and/or media for which permission is hereby given.

5. Altering/Modifying Material: Not Permitted. However figures and illustrations may be altered/adapted minimally to serve your work. Any other abbreviations, additions, deletions and/or any other alterations shall be made only with prior written authorization of Elsevier Ltd. (Please contact Elsevier at permissions@elsevier.com)

6. If the permission fee for the requested use of our material is waived in this instance, please be advised that your future requests for Elsevier materials may attract a fee.

7. **Reservation of Rights:** Publisher reserves all rights not specifically granted in the combination of (i) the license details provided by you and accepted in the course of this licensing transaction, (ii) these terms and conditions and (iii) CCC's Billing and Payment terms and conditions.

8. **License Contingent Upon Payment:** While you may exercise the rights licensed immediately upon issuance of the license at the end of the licensing process for the transaction, provided that you have disclosed complete and accurate details of your proposed use, no license is finally effective unless and until full payment is received from you (either by publisher or by CCC) as provided in CCC's Billing and Payment terms and conditions. If full payment is not received on a timely basis, then any license preliminarily granted shall be deemed automatically revoked and shall be void as if never granted. Further, in the event that you breach any of these terms and conditions or any of CCC's Billing and Payment terms and conditions, the license is automatically revoked and shall be void as if never granted. Use of materials as described in a revoked license, as well as any use of the materials beyond the scope of an unrevoked license, may constitute copyright infringement and publisher reserves the right to take any and all action to protect its copyright in the materials.

9. **Warranties:** Publisher makes no representations or warranties with respect to the licensed material.

10. **Indemnity:** You hereby indemnify and agree to hold harmless publisher and CCC, and their respective officers, directors, employees and agents, from and against any and all claims arising out of your use of the licensed material other than as specifically authorized pursuant to this license.

11. **No Transfer of License:** This license is personal to you and may not be sublicensed, assigned, or transferred by you to any other person without publisher's written permission.

12. **No Amendment Except in Writing:** This license may not be amended except in a writing signed by both parties (or, in the case of publisher, by CCC on publisher's behalf).

13. **Objection to Contrary Terms:** Publisher hereby objects to any terms contained in any purchase order, acknowledgment, check endorsement or other writing prepared by you, which terms are inconsistent with these terms and conditions or CCC's Billing and Payment terms and conditions. These terms and conditions, together with CCC's Billing and Payment terms and conditions (which are incorporated herein), comprise the entire agreement between you and publisher (and CCC) concerning this licensing transaction. In the event of any conflict between your obligations established by these terms and conditions and those established by CCC's Billing and Payment terms and conditions, these terms and conditions shall control.

14. **Revocation:** Elsevier or Copyright Clearance Center may deny the permissions described in this License at their sole discretion, for any reason or no reason, with a full refund payable to you. Notice of such denial will be made using the contact information provided by you. Failure to receive such notice will not alter or invalidate the denial. In no event will Elsevier or Copyright Clearance Center be responsible or liable for any costs, expenses or damage

incurred by you as a result of a denial of your permission request, other than a refund of the amount(s) paid by you to Elsevier and/or Copyright Clearance Center for denied permissions.

LIMITED LICENSE

The following terms and conditions apply only to specific license types:

15. Translation: This permission is granted for non-exclusive world **English** rights only unless your license was granted for translation rights. If you licensed translation rights you may only translate this content into the languages you requested. A professional translator must perform all translations and reproduce the content word for word preserving the integrity of the article. If this license is to re-use 1 or 2 figures then permission is granted for non-exclusive world rights in all languages.

16. Website: The following terms and conditions apply to electronic reserve and author websites:

Electronic reserve: If licensed material is to be posted to website, the web site is to be password-protected and made available only to bona fide students registered on a relevant course if:

This license was made in connection with a course,

This permission is granted for 1 year only. You may obtain a license for future website posting,

All content posted to the web site must maintain the copyright information line on the bottom of each image,

A hyper-text must be included to the Homepage of the journal from which you are licensing at <http://www.sciencedirect.com/science/journal/xxxxx> or the Elsevier homepage for books at <http://www.elsevier.com>, and

Central Storage: This license does not include permission for a scanned version of the material to be stored in a central repository such as that provided by Heron/XanEdu.

17. Author website for journals with the following additional clauses:

All content posted to the web site must maintain the copyright information line on the bottom of each image, and

the permission granted is limited to the personal version of your paper. You are not allowed to download and post the published electronic version of your article (whether PDF or HTML, proof or final version), nor may you scan the printed edition to create an electronic version,

A hyper-text must be included to the Homepage of the journal from which you are licensing at <http://www.sciencedirect.com/science/journal/xxxxx>. As part of our normal production process, you will receive an e-mail notice when your article appears on Elsevier's online service ScienceDirect (www.sciencedirect.com). That e-mail will include the article's Digital Object Identifier (DOI). This number provides the electronic link to the published article and should be included in the posting of your personal version. We ask that you wait until you receive this e-mail and have the DOI to do any posting.

Central Storage: This license does not include permission for a scanned version of the material to be stored in a central repository such as that provided by Heron/XanEdu.

18. Author website for books with the following additional clauses:

Authors are permitted to place a brief summary of their work online only.

A hyper-text must be included to the Elsevier homepage at <http://www.elsevier.com>

All content posted to the web site must maintain the copyright information line on the bottom of each image

You are not allowed to download and post the published electronic version of your chapter, nor may you scan the printed edition to create an electronic version.

Central Storage: This license does not include permission for a scanned version of the material to be stored in a central repository such as that provided by Heron/XanEdu.

19. Website (regular and for author): A hyper-text must be included to the Homepage of the journal from which you are licensing at <http://www.sciencedirect.com/science/journal/xxxxx>, or for books to the Elsevier homepage at <http://www.elsevier.com>

20. Thesis/Dissertation: If your license is for use in a thesis/dissertation your thesis may be submitted to your institution in either print or electronic form. Should your thesis be published commercially, please reapply for permission. These requirements include permission for the Library and Archives of Canada to supply single copies, on demand, of the complete thesis and include permission for UMI to supply single copies, on demand, of the complete thesis. Should your thesis be published commercially, please reapply for permission.

21. Other ConditionsNone

v1.6

Gratis licenses (referencing \$0 in the Total field) are free. Please retain this printable license for your reference. No payment is required.

If you would like to pay for this license now, please remit this license along with your payment made payable to "COPYRIGHT CLEARANCE CENTER" otherwise you will be invoiced within 30 days of the license date. Payment should be in the form of a check or money order referencing your account number and this license number 2239660017481.

If you would prefer to pay for this license by credit card, please go to <http://www.copyright.com/creditcard> to download our credit card payment authorization form.

Make Payment To:
Copyright Clearance Center
Dept 001
P.O. Box 843006
Boston, MA 02284-3006

If you find copyrighted material related to this license will not be used and wish to cancel, please contact us referencing this license number 2239660017481 and noting

the reason for cancellation.

Questions? customercare@copyright.com or +1-877-622-5543 (toll free in the US) or +1-978-646-2777.

**ELSEVIER LICENSE
TERMS AND CONDITIONS**

Aug 30, 2009

This is a License Agreement between Erin M Quan ("You") and Elsevier ("Elsevier") provided by Copyright Clearance Center ("CCC"). The license consists of your order details, the terms and conditions provided by Elsevier, and the payment terms and conditions.

All payments must be made in full to CCC. For payment instructions, please see information listed at the bottom of this form.

Supplier	Elsevier Limited The Boulevard, Langford Lane Kidlington, Oxford, OX5 1GB, UK
Registered Company Number	1982084
Customer name	Erin M Quan
Customer address	1700 4th St San Francisco, CA 94158
License Number	2239620676153
License date	Jul 31, 2009
Licensed content publisher	Elsevier
Licensed content publication	Cell
Licensed content title	A Luminol Surveillance Complex that Selects Misfolded Glycoproteins for ER-Associated Degradation
Licensed content author	Vladimir Denic, Erin M. Quan and Jonathan S. Weissman
Licensed content date	28 July 2006
Volume number	126
Issue number	2
Pages	11
Type of Use	Thesis / Dissertation
Portion	Full article
Format	Both print and electronic
You are an author of the Elsevier article	Yes
Are you translating?	No
Order Reference Number	
Expected publication date	Sep 2009

Elsevier VAT number	GB 494 6272 12
Permissions price	0.00 USD
Value added tax 0.0%	0.00 USD
Total	0.00 USD
Terms and Conditions	

INTRODUCTION

1. The publisher for this copyrighted material is Elsevier. By clicking "accept" in connection with completing this licensing transaction, you agree that the following terms and conditions apply to this transaction (along with the Billing and Payment terms and conditions established by Copyright Clearance Center, Inc. ("CCC"), at the time that you opened your Rightslink account and that are available at any time at <http://myaccount.copyright.com>).

GENERAL TERMS

2. Elsevier hereby grants you permission to reproduce the aforementioned material subject to the terms and conditions indicated.

3. Acknowledgement: If any part of the material to be used (for example, figures) has appeared in our publication with credit or acknowledgement to another source, permission must also be sought from that source. If such permission is not obtained then that material may not be included in your publication/copies. Suitable acknowledgement to the source must be made, either as a footnote or in a reference list at the end of your publication, as follows:

"Reprinted from Publication title, Vol /edition number, Author(s), Title of article / title of chapter, Pages No., Copyright (Year), with permission from Elsevier [OR APPLICABLE SOCIETY COPYRIGHT OWNER]." Also Lancet special credit - "Reprinted from The Lancet, Vol. number, Author(s), Title of article, Pages No., Copyright (Year), with permission from Elsevier."

4. Reproduction of this material is confined to the purpose and/or media for which permission is hereby given.

5. Altering/Modifying Material: Not Permitted. However figures and illustrations may be altered/adapted minimally to serve your work. Any other abbreviations, additions, deletions and/or any other alterations shall be made only with prior written authorization of Elsevier Ltd. (Please contact Elsevier at permissions@elsevier.com)

6. If the permission fee for the requested use of our material is waived in this instance, please be advised that your future requests for Elsevier materials may attract a fee.

7. Reservation of Rights: Publisher reserves all rights not specifically granted in the combination of (i) the license details provided by you and accepted in the course of this licensing transaction, (ii) these terms and conditions and (iii) CCC's Billing and Payment

**ELSEVIER LICENSE
TERMS AND CONDITIONS**

Aug 30, 2009

This is a License Agreement between Erin M Quan ("You") and Elsevier ("Elsevier") provided by Copyright Clearance Center ("CCC"). The license consists of your order details, the terms and conditions provided by Elsevier, and the payment terms and conditions.

All payments must be made in full to CCC. For payment instructions, please see information listed at the bottom of this form.

Supplier	Elsevier Limited The Boulevard, Langford Lane Kidlington, Oxford, OX5 1GB, UK
Registered Company Number	1982084
Customer name	Erin M Quan
Customer address	1700 4th St San Francisco, CA 94158
License Number	2239640308825
License date	Jul 31, 2009
Licensed content publisher	Elsevier
Licensed content publication	Molecular Cell
Licensed content title	Defining the Glycan Destruction Signal for Endoplasmic Reticulum-Associated Degradation
Licensed content author	Erin M. Quan, Yukiko Kamiya, Daiki Kamiya, Vladimir Denic, Jimena Weibezahn, Koichi Kato and Jonathan S. Weissman
Licensed content date	26 December 2008
Volume number	32
Issue number	6
Pages	8
Type of Use	Thesis / Dissertation
Portion	Full article
Format	Both print and electronic
You are an author of the Elsevier article	Yes
Are you translating?	No

Order Reference Number	
Expected publication date	Sep 2009
Elsevier VAT number	GB 494 6272 12
Permissions price	0.00 USD
Value added tax 0.0%	0.00 USD
Total	0.00 USD
Terms and Conditions	

INTRODUCTION

1. The publisher for this copyrighted material is Elsevier. By clicking "accept" in connection with completing this licensing transaction, you agree that the following terms and conditions apply to this transaction (along with the Billing and Payment terms and conditions established by Copyright Clearance Center, Inc. ("CCC"), at the time that you opened your Rightslink account and that are available at any time at <http://myaccount.copyright.com>).

GENERAL TERMS

2. Elsevier hereby grants you permission to reproduce the aforementioned material subject to the terms and conditions indicated.

3. Acknowledgement: If any part of the material to be used (for example, figures) has appeared in our publication with credit or acknowledgement to another source, permission must also be sought from that source. If such permission is not obtained then that material may not be included in your publication/copies. Suitable acknowledgement to the source must be made, either as a footnote or in a reference list at the end of your publication, as follows:

"Reprinted from Publication title, Vol /edition number, Author(s), Title of article / title of chapter, Pages No., Copyright (Year), with permission from Elsevier [OR APPLICABLE SOCIETY COPYRIGHT OWNER]." Also Lancet special credit - "Reprinted from The Lancet, Vol. number, Author(s), Title of article, Pages No., Copyright (Year), with permission from Elsevier."

4. Reproduction of this material is confined to the purpose and/or media for which permission is hereby given.

5. Altering/Modifying Material: Not Permitted. However figures and illustrations may be altered/adapted minimally to serve your work. Any other abbreviations, additions, deletions and/or any other alterations shall be made only with prior written authorization of Elsevier Ltd. (Please contact Elsevier at permissions@elsevier.com)

6. If the permission fee for the requested use of our material is waived in this instance, please be advised that your future requests for Elsevier materials may attract a fee.

TABLE OF CONTENTS

Preface	Acknowledgements	iv
	Abstract	viii
	Contributions	x
	Permissions	xii
	Table of Contents	xxii
	List of Tables and Figures	xxiii
Chapter 1	Introduction	1
Chapter 2	Exploration of the Topological Requirements of ERAD Identifies Yos9p as a Lectin Sensor of Misfolded Glycoproteins in the ER lumen	14
Chapter 3	A Luminal Surveillance Complex that Selects Misfolded Glycoproteins for ER-Associated Degradation	54
Chapter 4	Defining the Glycan Destruction Signal for Endoplasmic Reticulum-Associated Degradation	99
Chapter 5	Conclusions	129
Appendix A	Unpublished Data	134
Appendix B	References	144

LIST OF TABLES AND FIGURES

CHAPTER 1

Figure 1 N-linked glycan

CHAPTER 2

Figure 1	Presence of a stable C-terminal DHFR domain provides an impediment to ER-associated degradation of CPY*	21
Figure 2	Yos9p is required for ER-associated degradation of CPY*	25
Figure 3	Yos9p is required for degradation of proteins containing misfolded luminal but not cytosolic domains	28
Figure 4	Yos9p contains an intact sugar binding site that is required for its ability to support ERAD	30
Figure 5	Interaction of misfolded ER proteins with Yos9p	33
Figure 6	Sugar-independent recognition of CPY* by Yos9p	35
Figure S1	Western blots monitoring the degradation of DHFR-CPY*-DHFR and CPY*-DHFR-HA	46
Figure S2	Yos9p sugar-binding mutants show enhanced association with CPY*-DHFR	46
Figure S3	Yos9p interacts with substrate as part of a large protein complex	47
Figure S4	Yos9p and R200A Yos9p interaction with substrate is unaffected in the absence of Htm1p	47

CHAPTER 3

Figure 1	Yos9p associates with the core ERAD machinery at the ER membrane	62
-----------------	--	----

Figure 2	The integrity of the Yos9p-core ERAD machinery complex is not dependent on Der1p, Htm1p or Yos9p's sugar binding pocket	64
Figure 3	Dissection of the Hrd3p/Yos9p interaction by domain mapping/over-expression and a model of how Yos9p interacts with other members of the ERAD machinery	67
Figure 4	Yos9p interacts with CPY* and CPY*0000 in a <i>HRD3</i> -independent manner	69
Figure 5	Hrd3p interacts specifically with CPY* and CPY*0000 but not wild type CPY in a <i>YOS9</i> -independent manner	71
Figure 6	Sugar-independent association of misfolded carboxypeptidase Y with Usa1p	73
Figure 7	Over-expression of Hrd1p in a Δ <i>hrd3</i> background results in increased degradation of CPY* and CPY*0000 in a <i>YOS9</i> -independent manner	75
Figure S1	Yos9-FLAG genomic is function for ERAD-L	86
Figure S2	Mass spectrometry statistics	87
Figure S3	Yos9p associates with Hrd1p	88
Figure S4	Yos9p/Kar2p association is independent of Hrd3p	89
Figure S5	Deglycosylated Yos9p interacts with deglycosylated Hrd3p	90
Figure S6	Yos9p and R200A Yos9p interact with CPY* but not CPY wild-type	91
Figure S7	Hrd3 ₁₋₇₆₇ -MYC is functional for CPY* degradation	92
Figure S8	Usa1p is in a multiprotein complex containing misfolded carboxypeptidase Y prior to cell lysis	93
Figure S9	Degradation of CPY* when Hrd1p is overexpressed in a Δ <i>hrd3</i> background is suppressed by Δ <i>cue1</i>	94

CHAPTER 4

Figure 1	Purification of biochemical amounts of Yos9p from <i>E.coli</i> .	106
Figure 2	Yos9 recognizes glycans containing a terminal α 1,6-linked mannose	108
Figure 3	Production of Man ₇ GlcNAc ₂ sugars in vivo results in ERAD dependent degradation and bypass of <i>HTMI</i>	110
Figure 4	Model of dual recognition of substrates by ERAD	113
Figure S1	Native Yos9p forms disulfide-crosslinked aggregates	121
Figure S2	Refolding process of denatured Yos9p	122
Figure S3	Production of Man ₇ GlcNAc ₂ sugars results in degradation of CPY*	123
Figure S4	An exposed α 1,6-linked mannose on CPY* or KHN results in bypass of <i>HTMI</i>	124

APPENDIX A

Figure 1	Hrd3p requires its glycans to function in ERAD	136
Figure 2	Hrd3p interaction with non-glycosylatable DHFR-CPY* pieces	139
Figure 3	Bacterial expression of MBP-CPY* variants	140

CHAPTER 1

Introduction

INTRODUCTION

Genetic information is passed from DNA to mRNA, which is then translated into polypeptides. In order to perform their cellular functions, these polypeptides must, reproducibly fold into the proper three dimensional conformation. The remarkable assembly of linear polypeptides into folded proteins is governed by primary amino acid sequence (Anfinsen, 1973), but a complex energy landscape with several off-pathway and non-native states, presents a number of challenges for the folding polypeptide (Jahn and Radford, 2005; Onuchic and Wolynes, 2004). Indeed, protein folding in vitro can be slow and inefficient. To ensure the efficient production of functional proteins in vivo, the cell has evolved an intricate system of factors to facilitate proper protein folding (Hartl and Hayer-Hartl, 2009). Importantly, because functional proteins are fundamental to life, quality control systems exist to limit the number of errors and eliminate terminally misfolded proteins (McClellan et al., 2005).

Quality control mechanisms exist throughout the cytoplasm and organelles of eukaryotic cells, and are functionally tuned to the environment of each compartment. A network of organelles, collectively known as the secretory pathway, handles the production of secretory proteins: proteins to be displayed on the cell surface, along the secretory pathway or to be secreted out of the cell. These proteins participate in a variety of important functions such as cell-cell communication, signaling and defense and account for approximately one third of all eukaryotic proteins. This number can increase to greater than 90% for some specialized cells such plasma cells, hepatocytes and pancreatic cells (Kaufman, 2004) making it an important compartment in which to study

protein folding, and the associated chaperone and quality control systems. Central to the secretory pathways is the entry compartment, the endoplasmic reticulum (ER), which serves as the folding center -- an organelle largely dedicated to protein biogenesis of secretory proteins. The ER provides a specialized folding environment for these proteins to survive in the extracellular milieu. Mature proteins then exit the ER, and traffic through the Golgi, another organelle along the secretory pathway, and on to their site of action (Stevens and Argon, 1999; van Anken and Braakman, 2005).

In addition to the intrinsic difficulty of protein folding, the cellular environment presents a number of additional challenges. The large flux of proteins through the ER and an estimated 100mg/ml concentration of proteins in the ER lumen, results in a large risk of intra- and inter- polypeptide aggregation (Stevens and Argon, 1999). Additionally, secretory proteins often have to go through the slow process of forming correct disulfide bonds, or forming oligomeric complexes before being ready for export. Furthermore, transcription and translation errors as well as environmental damage can lead to a defined fraction of misfolded proteins (Hebert and Molinari, 2007). Finally, folding efficiency varies by protein. One example of low protein folding-efficiency is the cystic fibrosis transmembrane conductance regulator (CFTR). Only an estimated 25% of newly synthesized wild-type CFTR will reach the cell surface (Kopito, 1999; Ward et al., 1995). Combined, all these challenges result in an estimated range of a few percent (Vabulas and Hartl, 2005) up to 30% (Schubert et al., 2000) of newly synthesized proteins that are rapidly degraded.

The ER contains a high concentration of chaperones to help proteins fold -- namely protein disulfide isomerase (PDI), the ER Hsp70, Kar2p (BiP in mammals), and

lectin chaperones. PDI assists in the formation and/or isomerization of disulfide bonds to native linkages critical for the correct structure and stability of many proteins (Goldberger et al., 1963). Kar2p binds to hydrophobic patches to help prevent substrate aggregation and assist in the folding process (Flynn et al., 1991; Kabani et al., 2003; Nishikawa et al., 2001a; Simons et al., 1995). As proteins are translocated into the ER lumen, many are attached with asparagine-linked glycans. In most eukaryotes (As proteins are translocated in eukaryotes (*Saccharomyces cerevisiae* being a prime exception), sugar binding (lectin) chaperones, calnexin (CNX) and calreticulin (CRT) promote correct folding and inhibit aggregation by cyclically binding and releasing glycans on folding polypeptides until the proteins achieve their native state. These N-linked glycans themselves can also have a chaperone-like effect, as their hydrophilicity can help to keep proteins soluble. Glycans also have a positive effect on the protein folding process perhaps by sterically limiting the number of conformations (Helenius and Aebi, 2001).

In addition to helping proteins fold, chaperones perform a quality control function of monitoring folding and assembly to guarantee the structural integrity of the protein before it progresses through the secretory pathway to its destination. Chaperones, Kar2p, PDI and CNX/CRT retain immature and nonnative proteins to give them an increased chance of folding and to prevent these incorrect forms from exiting the ER where they could potentially be toxic. Kar2p retains misfolded proteins for disposal because native proteins bury the hydrophobic regions while misfolded proteins continually expose these residues (Ellgaard and Helenius, 2003). CNX and CRT polypeptides by binding to monoglucosylated glycans (Helenius and Aebi, 2004). After a round of folding attempts while bound to CNX/CRT, substrates are released and are deglucosylated by glucosidase

II to prevent reassociation with CNX/CRT. The folding sensor, UDP-glucose:glycoprotein glucosyltransferase (GT) scans proteins and reglucosylates those that are non-native (Caramelo and Parodi, 2007) to create a cycle of interaction with CNX/CRT where immature proteins re-enter the cycle and folded ones exit (Solda et al., 2007).

Despite the highly specialized ER folding environment, the challenges of intracellular folding inevitably result in some fraction of ER proteins becoming irreversibly misfolded. In order not to let potentially toxic proteins accumulate or be sent to their site of action, retention of misfolded proteins in the ER is linked to a disposal system called ER-associated degradation (ERAD) that is responsible for degrading terminally misfolded proteins (Hebert and Molinari, 2007). The budding yeast, *S. cerevisiae* has served as a critical model organism and enabled the discovery of many key ERAD factors and mechanisms. For the most part the basic conclusions about the ERAD pathways seem conserved from yeast to mammals, although in many cases the number of components have expanded. On account of this conservation, and the fact that the research in the following chapters has been performed using yeast as a model system, the remainder of this introduction is written using research in yeast to delineate the fundamental points.

The ERAD machinery eliminates misfolded proteins in a multi-step process that includes recognition of the misfolded substrate, dislocation of the protein into the cytosol and ends with ubiquitination and degradation by the 26S proteasome in the cytoplasm (Romisch, 2005). Many structurally diverse proteins fold in the ER including soluble luminal proteins and integral membrane proteins with varying transmembrane topologies,

all of which must be degraded by ERAD (Sayeed and Ng, 2005). Key genetic screens in budding yeast using a membrane protein, Hmg2p (Hampton et al., 1996), and a soluble misfolded form of carboxypeptidase Y, CPY* (Knop et al., 1996a), revealed that some of the same components were necessary for degradation of these two substrates. They included the E3 ubiquitin ligase Hrd1p and its associated factor Hrd3p (Bays et al., 2001; Bordallo et al., 1998; Gardner et al., 2000; Plemper et al., 1999), the E2 Ubc7p which is anchored to the membrane by Cue1p (Biederer et al., 1997; Hampton and Bhakta, 1997; Hiller et al., 1996) and the 26S proteasome (Hampton and Bhakta, 1997; Hiller et al., 1996). These results indicated that membrane and soluble substrates seem to use the same core proteins. Since then, multiple ERAD pathways have been defined in yeast based on the location of the misfolded lesion. Lesions that are cytoplasmic, luminal and membrane spanning are monitored and acted upon by the ERAD-C, ERAD-L or ERAD-M pathway, respectively (Vashist and Ng, 2004). These pathways require different upstream recognition factors but converge on to two ubiquitin ligases: Hrd1p for ERAD-L and ERAD-M and Doa10p for ERAD-C (Vashist and Ng, 2004; Vembar and Brodsky, 2008). Following ubiquitination, substrates are extracted from the membrane by the Ubx2p-recruited Cdc48p AAA ATPase (with cofactors Npl4p and Ufd1p) (Jarosch et al., 2002; Neuber et al., 2005; Schuberth and Buchberger, 2005; Ye et al., 2001) and escorted by ubiquitin binding proteins to the proteasome (Richly et al., 2005). Additional components Der1p (Derlin1-3 in mammals), an integral membrane protein (Knop et al., 1996a), and ER resident Htm1p (EDEM1-3 in mammals), a proposed lectin based on its homology to class I α 1,2-mannosidases (Jakob et al., 2001; Nakatsukasa et al., 2001), were found to be necessary only for ERAD-L (Vashist and Ng, 2004). Thanks in part to

the success of genetic screens, there are an increasing array of factors implicated in ERAD but in many cases there is minimal information about their molecular function, especially for proposed upstream components. Thus the fundamentally important question of how the ERAD machinery specifically recognizes misfolded proteins from folding intermediates and targets them for destruction remains unclear. To answer this question, identification of what proteins are involved, elucidation of what their functional role is, and discovery of how these individual functions are integrated to complete this complex task is necessary.

The ERAD machinery must achieve a fine balance so that it does not degrade functional proteins prematurely but at the same time does not let potentially toxic proteins escape detection. Tipping the balance either way can result in disease. Cystic fibrosis is an example of a disease caused by premature degradation which results in a lack of CFTR chloride channels at the cell surface. The most prominent mutation, $\Delta F508$, results in delayed folding and thus in recognition and degradation by ERAD even though the mutation does not render the chloride channel inactive (Riordan, 2008). On the other hand, loss of function mutations in ERAD components can lead to accumulation of misfolded proteins, as in the case of Parkin, a mammalian E3 ligase that, when mutated, is associated with Parkinson's disease (Takahashi and Imai, 2003). Central to this balancing act is substrate recognition. This is not a simple problem, as many of the possible features of ERAD substrates, such as exposed hydrophobic regions or unfolded domains, are shared with polypeptides that are in the process of folding.

Studies using glycoproteins have been essential towards making progress to understanding ERAD recognition. Nearly all ER proteins are covalently modified with a

pre-assembled, branched Glc₃Man₉GlcNAc₂ moiety at N-X-S/T consensus sites as the protein is translocated in to the ER. Key studies using CPY* in yeast indicated that N-linked glycans are necessary for ERAD. CPY* is a model ERAD-L substrate resulting from a single point mutation in a vacuolar protease, carboxypeptidase Y, that contains four glycosylation sites. The mutation causes the protein to globally misfold, which results in retention in the ER and degradation by ERAD, instead of being trafficked through the Golgi to the vacuole (Finger et al., 1993). If the glycan consensus sites in CPY* are mutated, this non-glycosylatable version of CPY* is retained in the ER but not degraded (Knop et al., 1996b), indicating that the N-linked glycans are necessary for entry into ERAD.

The role of glycosylation in ERAD was revealed by studies examining glycan trimming. In *S. cerevisiae*, the terminal glucoses on the glycan are quickly removed by glucosidase I and II (in mammalian cells, the rate of glucose trimming varies, depending on the length of time spent in the CNX/CRT cycle) followed by the removal of a single mannose in the middle B branch by an α 1,2-mannosidase, Mns1p (ER mannosidase I in mammals) (Helenius and Aebi, 2004). Studies indicating that these trimming steps are necessary for efficient degradation (Jakob et al., 1998a; Liu et al., 1999) supported the “timer hypothesis,” which proposed that the period of time it takes to reach a certain glycan structure provides proteins a protected period of time in which to fold without risk of being degraded (Helenius, 1994; Jakob et al., 1998b; Wu et al., 2003). Glycan trimming raises the question of what the identity of this signal might be and how such signals are specifically generated on misfolded proteins. Man₈GlcNAc₂ was proposed to be the specific glycan that signals destruction because Mns1p’s removal of the mannose

to generate $\text{Man}_8\text{GlcNAc}_2$ was shown to be relatively slow compared to glucosidase I and II trimming (Jakob et al., 1998a) in addition to the fact that lack of Mns1p activity delays degradation (Jakob et al., 1998a; Su et al., 1993). However, proteins have different folding rates and even correctly folded proteins and ER resident proteins can have their glycans trimmed to $\text{Man}_8\text{GlcNAc}_2$ (Byrd et al., 1982), indicating that perhaps recognition of an unfolded protein determinant or a unique glycan destruction signal is necessary. The discovery that only a single glycan in a non-interchangeable location is necessary for CPY* or PrA* (another misfolded vacuolar yeast protease) degradation, reinforced the idea that there might be a bipartite signal composed of a glycan and a protein determinant (Kostova and Wolf, 2005; Spear and Ng, 2005). Additionally, in mammalian cells, there have been reports of glycan trimming on substrates down to $\text{Man}_{5-6}\text{GlcNAc}_2$ and it thought that is this extended trimming that commits substrates for ERAD (Frenkel et al., 2003; Hosokawa et al., 2003; Kitzmuller et al., 2003; Lederkremer and Glickman, 2005), indicating that perhaps these more processed forms act as a distinctive glycan signal for degradation.

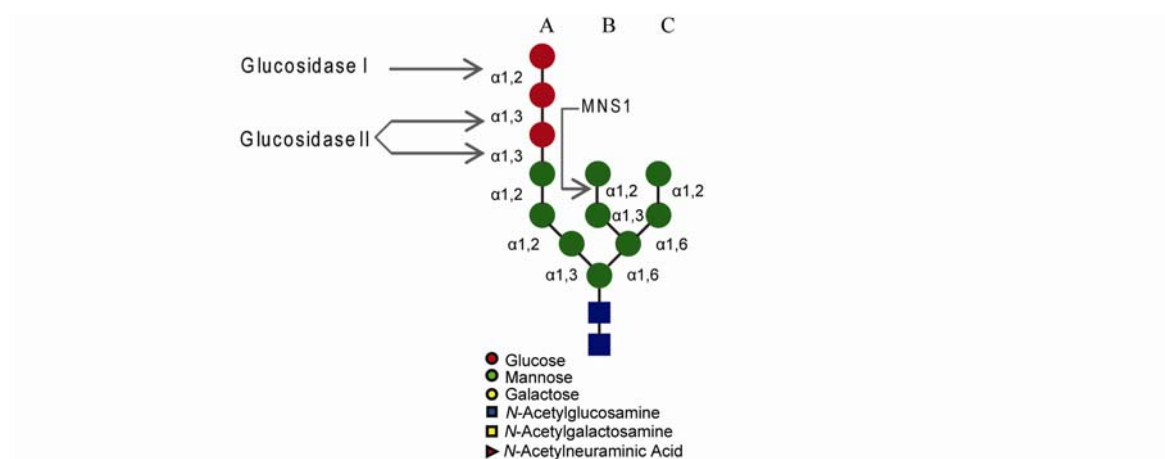


Figure 1. The N-linked glycan.

This core oligosaccharide is attached to proteins at N-X-S/T consensus sites. The terminal glucose residues are removed by glucosidase I and II. The B branch mannose is removed by Mns1p (ER α -mannosidase I). The linkages and symbols for the different sugars are indicated.

The key role for glycosylation not only brought into question the nature of the glycan signal recognized by ERAD but also established a need for a glycan binding protein, or lectin, to recognize the glycan destruction signal and target the substrate for degradation. One candidate protein for this function was Htm1p, and its mammalian homolog, EDEM1. Deletion of Htm1p causes a defect in ERAD-L substrate degradation (Jakob et al., 2001; Nakatsukasa et al., 2001) and over-expression of EDEM1 accelerates turnover of a mammalian ERAD substrate (Hosokawa et al., 2001; Molinari et al., 2003) thus establishing Htm1p/EDEM1 as ERAD factors. Htm1p and EDEM1 have homology to class I mannosidases, however, neither *in vivo* (Jakob et al., 2001) nor *in vitro* (Hosokawa et al., 2001) activity was initially reported. Additionally, they lack conserved cysteines thought to be important for mannosidase activity (Nakatsukasa et al., 2001) and thus they were proposed to act as lectins. EDEM1 interacts with misfolded proteins and CNX, and when over-expressed, ERAD was accelerated by increased release of substrate from CNX, suggesting that EDEM1 extracts terminally misfolded proteins out of the CNX cycle for degradation (Molinari et al., 2003; Oda et al., 2003). However, direct biochemical evidence for glycan binding by Htm1p or EDEM1 (or EDEM homologs EDEM2 and EDEM3) or a definitive mechanism are lacking, leaving the identity of the targeting lectin and its mechanism unknown.

Because glycans play an important role in ERAD recognition, the discovery and characterization of a new proposed lectin in yeast, Yos9p, created an exciting new avenue for investigating glycoprotein ERAD recognition (Chapter 2) Yos9p is a soluble glycoprotein with a C-terminal HDEL sequence that acts as an ER retrieval sequence and a mannose 6-phosphate receptor homology (MRH) domain (Bhamidipati et al., 2005;

Buschhorn et al., 2004; Kim et al., 2005; Munro, 2001; Szathmary et al., 2005). Deletion of Yos9p causes a defect in degradation of luminal misfolded glycoproteins, revealing that it is necessary for ERAD-L (Bhamidipati et al., 2005; Buschhorn et al., 2004; Kim et al., 2005; Szathmary et al., 2005). Point mutations of conserved MRH residues that are likely to break contact between the sugar-binding pocket and the glycan (Hancock et al., 2002; Olson et al., 1999) result in a defect in ERAD of CPY* equal to the complete loss of Yos9p (Bhamidipati et al., 2005; Szathmary et al., 2005). Therefore, Yos9p's ability to bind glycans is essential for its function in ERAD and suggested that Yos9p may be involved in substrate recognition. This hypothesis was further strengthened when it was shown that Yos9p co-immunoprecipitates with CPY* (Bhamidipati et al., 2005; Kim et al., 2005; Szathmary et al., 2005). Surprisingly, Yos9p can also interact with substrate independently of its lectin domain or substrate glycosylation, thus suggesting that there may be a bipartite interaction between Yos9p and substrate (Bhamidipati et al., 2005).

The initial characterization of Yos9p suggests that it is an important player in recognizing and targeting misfolded glycoproteins for ERAD, but it also highlights important unanswered questions, such as: How does Yos9p function with the rest of the ERAD machinery to degrade only misfolded substrates? Is Yos9p the critical lectin involved in recognition, and if so, what glycan signal does it recognize on substrates?

As described in Chapter 3, I discovered, using a series of affinity purifications, that Yos9p is part of a multi-protein complex that contains many previously identified ERAD components. Remarkably, this complex includes proteins in the ER lumen (Yos9p, Kar2), ER membrane (Hrd3p, Hrd1p, Ubx2p, Usa1p) and the cytosol (Cdc48p) and therefore showed for the first time that a large complex organizes ERAD proteins

involved in the initial substrate recognition steps down through the later steps of ubiquitination and extraction from the membrane. My further characterization of the organization of the complex revealed that in addition to Yos9p, the large luminal domain of Hrd3p was potentially an important factor for identifying substrates in the lumen. Surprisingly, Yos9p/Kar2 and Hrd3p each independently interact with misfolded CPY* but not wild-type CPY in a manner that does not depend on substrate glycosylation. Thus, Yos9p/Kar2p/Hrd3p form a luminal surveillance complex that brings misfolded proteins to the ubiquitination and extraction machinery. Since Yos9p's sugar-binding domain and substrate glycosylation are necessary for ERAD dependent substrate degradation, Yos9p participates in a distinct sugar-dependent step essential for degradation of legitimate substrates. Previous work had demonstrated that over-expression of Hrd1p allows for partial degradation in the absence of Hrd3p (Gardner et al., 2000; Plemper et al., 1999), and I showed this to be true in the absence of Yos9p as well. However, I found that this bypass of the recognition machinery results in promiscuous degradation, suggesting that Yos9p and Hrd3p act as gatekeepers by selecting only legitimate substrates for degradation.

With an increasingly sophisticated model of the mechanism of glycoprotein recognition, it became evident that biochemical proof that Yos9p is a lectin and deciphering its glycan specificity were critical advancements for understanding substrate recognition. As described in Chapter 4, to address this question I purified Yos9p under denaturing conditions and refolded it under optimized conditions. In collaboration with Dr. Koichi Kato's lab, frontal affinity chromatography then revealed that Yos9p has a specificity for glycans containing a terminal α 1,6-linked mannose. It is interesting to

note that Yos9p has little affinity for the final trimming product of the glucosidase I and II or the Mns1p-generated $\text{Man}_8\text{GlcNAc}_2$. Further trimming from $\text{Man}_8\text{GlcNAc}_2$ would have to occur to expose a terminal $\alpha 1,6$ -linked mannose. To show that Yos9's glycan specificity has in vivo relevance, I engineered a yeast strain to directly modify proteins with $\text{Man}_7\text{GlcNAc}_2$ glycans and then demonstrated that CPY* displaying $\text{Man}_7\text{GlcNAc}_2$ glycans is degraded by the canonical ERAD-L pathway. Strikingly, this degradation is not dependent on Htm1p, indicating that Htm1p is involved in processing the oligosaccharide to $\text{Man}_7\text{GlcNAc}_2$ to reveal the terminal $\alpha 1,6$ -linked mannose for Yos9p to recognize. Htm1p's role in generating terminal $\alpha 1,6$ -linked mannose on $\text{Man}_7\text{GlcNAc}_2$ to form a unique glycan signal adds another of another potential level of specificity to the bipartite recognition described above.

Please see Appendix A for unpublished results and the Chapter 5 for a brief discussion on how our glycoprotein recognition model fits within the present state of the field as well as enumeration of some of the important future questions.

CHAPTER 2

Exploration of the Topological Requirements of ERAD Identifies Yos9p as a Lectin Sensor of Misfolded Glycoproteins in the ER Lumen

Exploration of the Topological Requirements of ERAD Identifies Yos9p as a Lectin Sensor of Misfolded Glycoproteins in the ER Lumen

Arunashree Bhamidipati, Vladimir Denic, Erin M. Quan and Jonathan Weissman

Howard Hughes Medical Institute, Department of Cellular and Molecular Pharmacology,
University of California-San Francisco, San Francisco, CA94143

Correspondence:

Jonathan S. Weissman

415-502-7642 (phone)

415-514-2073 (fax)

weissman@cmp.ucsf.edu

[Reprinted with permission from Molecular Cell, Vol. 19, Bhamidipati, A., Denic V., Quan, E. M., Weissman, J. S., Exploration of the topological requirements of ERAD identifies Yos9p as a lectin sensor of misfolded glycoproteins in the ER lumen, 741-751, Copyright (2005) with permission from Elsevier.]

Summary

ER-associated degradation (ERAD) of glycoproteins depends on dual recognition of protein misfolding and remodeling of the substrate's N-linked glycans. After recognition, substrates are retrotranslocated to the cytosol for proteasomal degradation. To explore the directionality of this process, we fused a highly stable protein, DHFR, to the N or C terminus of the soluble ERAD substrate CPY* in yeast. Degradation of the C-terminal CPY*-DHFR fusion is markedly slowed and is accompanied by DHFR release in the ER lumen. Thus, folded luminal domains can impede protein retrotranslocation. The ER luminal protein Yos9p is required for both release of DHFR and degradation of multiple ERAD substrates. Yos9p forms a complex with substrates and has a sugar binding pocket that is essential for its ERAD function. Nonetheless, substrate recognition persists even when the sugar binding site is mutated or CPY* is unglycosylated. These and other considerations suggest that Yos9p plays a critical role in the bipartite recognition of terminally misfolded glycoproteins.

Introduction

Proteins entering the secretory pathway are first translocated in an unfolded form across the ER membrane (Matlack et al., 1998). Once in the ER, they acquire N-linked glycans and attempt to fold into their native states with the help of a variety of resident chaperone and redox proteins (Helenius and Aebi, 2001) and (Hirsch et al., 2004). The high flux of proteins through the ER, together with the fact that many secreted proteins have multiple domains and fold slowly, poses a significant recognition problem: how does the ER distinguish between bona fide folding intermediates and terminally misfolded proteins? The severity of this problem is illustrated by the fact that even in the absence of acute luminal stress, a large fraction of nascent ER proteins fails to fold and is consequently targeted for destruction (Casagrande et al., 2000; Friedlander et al., 2000; Jensen et al., 1995; Travers et al., 2000; Ward et al., 1995).

To avoid accumulation of unsalvageable, misfolded polypeptides that would otherwise impair ER function, the cell has evolved a series of mechanisms, commonly referred to as ER-associated degradation (ERAD), to dispose of such species (Fewell et al., 2001; Hirsch et al., 2004; Tsai et al., 2002). Over the last ten years, it has emerged that degradation comprises the following sequence of events: recognition of the misfolded protein, targeting for retrotranslocation across the ER membrane, and finally ubiquitin-dependent degradation by the cytosolic proteasome. Insight into how the ER distinguishes folding intermediates from terminally misfolded proteins has come from findings that misfolded glycoproteins undergo slow trimming of their N-glycans by a variety of glycosidases in the ER (Liu et al., 1999; Spiro, 2004). This time-dependent

remodeling of N-glycans in conjunction with persistent protein misfolding is thought to result in a bipartite signal for degradation by the ERAD machinery. This affords folding intermediates a protected period of time, before they acquire remodeled N-glycans, to reach their native state (Wu et al., 2003). Indeed, complete elimination or specific alterations of N-linked glycans leads to severe defects in the degradation of a number of substrates (Jakob et al., 1998a; Knop et al., 1996b). Although the requirement for proper glycosylation in ERAD is well established, far less is known about how the glycosylation state of substrates is monitored by the ERAD machinery. One important clue comes from the finding that a conserved ER localized mannosidase-like protein, EDEM/*HTMI*, plays a critical role in ERAD (Hosokawa et al., 2001; Jakob et al., 1998a; Molinari et al., 2003; Nakatsukasa et al., 2001; Oda et al., 2003). The presence of a mannosidase-like domain lacking a critical catalytic residue and the absence of any in vitro mannosidase activity (Jakob et al., 2001) have led to the suggestion that EDEM/*HTMI* acts as a lectin in ERAD. Nonetheless, it remains to be established whether EDEM/*HTMI* binds specific N-glycans and if such lectin activity contributes to its role in substrate degradation.

Although such studies have yielded a conceptual and molecular framework for thinking about the recognition problem, they have, in turn, raised a second question, namely, how are misfolded ER proteins transported across the ER membrane to the degradation machinery in the cytosol. This separation, while shielding proteolytically sensitive folding intermediates from being exposed to the protease machinery, poses a potential problem for terminally misfolded multidomain proteins, as these typically will have stable folded regions that may inhibit the retrotranslocation process (for review see (Romisch, 2005). At the heart of this multidomain problem lies the poorly defined

process of retrotranslocation itself (Johnson and Haigh, 2000; Lilley and Ploegh, 2004; Ye et al., 2004). To gain insight into this process, we generated a series of reporters comprising a highly stable protein, dihydrofolate reductase (DHFR), fused to the N or the C terminus of misfolded mutant carboxypeptidase Y (CPY*), the well-characterized soluble ERAD substrate.

Here, we show that fusing a stable DHFR domain to the C terminus markedly slows down degradation and that degradation is accompanied by the release of free DHFR into the lumen. These studies establish that the ER possesses a mechanism for releasing folded domains from multidomain proteins prior to completion of retrotranslocation and led us to perform a genetic screen for components necessary for the generation of the DHFR fragments. We further describe the characterization of one such component, Yos9p, a lectin required for the recognition of luminal misfolded glycoproteins.

Results

Revealing the Vectorial Nature of Retrotranslocation

To explore if there is an intrinsic directionality to the process by which luminal misfolded proteins are recognized and retrotranslocated into the cytosol, we investigated the effects of fusing a highly stable protein to either the N or C terminus of the well-characterized ERAD substrate CPY* on degradation kinetics (Hiller et al., 1996) (Figure 1A). In each case, the fusion protein was expressed in *S. cerevisiae* from the endogenous CPY promoter on a low-copy (CEN/ARS) plasmid, and a C-terminal triple HA epitope tag was appended to facilitate detection. Fusion proteins were targeted to the ER by the N-terminal signal sequence from *KAR2* (Ng et al., 1996). The logic behind this approach is that if substrate recognition and retrotranslocation require a flexible end, then the addition of a stable domain—in our case, *E. coli* dihydrofolate reductase protein (DHFR)—will provide a physical block to the process. A similar strategy has been used to monitor a range of other biological translocation events including protein import into mitochondria and threading of proteins into the proteolytic chamber of the proteasome (Eilers and Schatz, 1986; Johnston et al., 1995; Matouschek et al., 1997). Such studies have typically exploited the high stability of mammalian DHFR when complexed with its inhibitor, methotrexate. However, as it was unclear if the charged methotrexate molecule could effectively enter the ER lumen, we used the *E. coli* protein, which is structurally similar to the mammalian protein but folds more rapidly and is significantly more stable (Lee et al., 2001).

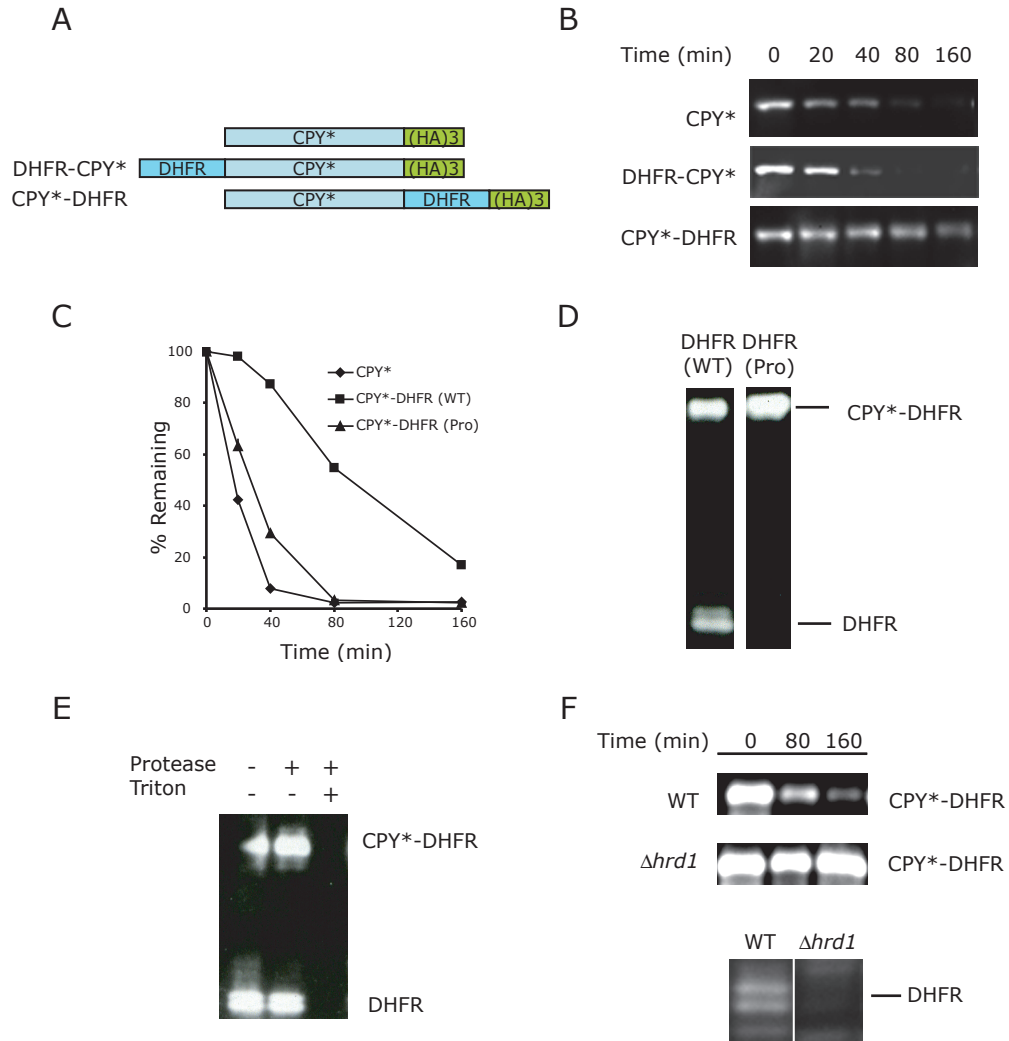


Figure 1. Presence of a Stable C-Terminal DHFR Domain Provides an Impediment to ER-Associated Degradation of CPY*

(A) A schematic of the fusion constructs used to explore the vectorial nature of retrotranslocation. All constructs were expressed from a low-copy (CEN/ARS) plasmid with the CPY (*Prc1*) promoter, targeted to the ER by an N-terminal *KAR2* signal sequence and C terminally tagged with three copies of the HA epitope ([HA]3).

(B) The rates of degradation of CPY*-HA (top), DHFR-CPY*-HA (middle), or CPY*-DHFR-HA (lower) were assessed by monitoring their disappearance at the indicated time after cycloheximide treatment by using SDS-PAGE and Western blot analysis.

(C) Quantitative Analysis of Western blots monitoring the degradation of CPY*-HA (♦), CPY*-DHFR-HA (■), and the destabilized mutant CPY*-DHFR(Pro)-HA (▲).

(D) Cells expressing CPY*-DHFR-HA (left) or CPY*-DHFR(Pro)-HA (right) were analyzed 80 min after the addition of cycloheximide as in Figure 1A. The migration position of full-length CPY*-DHFR-HA and released DHFR-HA fragments is indicated.

(E) Microsomes were prepared from cells expressing the CPY*-DHFR-HA fusion protein after 90 min of cycloheximide treatment. After proteinase K treatment in the presence or absence of Triton X-100, as indicated, samples were analyzed as in Figure 1B. The migration position of full-length CPY*-DHFR-HA and released DHFR-HA fragments is indicated.

(F) Western blots monitoring the degradation of CPY*-DHFR in *HRD1* (wt) (top) and isogenic *Δhrd1* strain (middle) after cycloheximide treatment. The DHFR fragment was visualized after 80 min of cycloheximide treatment in the *HRD1* (lower left) or *Δhrd1* (lower right) strains.

We found that fusion of DHFR to the N terminus did not significantly alter the rate or efficiency of degradation of CPY* or of the CPY*-DHFR C-terminal fusion (Figure 1B and Figure S1 in the Supplemental Data available with this article online). In contrast, addition of DHFR to the C terminus of CPY* led to strong stabilization of the fusion protein (Figure 1B). This overall stabilization was a direct consequence of the folded structure of the DHFR protein (as opposed to the presence of the ectopic sequence *per se*), as a similar fusion with a mutant form of DHFR [CPY*-DHFR(Pro)] in which the stability of the fold had been disrupted by mutating three residues to prolines (Ala-29-Pro, Trp-30-Pro, and Phe-31-Pro) failed to stabilize CPY* (Figure 1C). Remarkably, during degradation of the CPY*-DHFR fusion, we observe fragments (typically a doublet) that are recognized by both α -HA antibodies as well as α -DHFR antibodies (Figure 1D and data not shown). Moreover, the fragments do not accumulate during degradation of the CPY*-DHFR(Pro) mutant. Full-length CPY*-DHFR and the released DHFR fragments are associated with the microsome fraction and resist proteolysis by proteinase K until the addition of detergent, thus confirming that they remain in the ER lumen (Figure 1E and data not shown).

We observe that degradation of CPY*-DHFR fusion and generation of the DHFR fragments are dependent on two previously identified ERAD components required for cytosolic ubiquitination of CPY*: *HRDI*, a ubiquitin ligase (Bays et al., 2001), and *DER1*, a four-pass transmembrane protein (Hitt and Wolf, 2004a) that plays a central and conserved role in ERAD (Hiller et al., 1996; Knop et al., 1996a), possibly even in directly facilitating passage across the membrane (Lilley and Ploegh, 2004; Ye et al., 2004) (Figure 1F and data not shown).

The above findings provide a number of insights into the mechanism by which misfolded proteins are recognized and removed from the ER. First, they demonstrate an intrinsic directionality to the process (see Discussion). Second, they show that the presence of a stable, folded luminal domain can strongly inhibit degradation of a partly misfolded multidomain protein, implying that retrotranslocation (or possibly recognition) of folded regions within a misfolded substrate is at least in some instances disfavored or even prohibited. Third, they demonstrate that at least in part, the ERAD machinery circumvents the inhibitory effect of stable luminal domains by releasing them into the ER lumen through an uncharacterized clipping process. Finally, they establish that liberation of stable folded domains is dependent on the same machinery responsible for the normal degradation of ERAD substrates.

Role for Yos9p in the Degradation of Luminal Misfolded Proteins

We next reasoned that because generation of the DHFR fragments from the CPY*-DHFR fusion depended on known components of the ERAD machinery (e.g., Der1p and Hrd1p), we could identify players acting at or upstream of the clipping event by looking for yeast mutants that fail to generate the DHFR fragments. To this end, we screened a bank of yeast strains, each deleted for one of ~400 nonessential genes shown to encode proteins localized to the ER or to the early secretory pathway (Huh et al., 2003; Kumar et al., 2002; Schuldiner et al., 2005). Each strain was transformed with a plasmid carrying CPY*-DHFR, and the half-life of the fusion protein as well as the release of fragments were monitored by Western blot analysis of cell extracts after inhibition of protein synthesis with cycloheximide. For the remainder of the present work, we will focus on a

single protein, Yos9p, identified in this screen (Figure 2A). A full analysis of the results of the screen will be presented elsewhere. Yos9p, previously named on the basis of similarity to a mammalian gene (OS-9) that is amplified in patients with osteosarcoma (Su et al., 1996), is a poorly characterized protein with two notable features: a mannose 6-phosphate receptor homology (MRH) domain (Munro, 2001) and a C-terminal HDEL sequence that acts as an ER retrieval signal (Pelham et al., 1988) and also is found in a handful of other luminal ER resident proteins such as Kar2p and PDI.

An earlier report had suggested that deletion of *YOS9* leads to a modest defect in the trafficking of GPI-anchored proteins (Friedmann et al., 2002). However, a more recent analysis (Kim et al., 2005; Szathmary et al., 2005) failed to observe such a defect in a range of different strain backgrounds including those used in the original report. In addition, as this work was being prepared for publication, Wolf and coworkers (Buschhorn et al., 2004) reported that Yos9p is required for the ER-associated degradation of glycoproteins. Similarly, we see that loss of Yos9p, in addition to stabilizing the CPY*-DHFR fusion (Figure 2A), results in a profound defect in CPY* degradation, comparable to that caused by the loss of *DER1* (Figures 2B and 2C). Interestingly, the defect seen in the $\Delta yos9$ strain is considerably stronger than that seen in a $\Delta mns1$ strain (Figures 2B and 2C). Mns1p is the α -1,2 mannosidase that removes one mannose residue from the core oligosaccharide, resulting in the conversion of the Man₉GlcNAc₂ form to the Man₈GlcNAc₂ form. Mns1p acts as a “timer” whose delayed action provides a grace period for proteins to fold before they are subjected to surveillance by the ERAD machinery (Liu et al., 1999; Spiro, 2004). Additionally, the rate of CPY* degradation in the double deletion strain $\Delta mns1\Delta yos9$ is indistinguishable

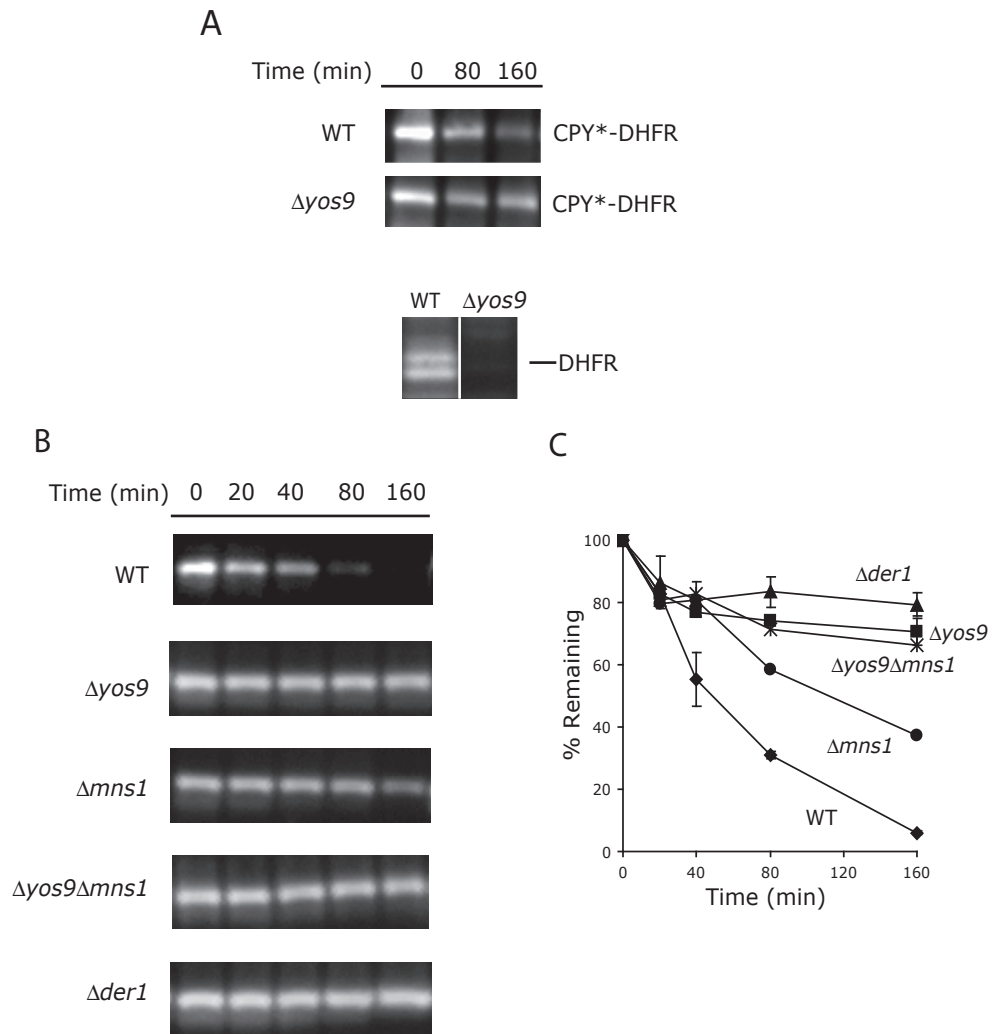


Figure 2. Yos9p Is Required for ER-Associated Degradation of CPY*

(A) Western blots monitoring the degradation of CPY*-DHFR-HA (top) and generation of released DHFR fragments (bottom) in the wild-type and the isogenic $\Delta yos9$ strain.

(B) Western blots monitoring the degradation of CPY*-HA in isogenic wild-type, $\Delta yos9$, $\Delta mns1$, $\Delta yos9\Delta mns1$, and $\Delta der1$ backgrounds.

(C) Quantitative analysis of Western blots monitoring the degradation of CPY*-HA in isogenic wild-type (\blacklozenge), $\Delta yos9$ (\blacksquare), $\Delta mns1$ (\bullet), $\Delta yos9\Delta mns1$ ($*$), and $\Delta der1$ (\blacktriangle) backgrounds. The error bars indicate the deviation from the mean of at least two independent experiments.

from that observed in the single *Yos9* strain. Thus, Yos9p is a critical component of the ERAD machinery whose action may be enhanced by, but is not fully dependent on, the Mns1p mannosidase timer.

Earlier studies indicated that there are at least two distinct surveillance mechanisms for identifying terminally misfolded ER proteins (Ahner and Brodsky, 2004; Hoyer et al., 2004): one (designated ERAD-L) that inspects for proteins like CPY*, which contain misfolded luminal (soluble or membrane tethered) domains, and a second (termed ERAD-C) that detects misfolded cytosolic domains of transmembrane proteins. Although both of these pathways ultimately converge on the ubiquitin proteasome degradation system, they depend on different sets of ER-associated components to detect misfolded species and to deliver them to the cytosol.

To explore the role of Yos9p in these two ERAD pathways, we took advantage of three substrates developed by Ng and coworkers (Vashist and Ng, 2004) that contain misfolded domains oriented to the luminal and/or cytosol face. One ERAD-L substrate, KHN, consists of a Kar2p signal sequence fused to the simian virus 5 HA-Neuraminidase ectodomain and, like CPY*, is a soluble luminal protein. A second ERAD-L substrate, KWW, consists of KHN fused to the transmembrane domain from the Wsc1p protein such that KHN is oriented to the luminal side of the ER. A third substrate, KWS, is designed to monitor the ERAD-C process. KWS contains a luminal KHN domain, the transmembrane Wsc1p domain, and a cytosolic domain of the misfolded Ste6-166p mutant. For the two ERAD-L substrates (KHN and KWW), loss of Yos9p led to a profound defect in degradation comparable to that seen with loss of components of the core ERAD-L machinery (e.g., Der1p and Htm1p) and substantially greater than the

defect seen in the absence of Mns1p (Figures 3A and 3B). In contrast, the degradation of the ERAD-C substrate, KWS, was not affected by loss of Yos9p (Figure 3C). Thus, Yos9p plays a critical role in the recognition and/or subsequent retrotranslocation of a range of proteins containing misfolded luminal domains.

Yos9p Is a Lectin Whose Sugar Binding Pocket Is Required for ERAD

The presence of the MRH domain in Yos9p is particularly intriguing in light of the broad and incompletely understood role that substrate glycosylation plays in allowing proteins to be recognized by the ERAD machinery. Whereas some MRH domains are genuine mannose 6-phosphate lectins, other MRH domains recognize protein substrates in a sugar-independent manner (Ghosh et al., 2003). In particular, the cation-independent mannose 6-phosphate receptor (CI-MPR) contains 15 MRH repeats, only two of which (repeat 3 and 9) are thought to contain high affinity mannose 6-phosphate binding sites. Structural analysis of the single MRH domain in the cation-dependent MPR (CD-MPR) complexed with mannose 6-phosphate, in conjunction with mutational studies, have identified four residues (Gln66, Arg111, Glu133, and Tyr143) that are in direct contact with the mannose sugar and are critical for carbohydrate recognition (Hancock et al., 2002; Olson et al., 1999) (Figures 4A and 4B). These residues provide a strong signature diagnostic of sugar binding activity, as they are highly conserved among the MRH repeats of the CI-MPR that tightly bind mannose 6-phosphate (repeats 3 and 9) but diverge rapidly in the MRH repeats not involved in sugar binding (Ghosh et al., 2003). Of these four signature residues, the final three are located at well-defined positions relative to conserved cysteines and, thus, their location in Yos9p (Arg200, Glu223, and Tyr229)

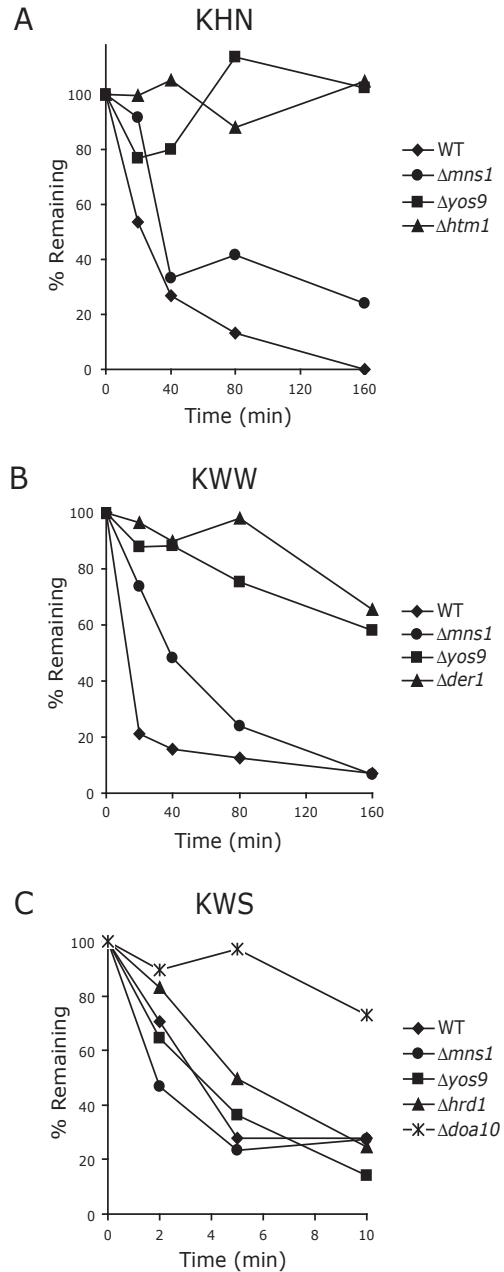


Figure 3. Yos9p Is Required for Degradation of Proteins Containing Misfolded Luminal but Not Cytosolic Domains

(A) Quantitative analysis of Western blots monitoring the degradation of KHN-HA, a soluble luminal ERAD substrate, in wild-type (♦), $\Delta mns1$ (●), $\Delta yos9$ (■), and $\Delta htm1$ (▲) backgrounds (Vashist and Ng, 2004).

(B) Quantitative analysis of Western blots monitoring the degradation of KWW-HA, an integral membrane ERAD substrate containing a misfolded luminal domain, in isogenic wild-type (♦), $\Delta mns1$ (●), $\Delta yos9$ (■), and $\Delta der1$ (▲) backgrounds.

(C) Quantitative analysis of Western blots monitoring the degradation of KWS-HA, an integral membrane ERAD substrate that also has a cytosolic misfolded domain, was assessed in wild-type (♦), $\Delta mns1$ (●), $\Delta yos9$ (■), $\Delta hrd1$ (▲), and $\Delta doa10$ (*).

and its homologs (Figure 4A) can be unambiguously determined despite the weak overall similarity between the various MRH domain-containing proteins. Significantly, we find that conservative changes (Glu-to-Asp, Tyr-to-Phe, Arg-to-Ala) to these signature residues strongly inhibit or completely abrogate CPY* degradation (Figure 4C). Thus, sequence analysis in conjunction with mutational studies strongly support the notion that Yos9p is a lectin and that this sugar binding activity is critical to its ability to support ERAD.

Efficient recognition and degradation of misfolded glycoproteins requires the presence of specific oligosaccharide structures on the substrate polypeptide (Jakob et al., 1998a). Thus, in principle, the degradation defect seen in a strain lacking Yos9p could be a secondary consequence of either failure to properly synthesize N-linked core oligosaccharides or failure to correctly trim such oligosaccharides. To exclude the possibility that Yos9p is required for the synthesis of the core oligosaccharide, we examined the glycosylation state of mature wild-type CPY. As noted previously (Jakob et al., 1998a), failure to generate full-length high mannose sugars (e.g., caused by deletion of the *ALG9* or *ALG12* genes) leads to reduced efficiency of N-glycosylation of wild-type CPY by the oligosaccharyltransferase, resulting in a ladder of hypoglycosylated CPY species. In contrast, no such ladder is seen in a *Δyos9* strain, indicating that Yos9p is not required for the production or transfer of full-length high mannose oligosaccharides to nascent polypeptide chains (data not shown). Secondly, as it is known that interfering with glucose trimming of N-glycans can lead to stabilization of CPY* (Hitt and Wolf, 2004b; Jakob et al., 1998a), we wished to exclude such a role for Yos9p. This concern was heightened by the finding that glucosidase II, one of the enzymes that catalyzes

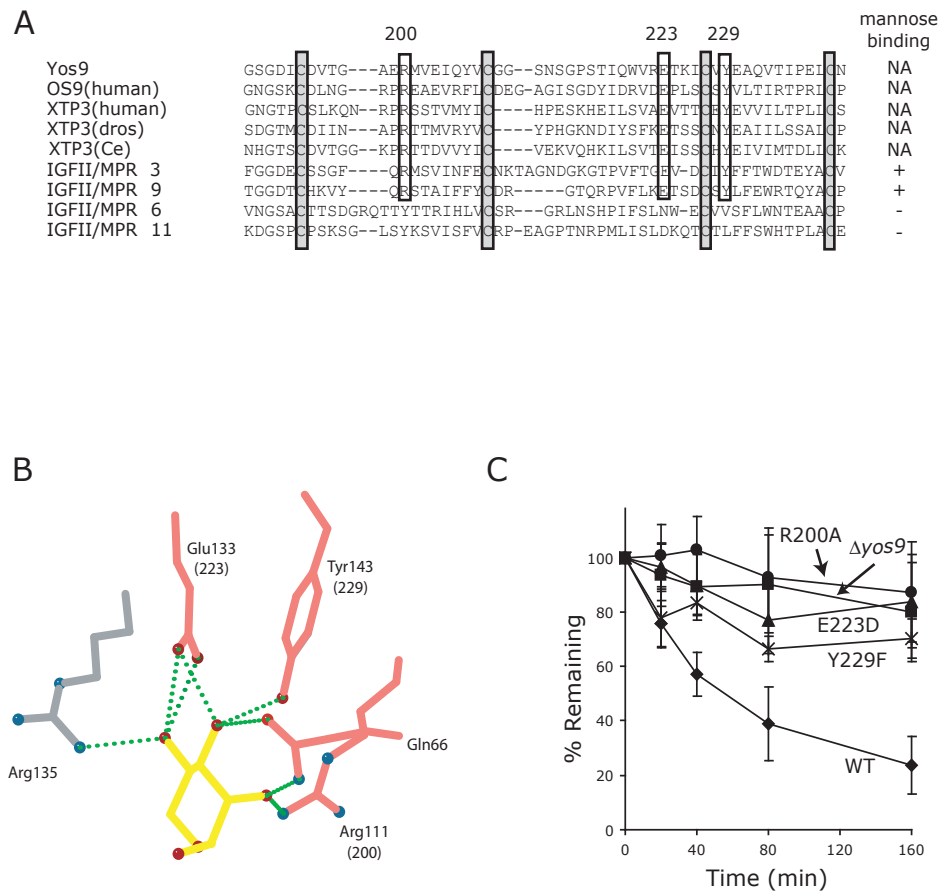


Figure 4. Yos9p Contains an Intact Sugar Binding Site that Is Required for Its Ability to Support ERAD

(A) Sequence alignment of corresponding C-terminal regions of the MRH domains from *S. cerevisiae* YOS9, human OS-9, human XTP3-B, *Drosophila* XTP3-B, *C. elegans* XTP3-B, and MRH domains 3, 6, 9, and 11 of the insulin-like growth factor II/cation-independent mannose 6-phosphate receptor (IGFII/MPR). The conserved cysteines are shaded in gray. The residues that are required for binding of the mannose sugar (R200, E223, and Y229 of Yos9p) are boxed (Hancock et al., 2002). Previously characterized mannose binding properties are shown on the right (NA: not assessed).

(B) Structure of the carbohydrate binding pocket of the cation-dependent mannose 6-phosphate receptor (CD-MPR) in complex with mannose 6-phosphate. Hydrogen bonds between the CD-MPR and mannose backbone are indicated by dotted lines. The four residues that have been shown by mutational analysis to be critical for mannose 6-phosphate binding (Hancock et al., 2002) are shown in red. The sequence numbers of corresponding residues in *S. cerevisiae* Yos9p are given in parenthesis.

(C) Quantitative analysis of Western blots monitoring the degradation of CPY*-HA in $\Delta yos9$ cells harboring an empty vector (■), or expressing wild-type Yos9p (♦) or the R200A (●), E223D (▲), or Y229F (*) mutant forms of Yos9p. The error bars indicate the standard deviation obtained from four independent experiments.

trimming of glucose residues, also contains an MRH domain (Munro, 2001). However, in contrast to the glucosidase mutants, the ERAD defect caused by loss of Yos9p is not suppressed by a mutation in the gene *ALG6*, which is responsible for the biosynthetic glucosylation of the high mannose oligosaccharide (Jakob et al., 1998a) (data not shown). Finally, as noted earlier, the ERAD defect in a strain deleted for both *YOS9* and *MNS1* is considerably stronger than the one seen in a strain deleted for *MNS1* alone, even though *MNS1*-deleted strains show a complete failure to undergo trimming to convert $\text{Man}_9\text{GlcNAc}_2$ forms to $\text{Man}_8\text{GlcNAc}_2$, arguing against the idea that Yos9p is performing a function linked solely to Mns1p-dependent mannose trimming (Jakob et al., 2001). Taken together, the above studies establish that the lectin activity of Yos9p is required for its ability to support substrate degradation but that Yos9p nonetheless acts downstream of generation of the proper oligosaccharide structure required for ERAD.

Substrate Recognition by Yos9p

To address whether Yos9p is involved in directly recognizing substrates, we performed immunoprecipitation experiments by using a tagged version of Yos9p. We tagged Yos9p with a triple FLAG epitope inserted immediately prior to the C-terminal HDEL signal and expressed it on a high-copy (2 μ) plasmid under the control of its natural promoter. This construct was able to complement the ERAD defect of a $\Delta yos9$ strain (data not shown). Additionally, to facilitate detection of what would most likely be a transient interaction with a short-lived CPY* substrate, we performed all experiments in a strain deleted for downstream ERAD components, either $\Delta hrd1$ or $\Delta der1$. Under such conditions, solubilization of a crude cellular membrane fraction with the mild amphoteric

detergent CHAPS revealed that Yos9-FLAG interacts specifically and equally well with both CPY* and CPY*-DHFR (Figure 5A). This latter observation suggests that the degradation defect caused by fusing DHFR to the C terminus of CPY* does not result from an inability to interact with Yos9p and is thus likely to result from interference with a downstream step in ERAD such as retrotranslocation.

The interaction between CPY* and Yos9p was confirmed with a crosslinking strategy (Gardner et al., 2000). Here, we treated intact microsomes with a short (12 Å) reversible crosslinker (DSP) and immunoprecipitated CPY* and any covalently associated proteins under denaturing conditions. We then reversed the crosslink and probed for Yos9-FLAG. As seen in Figure 5B, Yos9-FLAG interacts with CPY* and does so in a specific and crosslinker-dependent manner. Interestingly, when these experiments were repeated with non-reversible crosslinkers (DSS and DSG), both CPY* and Yos9p were found in a large (>200 kDa), discrete complex (Figure S3), suggesting that multiple copies of Yos9p or CPY* or other proteins are involved in the recognition complex.

Because we have shown that Yos9p's lectin activity is required for its ERAD function, we wanted to test if the Yos9p-substrate interaction we see is also abolished by sugar binding mutations in the MRH domain. Unexpectedly, the lectin mutants were still able to interact with the substrate (Figure 5C and Figures S2 and S4), and this interaction, if anything, was more pronounced (relative increase in pull down efficiency of 3.8 ± 0.4 by native IP, see Experimental Procedures) than the one seen with the wild-type Yos9p (see Discussion). We also find that the interaction between CPY* and both wild-type Yos9p and the R200A mutant persists in the absence of Htm1p (Figure 5D and Figure

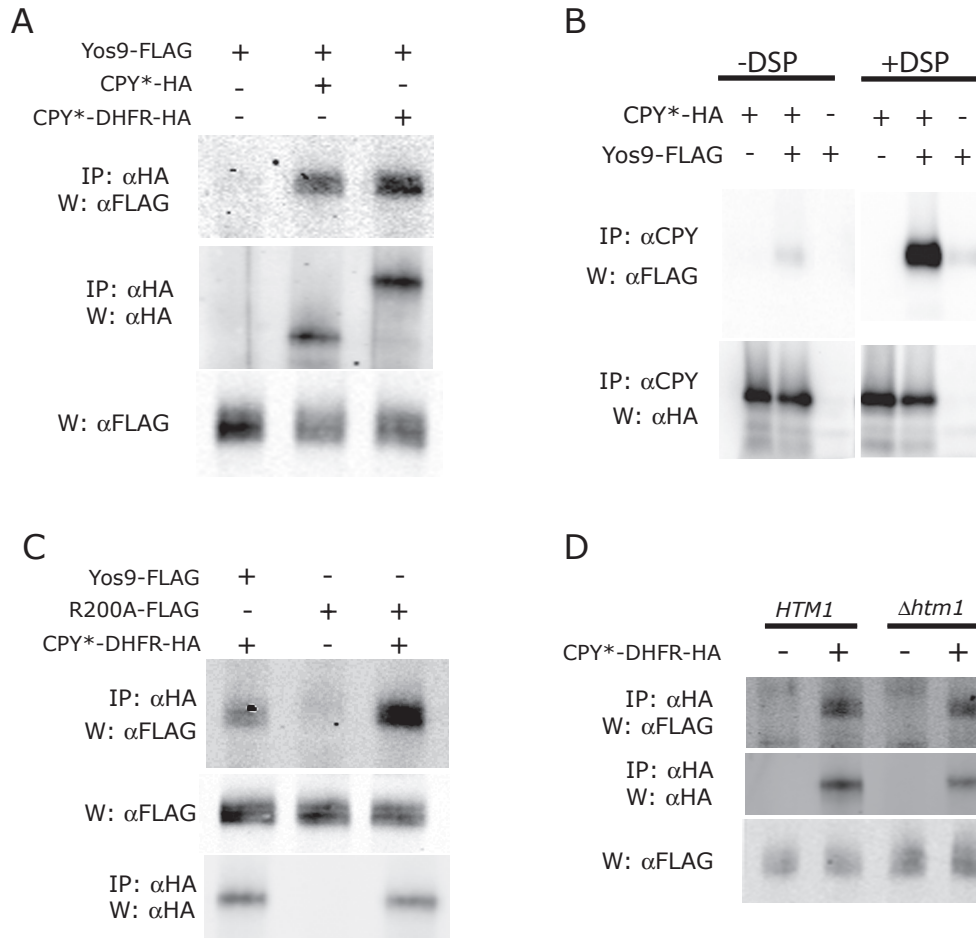


Figure 5. Interaction of Misfolded ER Proteins with Yos9p

(A) Native IP: Δ hrd1 Δ yos9 cells were transformed with constructs expressing Yos9-FLAG, CPY*-HA, or CPY*-DHFR-HA as indicated. Spheroplasts were prepared from mid-log phase cells, and lysates were incubated with protein A/G agarose prebound to α -HA antibodies for IP. Proteins eluted after IP (top and middle) or whole-cell lysate were subjected to SDS-PAGE followed by Western blot (W) analysis with the indicated antibodies (see Experimental Procedures for details).

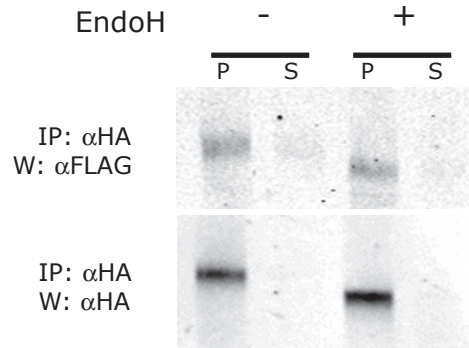
(B) Crosslinking followed by denaturing IP. Microsomes prepared from Δ der1 cells transformed with the indicated plasmid were incubated in the presence or absence of 800 μ g/ml of the reversible crosslinker, DSP. After denaturation of protein complexes, samples were immunoprecipitated with α -CPY antibodies and bound protein was analyzed by SDS-PAGE followed by Western blotting analysis.

(C) Δ hrd1 Δ yos9 cells expressing CPY*-DHFR-HA, Yos9-FLAG, or a Yos9-FLAG variant in which Arg 200, known to be critical for mannose binding in CD-MPR, has been replaced with alanine (R200A) were subjected to native IP as described in 5A. Similar results were obtained with two other YOS9 lectin mutants (Figure S2).

(D) Δ hrd1 Δ yos9 (*HTM1*) or Δ hrd1 Δ yos9 Δ htm1 (Δ htm1) cells harboring a plasmid expressing Yos9-FLAG and, where indicated, a second plasmid expressing CPY*-DHFR-HA were subjected to native IP analysis as described in Figure 5A.

S4), a putative lectin involved in ERAD. To exclude the possibility that the ability of substrate to bind the Yos9p lectin mutants resulted from additional sugar-dependent contacts, we subjected the native immunoprecipitates to digestion with endoglycosidase H, which cleaves off all but one residue of N-linked core oligosaccharides. This treatment quantitatively deglycosylated the substrate but failed to abolish the interaction with the wild-type Yos9p (data not shown) as well as with the R200A lectin mutant (Figure 6A). It remains a formal possibility that a small fraction of CPY* bound to Yos9p is resistant to endoH treatment. We therefore confirmed that the CPY*-Yos9p interaction did not depend on sugar recognition by using a mutant of CPY* (CPY*0000) in which the four glycosylation sites have been removed. CPY*0000 has a very slow rate of degradation in wild-type cells, which is unaffected by the loss of Yos9p (Buschhorn et al., 2004). Consistent with the above results, CPY*0000 could be immunoprecipitated with Yos9p, and this interaction was more pronounced in the R200A Yos9p lectin mutant (Figure 6B). Taken together, these data strongly argue that Yos9p is able to interact with a misfolded protein independent of its lectin domain or the presence of any N-glycans on the substrate.

A



B

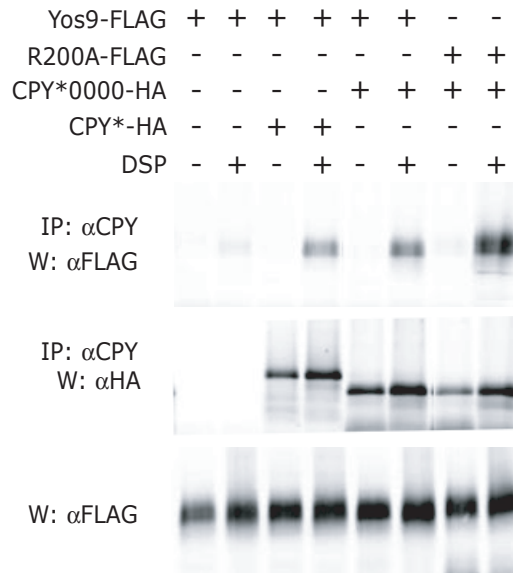


Figure 6. Sugar-Independent Recognition of CPY* by Yos9p

(A) The R200A Yos9p-CPY* interaction does not depend on continued substrate glycosylation. After immunoprecipitation of the R200A FLAG-CPY*-HA complex, the beads were split and incubated in the presence or absence of EndoH. The beads were subsequently pelleted, and equal fractions of the supernatant (S) and the washed pellet (P) were analyzed by SDS-PAGE followed by Western blot analysis. (B) *Δhrd1Δyos9* cells expressing either Yos9-FLAG or the MRH mutant of Yos9p, R200A-FLAG, with or without the non-glycosylated form of CPY* (CPY*0000-HA) were subjected to crosslinking with the cleavable crosslinker DSP followed by denaturing IP as described in Figure 5B. A control IP was performed with *Δhrd1Δyos9* cells expressing Yos9-FLAG and CPY*-HA. The faint band in lane 2 may be due to an interaction between Yos9-FLAG and misfolded endogenous wild-type CPY.

Discussion

The “signal hypothesis” (Blobel and Dobberstein, 1975), first formulated 30 years ago, has served as a conceptual framework for understanding how proteins are targeted for translocation across a variety of cellular membranes. By contrast, the reverse process by which misfolded ER proteins are targeted back into the cytosol for destruction remains poorly understood. This problem seems all the more challenging as it is known that luminal ERAD substrates have their N-terminal signal sequences cleaved and completely disengage from the translocon prior to being recognized by the ERAD machinery (Plempner et al., 1999). Moreover, the physical properties and exposed epitopes of terminally misfolded proteins are likely to resemble those found in productive folding intermediates. Thus, two outstanding questions in the field are one of information flow (i.e., what are the signals that mark proteins for destruction) and one of mechanics (i.e., how do substrates, once recognized, engage the retrotranslocation apparatus and emerge on the cytosolic side).

The multidomain nature of secreted proteins provides a particular mechanical challenge to retrotranslocation, as many misfolded proteins may contain stably folded luminal domains. Thus, retrotranslocation requires either that the cell is capable of transporting such native domains intact across the ER membrane or alternatively that there are mechanisms to unfold or proteolytically remove such domains prior to or during the process of retrotranslocation. Although there is evidence that the former possibility is used in some cases (Fiebigler et al., 2002; Tirosh et al., 2003), here we establish that the presence of folded luminal domains can provide a strong impediment to the degradation

of misfolded ER proteins. In particular, addition of the highly stable protein, *E. coli* DHFR, to the C terminus of the well-characterized soluble ERAD substrate CPY* (Hiller et al., 1996) greatly slows its rate of degradation. This inhibition is due specifically to the presence of the structured region and not the DHFR sequence per se, as a destabilized mutant of DHFR fails to have an effect on the CPY* degradation kinetics. The block in degradation appears to occur after substrate recognition, because the presence of the DHFR domain does not inhibit interaction of CPY* with Yos9p, the luminal lectin we show to play a critical role in ERAD (see below).

As part of the ERAD process, DHFR can be clipped from the remainder of CPY* and the released DHFR fragments remain in the ER lumen. In addition to facilitating degradation of proteins with stable luminal domains, proteolytic release may also be important in preventing such substrates from occluding the available retrotranslocons. The mechanism by which this clipping occurs remains an interesting open question; for example, are there luminal proteases dedicated to releasing stable domains, or is the clipping a result of incomplete proteasomal degradation of a partially retrotranslocated substrate?

The DHFR fusion strategy also reveals a strong directionality to the recognition and retrotranslocation of CPY*, as the C-terminal fusion showed marked inhibition of degradation whereas the N-terminal fusion had no effect. The observation that fusing DHFR to both termini of CPY* does not completely block degradation (Figure S1) indicates that an unfolded domain of a multidomain protein can be recognized even when sandwiched between two stable folded regions. These observations suggest that retrotranslocation can be initiated internally, even though in the absence of structured

regions there may typically be a strong preference for commencing this process at one or both of the termini. Extension of the fusion strategy used in the present work should help elucidate what types of sequence and structural information (e.g., conformation of the misfolded region, N-linked glycans, or ubiquitination sites) lead to such a bias.

A search for factors required for generating the DHFR fragments of the CPY*-DHFR fusion identified the resident ER protein Yos9p, which contains a mannose 6-phosphate receptor homology (MRH) domain. Consistent with a recent report from the Wolf lab (Buschhorn et al., 2004; Kim et al., 2005; Szathmary et al., 2005), Yos9p is required for the degradation of a range of different glycoproteins that contain lumenally exposed, misfolded domains. Yos9p may contribute directly to the recognition of misfolded substrates, as it can be efficiently coimmunoprecipitated with CPY* under native conditions and can be crosslinked with CPY* by using the short (12 Å) crosslinker DSP.

YOS9 was originally identified on the basis of its sequence similarity to mammalian OS-9. However, in light of our current findings regarding Yos9p's critical role in ERAD of lumenal misfolded glycoproteins, two earlier studies raise significant doubts as to whether OS-9 is a functional homolog of Yos9p. First, in contrast to Yos9p's lumenal disposition (Friedmann et al., 2002), OS-9 has been shown to be peripherally associated with the cytosolic face of the ER, where it transiently interacts with meprin β to facilitate its trafficking along the early secretory pathway (Litovchick et al., 2002). Second, a recent report demonstrated that OS-9 interacts with and promotes the degradation of the cytosolically localized protein hypoxia-inducible factor 1 α (HIF-1 α) (Baek et al., 2005). Although these data argue that OS-9 is performing a distinct function

from Yos9p, the presence of an MRH domain in OS-9 raises the interesting question of what function such a domain, with its sugar binding pocket intact, would be performing in the cytosol. Thus, either a fraction of OS-9 is localized to the ER or OS-9 recognizes glycoproteins that have escaped from the ER in a role possibly similar to the one proposed for the E3 lectin Fbs1 (Yoshida et al., 2002). The human genome contains a second protein (XTP3-transactivated protein B [XTP3-B]) with similarity to Yos9p that is a more attractive candidate for a true functional homolog of Yos9p. XTP3-B contains two MRH domains and shows greater similarity to Yos9p compared to OS-9. The localization of XTP3-B proteins is unknown, but close homologs are found throughout metazoans including a *C. elegans* protein (WP:CE34218) with a C-terminal HEDL that likely confers residence in the ER lumen.

The presence of an MRH domain in Yos9p is particularly intriguing in light of the critical role that substrate glycosylation plays in protein degradation. Whereas only a subset of MRH domains are competent to bind sugars (Ghosh et al., 2003), our analysis of Yos9p and related sequences together with the structure of the MRH domain complexed with mannose argues strongly that the sugar binding site is intact and conserved in Yos9p. Moreover, this sugar binding pocket is required for Yos9p function, as conservative mutations in solvent-exposed residues known to be critical for sugar recognition abrogate the ability of Yos9p to degrade CPY*. Despite the critical role of the Yos9p lectin activity, interaction between Yos9p and substrate persists even when the sugar binding site is mutated or the substrate is deglycosylated, suggesting that Yos9p recognizes misfolded polypeptides in a sugar-independent manner. Indeed, MRH

domains have been found to be involved in sugar-independent interactions (Ghosh et al., 2003).

What then is the role of the Yos9p lectin in ERAD? Three distinct possibilities exist for Yos9p's role in the bipartite recognition of terminally misfolded proteins involving both substrate recognition and read out of the glycosylation status. First, binding of ERAD substrates by Yos9p involves both recognition of sugars and direct interaction with the substrate, and this latter mode is sufficient to support coimmunoprecipitation in the presence of the mild detergent CHAPS. Consistent with the notion that sugar binding contributes to Yos9p-substrate interactions, Szathmary et al. (2005) find that in the presence of Triton X-100, coimmunoprecipitation of Yos9p and CPY* is not observed in yeast strains containing mutations in some of the *ALG* genes, which alter the structure of N-linked glycans. Second, substrate recognition by Yos9p predominantly involves direct, lectin-independent recognition of misfolded species. Yos9p then queries the sugar status of the substrate to determine whether the N-glycans are in a configuration instructive for hand-off to downstream effectors (e.g., they have undergone proper time-dependent trimming). Third, carbohydrate binding by Yos9p is required for its productive interaction with downstream ERAD components, but is not involved in substrate binding. In accordance with this intriguing possibility, we consistently find a marked increase in the amount of substrate coimmunoprecipitated with Yos9p when its sugar binding site is ablated. Regardless, identification of Yos9p as a critical lectin that is required for ERAD and that interacts with substrates provides a key tool for understanding the molecular basis of how the ER quality control machinery distinguishes right from wrong.

Experimental Procedures

Plasmid Construction

CPY* and the indicated derivatives of CPY* were expressed from the natural promoter based on a CEN/ARS plasmid (see Supplemental Data).

Untagged Yos9p and R200A, E223D, and Y229F YOS9 lectin mutants were expressed from the YOS9 endogenous promoter on a CEN/ARS plasmid. Flag-tagged YOS9 constructs were generated on a high-copy 2 μ plasmid (see Supplemental Data).

KHN-HA, KWS-HA, KWW-HA ((Vashist et al., 2001; Vashist and Ng, 2004), and non-glycosylated CPY* were a gift from Davis Ng.

Strains

Δ prc1, *Δ yos9*, and *Δ rpn4 Δ pdr5* were derived from W303-1A (MATa; *leu2-3, -112 his3-11, -15 trp1-1 ura3-1 ade2-1 can1-100*). *PRC1* and *YOS9* were deleted by using chimeric polymerase chain reaction (PCR) (Longtine et al., 1998) with the *TRP1* and *HIS3* auxotrophic markers. *Δ rpn4 Δ pdr5* was generated by sequentially deleting *RPN4* and *PDR5* with *HIS3* and *LEU2* auxotrophic markers.

Δ yos9, *Δ der1*, *Δ hrd1 Δ mns1*, *Δ htm1*, *Δ alg6*, *Δ alg9*, and *Δ alg12* are derivatives of a BY4741: S288c background (*MATa his3 Δ 1 leu2 Δ 0 met15 Δ 0 ura3 Δ 0*) or Y3656 (*MAT α can1 Δ ::MFA1pr-HIS3-MFA1pr-Leu2 his3 Δ 1 leu2 Δ 0 met15 Δ 0 ura3 Δ 0 lys2 Δ 0*). Deletion strains in MATa were generated by the *S. cerevisiae* deletion consortium (Winzeler et al., 1999) by using a kanamycin resistance cassette. Deletion strains in MAT α were generated with a NAT antibiotic resistance cassette (pFA6-NAT-MX3) (Goldstein and

McCusker, 1999). Double deletions were generated by crossing opposite mating types, using standard yeast manipulation techniques (Guthrie and Fink, 1991).

For native immunoprecipitations (IPs), *YOS9* was deleted with *MET15* in the *HTM1-TAP::HIS* strain (Ghaemmaghami et al., 2003). This strain was then crossed to *Δhrd1::NAT*. The *Δhrd1Δyos9* isolate obtained from this was used for native IPs with wild-type *YOS9* and *YOS9* lectin mutants. The *Δhtm1Δhrd1Δyos9* triple mutant was obtained by crossing *Δhrd1Δyos9* with *Δhtm1::Kan*.

Cycloheximide Chase Degradation Assay

Cycloheximide chase degradation assays were done as previously described (Gardner et al., 2000) with minor modifications (see Supplemental Data).

Protease Protection Assays

Protease protection experiments were done in a W303-1A *Δrpn4Δpdr5* strain, but similar results were observed in the wild-type background. Microsomes from cells expressing CPY*-DHFR-HA were prepared as described in the Supplemental Data and incubated in the presence or absence of 10 µg/ml proteinase K and with or without 1% Triton X-100 at room temperature (RT) for 10 min. The reaction was terminated by the addition of PMSF to a final concentration of 0.05 mM. Samples were analyzed by sodium dodecyl-sulfate-polyacrylamide gel electrophoresis (SDS-PAGE) followed by Western blotting with 12CA5 mouse α-HA and goat α-mouse antibodies.

Crosslinking Experiments

These experiments were done as described before (Gardner et al., 2000) with some modifications (see Supplemental Data).

Native Immunoprecipitations

For native IPs, 25 OD₆₀₀ units of mid-log phase cells were spheroplasted by using the protocol described under Protease Protection Assays. The spheroplasts were washed in Lysis buffer containing 0.7 M sorbitol and were lysed in 1.25 ml cold lysis buffer containing 50 mM Hepes (pH 6.8), 150 mM KOAc, 2 mM Mg(OAc)₂, 1 mM CaCl₂, and protease inhibitors. The lysate was cleared at 21,000 × g for 10 min at 4°C. The pellet was resuspended in 1.25 ml LB containing 0.5% CHAPS. The samples were incubated on ice for 10 min and centrifuged at 21,000 × g for 10 min. BSA was added to 0.1% to the supernatant, and 1 ml of this was subjected to IP with protein A/G agarose prebound to α -HA antibodies (combination of Roche 12CA5 and Santa Cruz HA probe Y11) at 4°C for 2 hr with rotating. IPs were washed four times with 1 ml of LB containing 0.5% CHAPS and once with 1 ml of 0.1% DOC/SDS. Each wash lasted 2 min. Immune complexes were eluted by boiling the beads in SDS-PAGE sample buffer and were analyzed by SDS-PAGE electrophoresis and Western blotting. Protein bands were detected by using fluorescent antibodies and the LI-COR Odyssey detection system.

For EndoH treatment, 20 μ l of 100 mM NaCitrate (pH 5.5) and protease inhibitors were added to duplicate IPs after the final wash. The duplicate IPs were pooled and split into two. They were incubated with or without 1 μ l of EndoH (Roche; 1U [200 μ l]) and incubated at 37°C for 30 min with occasional mixing. The supernatant was taken out and

the beads were washed with LB containing 0.5% CHAPS. Immune complexes were eluted as described above.

The relative efficiency of interaction of wild-type Yos9p (wt) versus R200A lectin mutant was determined with the following formula:

$$\frac{(IP_{FLAGR200A}/[IP_{CPY(R200A)}(Total_{FLAGR200A})])}{(IP_{FLAGwt}/[IP_{CPY(wt)}(Total_{FLAGwt})])}$$

CPY* and total amount of wild-type Yos9p or R200A lectin mutant varied by at most 20%. IP_{FLAG} is the amount of FLAG-tagged Yos9p or R200A lectin mutant immunoprecipitated. IP_{cpy*} is the amount of CPY* pulled down. Total_{FLAG} is the amount of FLAG-tagged Yos9p or R200A present in the reaction prior to the addition of antibodies used for immunoprecipitation.

Acknowledgments

We are grateful to D. Ng and C. Jakob for communicating results to us prior to publication; to R. Kopito and J. Christianson for helpful discussions; to members of the O'Shea and Weissman labs for helpful discussions; J. Hollien, M. Kulp, J. Newman, and M. Schuldiner for helpful comments on the manuscript; M. Schuldiner and M. Noble for the ER knockout library; S. Ghaemmaghami and A. Belle for technical help with the cycloheximide degradation assay screen. We are grateful for the support from American Cancer Society (A.B.), National Science Foundation (E.Q.) and the Howard Hughes Medical Institute.

Received 5 April 2005; revised 13 June 2005; accepted 23 July 2005.

Published: September 15, 2005.

Available online 15 September 2005.

Supplemental Data

Exploration of the Topological Requirements of ERAD Identifies Yos9p as a Lectin Sensor of Misfolded Glycoproteins in the ER Lumen

Arunashree Bhamidipati, Vladimir Denic, Erin M. Quan, and Jonathan S. Weissman

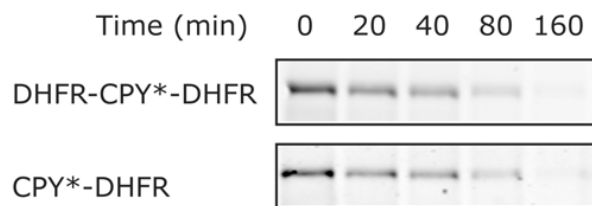


Figure S1. Western Blots Monitoring the Degradation of DHFR-CPY*-DHFR (Top) in which DHFR Was Fused to the N Terminus of CPY*-DHFR-HA and CPY*-DHFR-HA (Lower)

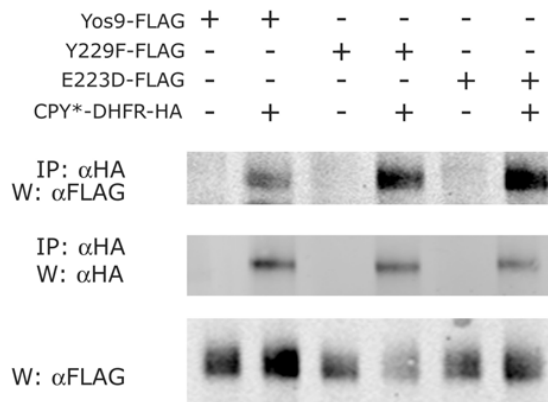


Figure S2. *Δhrd1 Δyos9* Cells Expressing CPY*-DHFR-HA and Yos9-FLAG or a Yos9-FLAG Variant in which One of the Residues Implicated in Mannose Binding in CD-MPR has Been Mutated (E223D, Y229F).

Transformed cells were subjected to native IP and samples were analyzed by SDS-PAGE and Western blotting as described for Figure 5A.

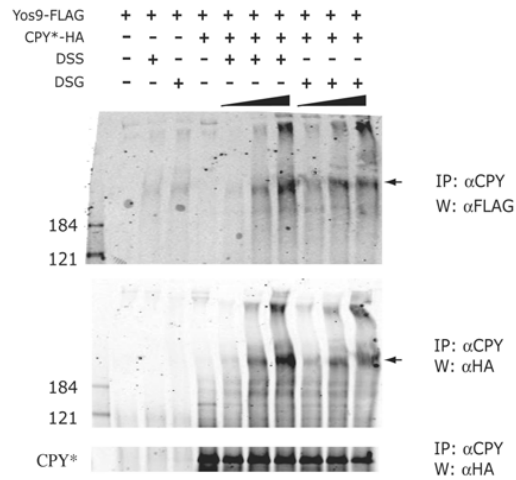


Figure S3. Microsomes Derived from $\Delta hrd1\Delta yos9$ Cells Expressing Yos9-FLAG with or without CPY*-HA Were Incubated in the Presence or Absence of Noncleavable Crosslinkers DSS (Disuccinimidyl Suberate) or DSG (Disuccinimidyl Gluterate) Followed by Denaturing IP as Described in Figure 5B

Crosslinkers were used at 800 $\mu\text{g/ml}$ for the negative controls and increasing concentrations were used (200 $\mu\text{g/ml}$ –800 $\mu\text{g/ml}$) in the strains expressing CPY*-HA. A crosslinker-specific high molecular weight species (indicated by arrow) can be detected by both α -HA and α -FLAG antibodies. In addition, a much larger aggregate that does not enter the main body of the gel becomes prominent as the crosslinker concentration is increased. Molecular weight markers (kDa) are shown on the left.

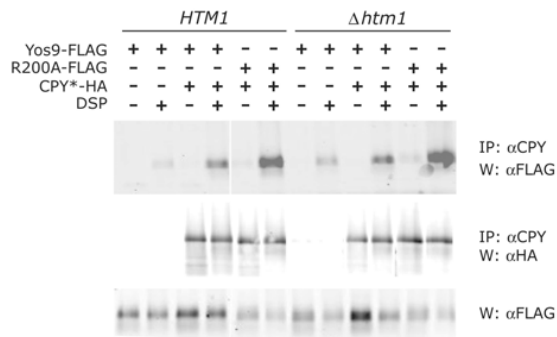


Figure S4. $\Delta hrd1\Delta yos9$ (*HTM1*) or $\Delta hrd1\Delta yos9\Delta htm1$ ($\Delta htm1$) Cells Expressing Either Yos9-FLAG or the MRH Mutant of Yos9, R200A-FLAG, with or without CPY*-HA Were Subjected to Crosslinking with the Cleavable Crosslinker DSP Followed by Denaturing IP as Described in Figure 5B.

Supplemental Experimental Procedures

Plasmid Construction

To facilitate construction of CPY* fusion proteins for retrotranslocation experiments a modular system was generated on a low copy CEN/ARS plasmid. Full-length *S. cerevisiae* CPY cDNA encoding wild type CPY (*PRC1*) along with its endogenous promoter (500bp upstream of start codon) and terminator (300bp downstream of stop codon) was cloned into *KpnI* and *EcoRI* sites of pRS316 (Sikorski and Hieter, 1989). Quikchange mutagenesis (Stratagene) was used to make an amino acid substitution G255R that transforms wild type CPY to the ERAD substrate CPY*. PCR based mutagenesis techniques were used to introduce an *SphI* restriction site immediately upstream of the start codon. *EagI* and *XhoI* sites were introduced immediately downstream of the CPY signal sequence and *HindIII* site was introduced immediately downstream of the stop codon. A triple HA epitope tag with a stop codon at the 3' end was obtained by PCR and cloned into the *HindIII* site to generate a C-terminally tagged CPY*. *SalI* and *NheI* restriction sites were introduced just upstream of the HA tag via the forward primer.

Constructs for directionality experiments were generated in the following manner: CPY*-HA was obtained by replacing the endogenous signal sequence flanked by *SphI* and *EagI* in the modular system with the *KAR2* (BIP) signal sequence (Craven et al., 1996). We replaced the endogenous post-translational CPY signal sequence with the co-translational *KAR2* signal sequence as it allowed for a greater fraction of the fusion proteins to enter the ER. The PCR fragment encoding the *KAR2* signal sequence was PCR amplified from yeast genomic DNA. *E. coli* DHFR was amplified by colony PCR

and cloned into *EagI-XhoI* sites of CPY*-HA to generate DHFR-CPY*-HA or into *Sall-NheI* sites to generate CPY*-DHFR-HA or into the *EagI-XhoI* and *Sall-NheI* sites to generate DHFR-CPY*-DHFR-HA. The CPY*-DHFR(Pro)-HA proline mutant was obtained by changing A29, W30 and F31 to prolines by fusion PCR.

An untagged Yos9p expression construct (pRS315-Yos9) was generated by amplifying *YOS9* along with its endogenous promoter (500bp upstream of start) and terminator (300bp downstream of stop) and cloning it into *XmaI-SacI* sites of the low copy CEN/ARS plasmid pRS315. Untagged R200A, E223D, Y229F *YOS9* lectin mutants were generated by fusion PCR using pRS315-Yos9 as a template. To construct the FLAG tagged *YOS9* (pRS425-Yos9-FLAG), the gene was subcloned into *XmaI-SacI* sites of the high copy 2 μ plasmid pRS425. Subsequently, *EagI* and *XhoI* sites were introduced upstream of the *YOS9* HDEL sequence by fusion PCR. Oligos encoding a triple FLAG tag were synthesized and cloned into *EagI-XhoI* sites. FLAG tagged mutants R200A-FLAG, E223D-FLAG, Y229F-FLAG were generated by cutting out *BglII-SpeI* fragments from the pRS425 Yos9-FLAG construct and replacing them with the corresponding fragments from the pRS315 mutant constructs.

Cycloheximide Chase Degradation Assay

For Figures 1B, C and D *Aprc1* strain was used and for Figure 4C *Δyos9::HIS3* strain was used. Yeast transformed with the indicated constructs were grown to mid-log phase in selective media. Cycloheximide (Sigma) was added to a final concentration of 100 μ g/ml – 200 μ g/ml (time 0) to terminate protein synthesis. Time points were taken by adding TCA to a final concentration of 10% to 0.6-0.8 OD₆₀₀ units of cells. TCA

precipitates were washed with 100% cold acetone twice, air dried for 20 min, and resuspended in 100µl of SDS boiling buffer. Cells were lysed by vortexing with glass beads at the maximum setting at 4°C. Lysates were cleared by centrifugation at 21,000g and boiled. 12µl of the samples were subjected to SDS-PAGE electrophoresis on 4-15% tris-glycine gels and analyzed by Western blotting with 12CA5 mouse α-HA antisera (1:1000, Roche) and goat α -mouse (1:3000, Bio-Rad) antibodies. Nitrocellulose blots were incubated in Super Signal West Femto Maximum Sensitivity Chemiluminescent Substrate (Pierce) and protein bands were visualized using chemiluminescence and a CCD camera (FluorChem 8800) and quantitated.

For Figures 1F and 2A, 1ml of cells were removed at each time point and the cycloheximide chase was terminated by flash-freezing cell pellets in liquid nitrogen. For Figure 4C chase was terminated at indicated times by the addition of 250µl of cold 5x YEP and 25µl of 1:1 mix of 1M NaF and NaN₃. Cells were immediately pelleted at 4°C and flash frozen in liquid nitrogen. Pelleted cells were thawed and lysed by the addition of hot SDS-PAGE sample buffer followed by boiling for 5 min. Bands were visualized using fluorescent secondary antibodies (Molecular Probes) and the LI-COR Odyssey system.

Protease Protection Assays

Microsomes for protease protection assays were prepared in the following manner. Cells containing CPY*-DHFR-HA were grown to mid-log in SD-Ura medium. Cycloheximide was added to 200µg/ml to 30 OD₆₀₀ units of mid-log cells and incubated at 30° for 90 min. NaN₃ was added to 10mM and cells were harvested. Cells were washed with water and

pretreated in 1ml of buffer containing 100mM Tris pH 9.4, 10mM DTT at room temperature (RT) for 5 min. Cells were pelleted and incubated in 1ml of spheroplasting buffer containing 10mM Tris pH7.5, 0.7M sorbitol, 100mM NaCl, 1mM DTT, 10mM NaN₃ and 100μl lyticase at 30⁰C for 30 min with occasional mixing. Spheroplasts were pelleted at 2500g for 3 min and subsequently washed gently in 1ml of buffer containing 50mM NaP pH 7, 0.7M sorbitol. Spheroplasts were resuspended in 0.5mls of cold lysis buffer containing 25mM NaP pH7, 0.2M sorbitol, 10mM NaCl, 1mM EDTA, and protease inhibitors and lysed by douncing. Lysate was cleared by centrifugation at 1000g for 10 min at 4⁰C twice. The supernatant was used to obtain a P13 fraction for protease protection assays.

Crosslinking Experiments

Yeast cells transformed with desired constructs were used to make ER-derived microsomes as described previously (Brodsky et al., 1993) with a few modifications. 600 OD₆₀₀ units of mid-log phase cells grown in selective media were harvested by centrifugation. Cells were washed in water and pretreated in 16ml of buffer containing 100mM Tris pH9.4, 10mM DTT at RT for 15 min. Cells were pelleted and resuspended in 8ml of lyticase buffer (50mM Tris pH7.8, 1M sorbitol, 5mM βMe). 2.5ml of lyticase was added to the resuspended cells and the cells were incubated at RT until 70% spheroplasting efficiency was achieved. Spheroplasting was checked by the drop in OD₆₀₀ units. Spheroplasts were pelleted for 4 min at 4⁰C and resuspended in cold 15ml of lysis buffer (25mM Hepes pH6.8, 10mM NaCl, 200mM sorbitol, 1mM MgCl₂, 1mM CaCl₂ and protease inhibitors). Resuspended spheroplasts were incubated in ice for about

15 min and lysed by douncing on ice. Lysates were cleared at 160g for 8 min at 4⁰C. Supernatants were subjected to two rounds of ultracentrifugation at 194,400g (27000rpm, Ti 70 rotor) for 24 min at 4⁰C. The final microsome pellets were resuspended in buffer 88 (20mM Hepes, 150mM KoAc, 250mM sorbitol and 5mM Mg(OAc)₂). 150μl aliquots of the microsomes were flash frozen in liquid nitrogen and stored at -80.

150μl of microsomes were used for each crosslinking reaction. Reactions were carried out with or without the reversible crosslinker, DSP (Dithiobis[succinimidylpropionate], Pierce), which was added to a final concentration of 800μg/ml, and incubated at RT for 30 min. For some experiments non-reversible crosslinkers, DSS (Disuccinimidyl suberate, Pierce) and DSG (Disuccinimidyl glutarate, Pierce) were at concentrations ranging from 200μg/ml-800μg/ml. Tris pH7.5 was added to a final concentration of 40mM to quench the crosslinker. Microsomes were centrifuged at 21,000g for 5 min at 4⁰C and resuspended in 100μl urea boiling buffer (50mM Tris pH7.5, 1mM EDTA, 1% SDS, 2M Urea). Microsomes were disrupted by vortexing at maximum setting with glass beads at 4⁰C. 900μl of Tween IP buffer (50 mM Tris pH7.5, 150mM NaCl, 0.5% Tween-20, 0.1mM EDTA) were added to each reaction and rabbit polyclonal α-CPY antisera made using full-length protein (1:100, Covance Research Products) was used for immunoprecipitating crosslinked species. Protein A/G beads (Santa Cruz) were used to capture immune complexes. The beads were boiled with SDS-PAGE sample buffer to release immune complexes which were then analyzed by SDS-PAGE electrophoresis and Western blotting. Western blots were probed with mouse α-HA 12CA5 antibodies or mouse α-FLAG (M2 Monoclonal antibody, Sigma) antibodies. Protein bands were visualized by using chemiluminescence and a CCD

camera (FluorChem 8800) or by using fluorescent secondary antibodies and the LI-COR Odyssey detection system.

CHAPTER 3

A Luminal Surveillance Complex that Selects Misfolded Glycoproteins for ER-Associated Degradation

A Luminal Surveillance Complex that Selects Misfolded Glycoproteins for ER-Associated Degradation

Vladimir Denic*, Erin M. Quan* and Jonathan S. Weissman

* These authors contributed equally to this work.

Howard Hughes Medical Institute, Department of Cellular and Molecular Pharmacology,
University of California-San Francisco and the California Institute of Quantitative
Biomedical Research, San Francisco, CA 94148, USA

Correspondence:

Jonathan S. Weissman

415-502-7642 (phone)

415-514-2073 (fax)

weissman@cmp.ucsf.edu

[Reprinted with permission from Cell, Vol. 126, Denic, V., Quan, E. M., Weissman J. S., A Luminal Surveillance Complex that Selects Misfolded Glycoproteins for ER-Associated Degradation, 349-359, Copyright (2006) with permission from Elsevier.]

Summary

How the ER-associated degradation (ERAD) machinery accurately identifies terminally misfolded proteins is poorly understood. For luminal ERAD substrates, this recognition depends on their folding and glycosylation status as well as on the conserved ER lectin Yos9p. Here we show that Yos9p is part of a stable complex that organizes key components of ERAD machinery on both sides of the ER membrane including the transmembrane ubiquitin ligase Hrd1p. We further demonstrate that Yos9p, together with Kar2p and Hrd3p, forms a luminal surveillance complex that both recruits non-native proteins to the core ERAD machinery and assists a distinct sugar-dependent step necessary to commit substrates for degradation. When Hrd1p is uncoupled from the Yos9p surveillance complex, degradation can occur independently of the requirement for glycosylation. Thus, Yos9p/Kar2p/Hrd3p acts as a gatekeeper, ensuring correct identification of terminally misfolded proteins by recruiting misfolded forms to the ERAD machinery, contributing to the interrogation of substrate sugar status, and preventing glycosylation-independent degradation.

Introduction

Proteins that traverse the secretory pathway fold in the endoplasmic reticulum (ER). This process is assisted by ER-resident chaperones, addition of N-linked glycans, and formation of disulfide bonds (Helenius and Aebi, 2001). The high flux of proteins into the ER together with the complicated multi-domain nature of many secreted proteins inevitably results in some fraction of proteins becoming terminally misfolded (Casagrande et al., 2000; Friedlander et al., 2000; Jensen et al., 1995; Travers et al., 2000; Ward et al., 1995). To protect cells from the deleterious effects of such forms, the ER employs a series of mechanisms collectively referred to as ER-associated degradation (ERAD) to bring about their efficient disposal (Romisch, 2005). In most instances, substrates are first specifically identified and then targeted for ubiquitination in preparation for their destruction in the cytosol by the proteasome (Meusser et al., 2005; Nishikawa et al., 2005; Romisch, 2005; Sayeed and Ng, 2005; Tsai et al., 2002). Depending on the position of the misfolded lesion, the recognition step can occur either on the luminal side (ERAD-L), the cytosolic side (ERAD-C), or in the context of the ER membrane itself (ERAD-M) (Bonifacino et al., 1990; Taxis et al., 2003; Vashist and Ng, 2004). For luminal targets, Kar2p (the major ER-localized Hsp70), has been shown to keep substrates in an ERAD-competent soluble state (Kabani et al., 2003; Nishikawa et al., 2001b) and additionally participates in a second less well-defined step of bringing them to the retrotranslocation machinery (Kabani et al., 2000), which then delivers substrates across the membrane to the cytosolically-located catalytic sites of the ubiquitin conjugation machinery. Following ubiquitination by membrane-associated ubiquitin

ligases (e.g., Hrd1p and Doa10p in yeast)(Bays et al., 2001; Deak and Wolf, 2001; Swanson et al., 2001), substrates are typically extracted from the membrane by the Ubx2p-recruited Cdc48p-Npl4p-Ufd1p AAA ATPase (Jarosch et al., 2002; Neuber et al., 2005; Schubert and Buchberger, 2005; Ye et al., 2001), which together with other ubiquitin-binding proteins escorts substrates to the proteasome (Richly et al., 2005).

Our understanding of the more downstream events in ERAD is becoming increasingly sophisticated. By comparison, detailed information is lacking on how proteins are initially selected for degradation and subsequently delivered to the ubiquitination/extraction machinery. The significance of understanding how the ER scans through the abundance of folding intermediates for terminally misfolded proteins is well illustrated by a recent study showing that the most dangerous variants of an amyloidogenic protein are those whose mutations are not so destabilizing as to trigger detection by the ERAD system (Sekijima et al., 2005). The complexity of the recognition problem is further underscored by the risk of over-vigilance, which can lead to the degradation of imperfect but potentially functional proteins, as appears to be the case for the CFTR chloride channel (Drumm et al., 1991).

Degradation of ERAD-L substrates depends not just on substrate misfolding but also on the presence of substrate sugars (Kostova and Wolf, 2005; Spear and Ng, 2005). The molecular basis of this dual requirement and how this information is communicated to the downstream ERAD machinery is unclear. Htm1p, a putative ER lectin required for ERAD-L, may contribute to sugar recognition (Jakob et al., 2001; Nakatsukasa et al., 2001). More recently, Yos9p has been identified as a conserved ER lectin with a critical role in the recognition of luminal misfolded glycoproteins (Bhamidipati et al., 2005;

Buschhorn et al., 2004; Kim et al., 2005; Szathmary et al., 2005). Furthermore, it was shown that Yos9p can associate with the prototypical ERAD-L substrate CPY* even when its sugar-binding site (critical for its ERAD function) is mutated and the substrate is deglycosylated (Bhamidipati et al., 2005). This suggests that Yos9p lies at the core of a poorly defined bipartite recognition machinery that specifically targets for retrotranslocation only those proteins that are simultaneously misfolded and have the correct sugars.

Following recognition, ERAD-L substrates are delivered to the cytosol, where they undergo ubiquitination by Hrd1p (Bays et al., 2001; Deak and Wolf, 2001). This membrane-bound ubiquitin ligase is associated stoichiometrically with another key component of ERAD-L, Hrd3p, whose presence is required to prevent Hrd1p from undergoing self-destruction (Gardner et al., 2000; Plemper et al., 1999). The highly conserved, large (~80 kDa) nature of the Hrd3p luminal region suggests that it may play an additional role in early ERAD-L events. Counteracting this view, however, is the finding that simply restoring Hrd1p levels by over-expression suppresses the substrate degradation defect associated with the loss of Hrd3p (Gardner et al., 2000; Plemper et al., 1999).

In the present study we investigate the molecular mechanism by which ERAD-L substrates are recognized and targeted for destruction. Specifically, we demonstrate that Yos9p, Hrd3p, and Kar2p, form a luminal surveillance complex that recognizes misfolded substrates independent of their glycosylation status and brings them to the downstream ubiquitination/extraction machinery. Degradation, however, requires a distinct commitment step that is dependent on substrate sugars and Yos9p's sugar-

binding site. Finally, we show that in addition to its positive role in enhancing recruitment of bona fide ERAD-L substrates, the surveillance complex also helps eliminate basal, indiscriminate degradation which otherwise leads to cellular toxicity.

Results

Yos9p forms a stable complex with the transmembrane and cytosolic ERAD machinery

Previous studies have shown that Yos9p associates with the misfolded, luminal ERAD substrate, CPY* (Bhamidipati et al., 2005; Kim et al., 2005; Szathmary et al., 2005). This recognition event is likely to occur in the context of a multiprotein assembly as Yos9p is membrane-associated but does not itself contain a transmembrane domain (Friedmann et al., 2002; Kim et al., 2005). Furthermore, crosslinking experiments suggested that substrate-associated Yos9p was part of a discrete high molecular weight complex (Bhamidipati et al., 2005). To gain insight into the composition of this complex, we used an affinity purification approach, taking advantage of a yeast strain expressing a functional 3xFLAG epitope-tagged version of Yos9p expressed from its endogenous locus (Supplementary Figure S1). Specifically bound proteins were isolated from detergent-solubilized microsomes and subjected to SDS-PAGE and Coomassie Blue staining, thus identifying several abundantly-associated polypeptides. Mass spectrometry (Supplementary Figure S2) indicated that the Yos9p-specific bands consisted of the following proteins: Cdc48p, Hrd3p, Kar2p, Yos9p/Ubx2p (co-migrating), Hrd1p, and Emp47p (Figure 1A). Additionally, this complex contained Usa1p, a new ERAD component identified and characterized in the accompanying paper (Carvalho et al., 2006). Strikingly, with the exception of Emp47p (the significance of whose association with Yos9p will be addressed elsewhere), all the Yos9p-associated proteins are known to be required for Yos9p-dependent ER-associated degradation and include luminal (Kar2p),

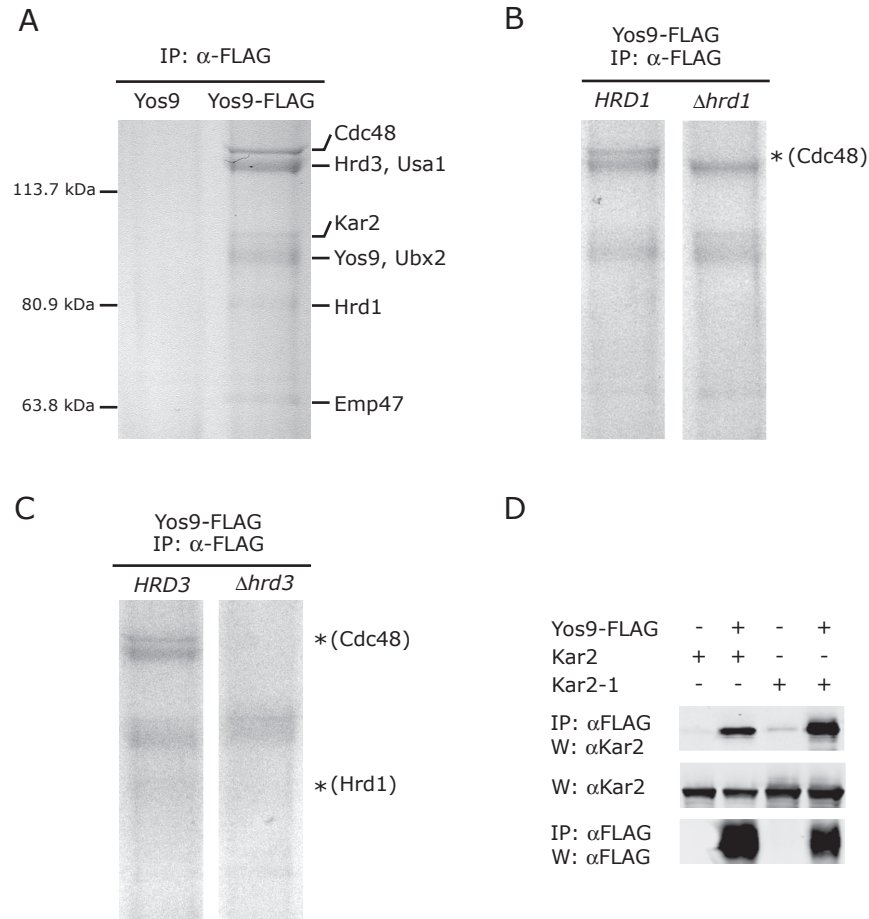


Figure 1. Yos9p associates with the core ERAD machinery at the ER membrane

Microsomes were prepared from late mid-log phase cells expressing genomic copies of either untagged Yos9p (A) or Yos9-FLAG (A-C) in wild type, Δ hrd1 or Δ hrd3 strain backgrounds as shown. The microsomes were solubilized with Triton X-100 and affinity purified using anti-FLAG beads. Immunoprecipitates were eluted with 3xFLAG peptide and resolved by SDS-PAGE followed by Coomassie blue staining. The identity of bands in (A) was determined by mass spectrometry. * denotes the position of missing bands. Molecular weights are labeled according to a prestained protein ladder.

(D) As indicated, wild type or *kar2-1* cells were transformed with empty vector or pRS425 expressing Yos9-FLAG. Prior to harvesting, cells were shifted to the nonpermissive *kar2-1* temperature (37°C) for 1 hour. Subsequently, total cell lysates were solubilized with 1% Triton X-100, cleared, and immunoprecipitated with anti-FLAG resin. Bound proteins were eluted by boiling in SDS loading buffer and along with total cell lysates were resolved by SDS-PAGE followed by Western blot analysis with the indicated antibodies.

transmembrane (Hrd1p, Hrd3p, Ubx2p, Usa1p) and fully cytosolic (Cdc48p) ERAD components (Romisch, 2005). Thus, Yos9p is part of a stable complex that organizes a series of key components of ERAD machinery on both sides of the ER membrane.

We performed further experiments to address two specific issues regarding the integrity of the complex. First, two membrane proteins critical for ERAD-L, Der1p and Htm1p, (Jakob et al., 2001; Knop et al., 1996a; Nakatsukasa et al., 2001) were not identified in our affinity purification. To exclude the possibility that these were integral components of this membrane complex whose presence was obscured for technical reasons, we repeated the purification using strains deleted for *der1* or *htm1*. These deletions had no apparent effect on the molecular composition of the Yos9p complex (Figure 2A and 2B). Second, we wished to explore the role of Yos9p's sugar-binding pocket in complex assembly. This was motivated by our previous finding that point mutations specifically ablating this region strongly eliminated Yos9p's ability to support ERAD-L but did not interfere with substrate interaction (Bhamidipati et al., 2005). We therefore repeated the purification with a sugar-binding mutant (R200A) but detected no changes in the composition of the complex with the apparent exception of a slight decrease in Coomassie staining of the Yos9p/Ubx2p region (Figure 2C). However, we demonstrated that the Yos9p/Ubx2p association was not affected by directly monitoring levels of coimmunoprecipitated Ubx2p using Western blotting (Figure 2D). These data suggest that sugar recognition by Yos9p acts at a step downstream of substrate binding and complex assembly.

Yos9p/Kar2p/Hrd3p form a luminal subcomplex

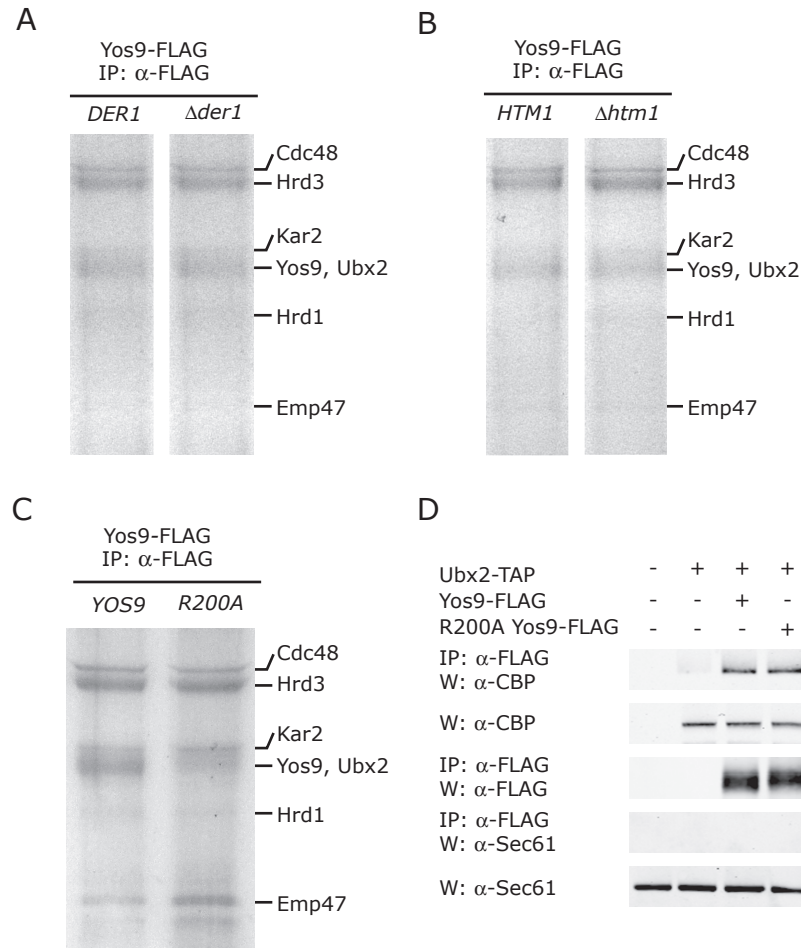


Figure 2. The integrity of the Yos9p-core ERAD machinery complex is not dependent on Der1p, Htm1p or Yos9p's sugar binding pocket

Microsomes were made from wild type, *Δder1*, or *Δhtm1* log phase cells expressing genomic Yos9-FLAG (A-B), or Yos9-FLAG and R200AYos9-FLAG from a plasmid (C) as indicated. Microsomes were solubilized and Yos9p was immunoprecipitated as described in Figure 1A. Note: Usa1p comigrates with Hrd3p. We did not explicitly test for the presence of Usa1p in the various deletion strains.

(D) Wild type or UBX2-TAP::HISM6 cells were transformed with either an empty vector, pRS425-Yos9-FLAG or pRS425-R200AYos9-FLAG as indicated and subjected to immunoprecipitation as described in Figure 1D. Anti-CBP was used to visualize the TAP fusion protein while anti-Sec61p served as a negative control.

Since Yos9p is a strictly luminal protein, we wished to determine the contribution of other members in the complex to Yos9p's ability to associate with Cdc48p on the cytosolic side. The multi-pass transmembrane protein Hrd1p was a good candidate for allowing communication between the complex components on opposing sides of the membrane (Deak and Wolf, 2001; Gardner et al., 2000). Indeed, when we repeated the purification procedure using a *hrd1* deletion strain, we observed a complete loss of Yos9p-associated Cdc48p (Figure 1B). In contrast, Hrd3p association remained unaffected. Together with IP-Western data confirming the presence of Hrd1p in the Yos9p immunoprecipitations (Supplementary Figure S3), this finding demonstrated that despite its faint appearance by Coomassie staining, Hrd1p is nonetheless absolutely required for Cdc48p's ability to associate in a complex with Yos9p.

The fact that Hrd3p has a large (~80 kD) luminal domain and exists in a 1:1 complex with the Hrd1p ubiquitin ligase (Gardner et al., 2000) suggests that Hrd3p might be responsible for anchoring Yos9p to Hrd1p/Cdc48p. In accordance with this idea, we observed a total absence of Cdc48p when we purified Yos9p from a Δ *hrd3* strain (Figure 1C). Given that Kar2p and Yos9p closely migrate by SDS-PAGE, we confirmed by Western blotting that the Kar2p/Yos9p interaction is independent of the presence of Hrd3p (Supplementary Figure S4) and Cdc48p (Figure 1C). Additionally, we demonstrated that the Kar2p-Yos9p interaction is still observed even when endogenous *KAR2* has been replaced by the *kar2-1* peptide-binding mutant (Figure 1D)(Kabani et al., 2003). This suggests that Kar2p's association with Yos9p is not solely mediated through Kar2p's ability to interact with unfolded proteins.

We further explored the Yos9p-Hrd3p interaction using truncations of Hrd3p. Hrd3p comprises a luminal region, consisting of domains A (residues 1-390) and B (residues 390-767), that is attached to a transmembrane anchor and a cytosolic tail (residues 767-833) (Gardner et al., 2000) Figure 3A). To investigate which of these regions was responsible for the observed interaction with Yos9p, we generated strains expressing from the endogenous locus, C-terminally tagged variants of Hrd3p and tested their ability to co-immunoprecipitate Yos9p. As shown in Figure 3B, both full-length and A-B (1-767) Hrd3p (but not the A domain alone) were able to pull down Yos9p indicating that the B domain is required for Yos9p binding while the transmembrane anchor and the cytosolic tail are dispensable. We further find that strong over-expression of either Yos9p or Hrd3p alone results in only a minor enhancement in the amount of Hrd3p pulled down with Yos9p (Figure 3C). However, concomitant over-expression of both proteins resulted in a synergistic ~20 fold increase in Yos9p/Hrd3p complex formation (Figure 3C). Moreover, this interaction persisted even following deglycosylation of both proteins by EndoH (Supplementary Figure S5). Thus the observed Yos9p interaction with Hrd3p is sugar-independent and unlikely to be bridged by other dedicated ERAD components.

Collectively, these findings lead us to propose the following model for the molecular organization of the complex (Figure 3D). Yos9p, Kar2p, and the luminal domain of Hrd3p form a complex, which is anchored to the transmembrane Hrd1p ubiquitin ligase (Gardner et al., 2000). In turn, Hrd1p, in a manner that depends on its ligase activity, recruits Ubx2p-tethered Cdc48p (Gauss et al., 2006b; Neuber et al., 2005; Schuberth and Buchberger, 2005), a cytosolic protein shown to be required for the

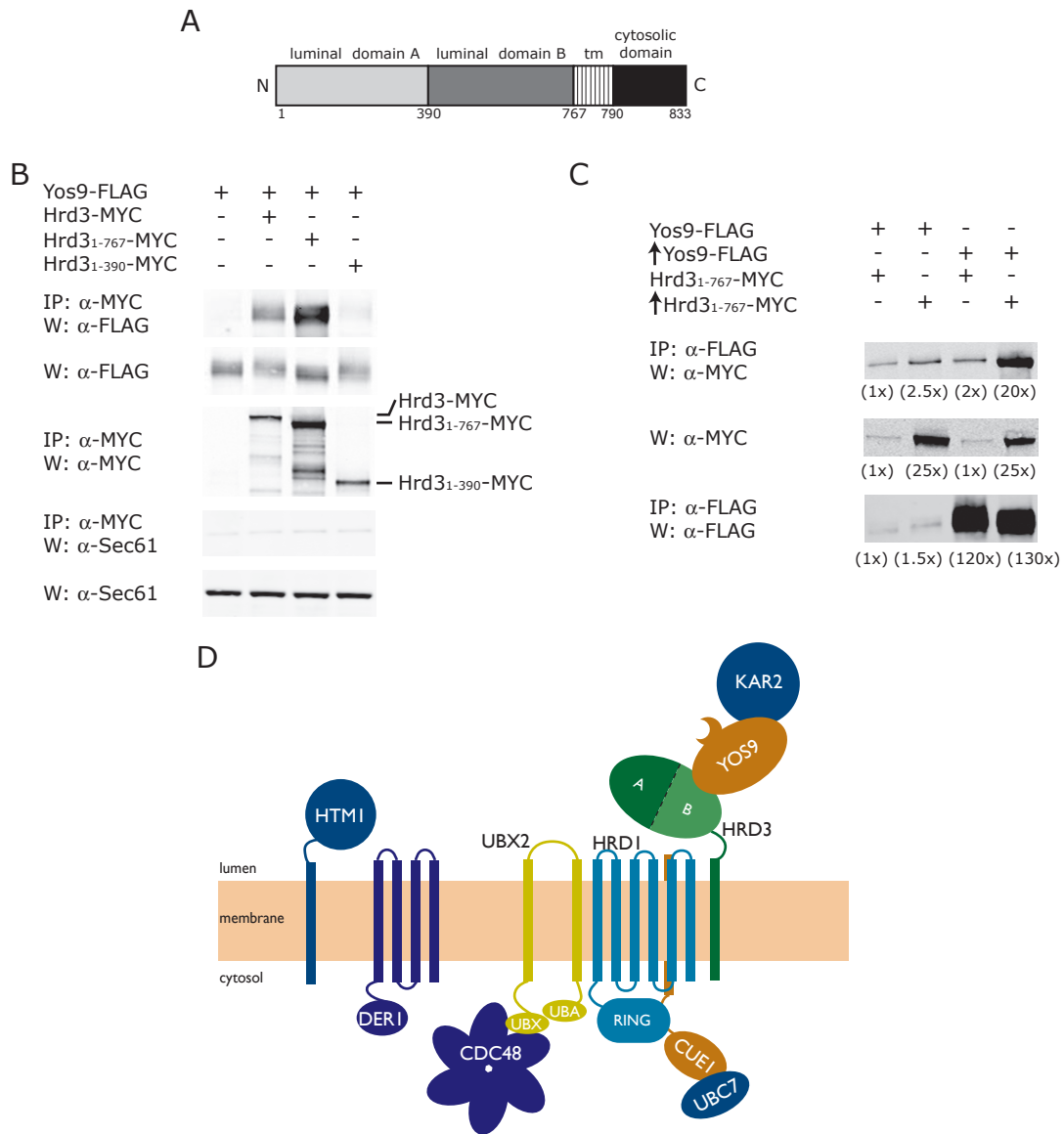


Figure 3. Dissection of the Hrd3p/Yos9p interaction by domain mapping/over-expression and a model of how Yos9p interacts with other members of the ERAD machinery

(A) Schematic of Hrd3p. Domain boundaries are demarcated with their amino acid position in the Hrd3p sequence. Tm denotes the transmembrane domain.

(B) A 13MYC tag was inserted at the *HRD3* locus following amino acids 390, 767 or 833 in a strain expressing Yos9 genomic FLAG. The cells were immunoprecipitated with anti-MYC as described in Figure 1D.

(C) Strains expressing endogenous or over-expressed (symbolized with \uparrow indicating *TDH3* promoter driven expression) tagged versions of Yos9p and Hrd3₁₋₇₆₇p were mated as shown, and subjected to immunoprecipitation as described in Figure 1D. The numbers in parentheses indicate the levels of each protein relative to the control strain expressing endogenous levels of both proteins.

(D) Proposed model of how Yos9p associates with other ERAD components in the ER membrane and cytosol. Hrd1p anchors at least a portion of the Yos9p/Kar2p/Hrd3p surveillance complex to the ER membrane and interacts with Ubx2p which recruits Cdc48p to the membrane complex (the dependence of Cdc48p recruitment on Hrd1p's ubiquitin ligase activity is not depicted in the figure). Der1p and Htm1p may associate but are not important for the integrity of the complex. Ubc7p and its membrane anchor Cue1p are necessary for the ubiquitination of substrates by Hrd1p. Usa1p not pictured.

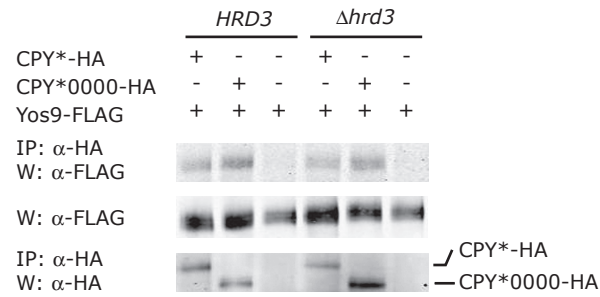
extraction of substrates from the ER membrane (Jarosch et al., 2002; Ye et al., 2001). The transmembrane proteins Der1p and Htm1p are central players in ERAD, but our results establish that they are not required for the integrity of the Yos9p complex described here.

Yos9p and Hrd3p can recruit misfolded proteins independently of each other

We next wanted to explore how ERAD-L substrates are recruited to the Hrd1p ubiquitin ligase complex. First we tested whether the Yos9p-substrate interaction is dependent on Hrd3p. As previously reported, Yos9p co-immunoprecipitated with the prototypical ERAD-L substrate CPY*, and this interaction did not depend on substrate sugars, either alone or in combination with the R200A Yos9p lectin mutant (Figure 4A and 4B) but was specific for the misfolded form (Bhamidipati et al., 2005; Kim et al., 2005; Szathmary et al., 2005) Supplementary Figure S6). Importantly, these interactions persisted even in strains lacking *HRD3*, suggesting that they were being mediated directly by Yos9p and/or Kar2p.

To investigate the simple model that Hrd3p is acting as a passive scaffold for bridging the Yos9p/Kar2p/substrate complex with the downstream ERAD machinery, we asked whether Yos9p was required for the ability of substrate to be co-immunoprecipitated with Hrd3p (Gardner et al., 2001; Gauss et al., 2006b). We initially found that various N- or C- terminally tagged versions of full-length Hrd3p either gave very weak Western signals or were non-functional (data not shown). However, as demonstrated in the case of HMG-CoA Reductase 2 degradation (Gardner et al., 2000), Hrd3₁₋₇₆₇-MYC efficiently supported CPY* degradation when tagged at the C-terminus

A



B

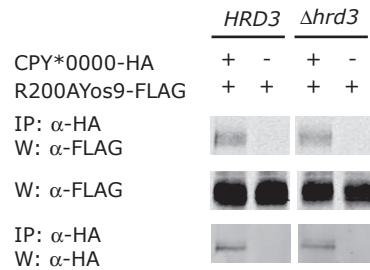


Figure 4. Yos9p interacts with CPY* and CPY*0000 in a HRD3-independent manner

(A) *Δyos9Δder1HRD3* or *Δyos9Δder1Δhrd3* cells were transformed with pRS425-Yos9-FLAG, together with an empty vector, or one expressing CPY* or CPY*0000 as indicated. Following spheroplasting and lysis by bead beating, crude membranes were solubilized with 1% Triton-X100 and subjected to immunoprecipitation with anti-HA essentially as described in Figure 1D.

(B) *Δyos9Δder1HRD3* or *Δyos9Δder1Δhrd3* cells were transformed with pRS425-R200AYos9-FLAG together with an empty vector or a vector expressing CPY*0000, as indicated. Spheroplasting and immunoprecipitation were performed as described in Figure 4A.

(Supplementary Figure S7) and robustly interacted with Yos9p (Figure 3B, 3C). As expected, based on its association with Yos9p, Hrd3p was able to interact with both CPY* as well as with an unglycosylated variant of CPY* (CPY*0000) which is not subject to ERAD-L (Figure 5A) (Kostova and Wolf, 2005; Spear and Ng, 2005). Surprisingly, we still observed co-immunoprecipitation of Hrd3p with CPY* and CPY*0000 in a strain deleted for *YOS9* (Figure 5A). This interaction is likely to be direct because it was observed even in the absence of Der1p, Htm1p, and Hrd1p (which is responsible for anchoring the Hrd3p luminal domain) (Figure 5A, 5B). Furthermore, we observed that over-expression of Hrd3p leads to a proportional increase in the amount of Hrd3p-CPY* complex recovered by immunoprecipitation (Figure 5C). Several lines of evidence argue for the validity and specificity of this interaction. First, the observed association between Hrd3p and substrate is unlikely to be an artifact of inadequate membrane disruption as we solubilized lysates using a large excess of Triton X-100, a strong non-ionic detergent and we observed no interaction with the abundant ER membrane protein Sec61p (Figure 5A, 5B). Second, this interaction is not due to the formation of a large substrate aggregate that non-specifically incorporates other proteins, because it remains in the supernatant even after clearing the solubilized lysates at 100,000xg for 45min. Finally, the interaction is highly specific for the misfolded form of carboxypeptidase Y, since we could vastly increase the amount of native CPY in the ER by deleting the gene for its ER export receptor, Erv29p (Belden and Barlowe, 2001), without observing a significant interaction with Hrd3p (Figure 5D). We therefore conclude that Yos9p/Kar2p and Hrd3p independently recognize misfolded ER luminal proteins.

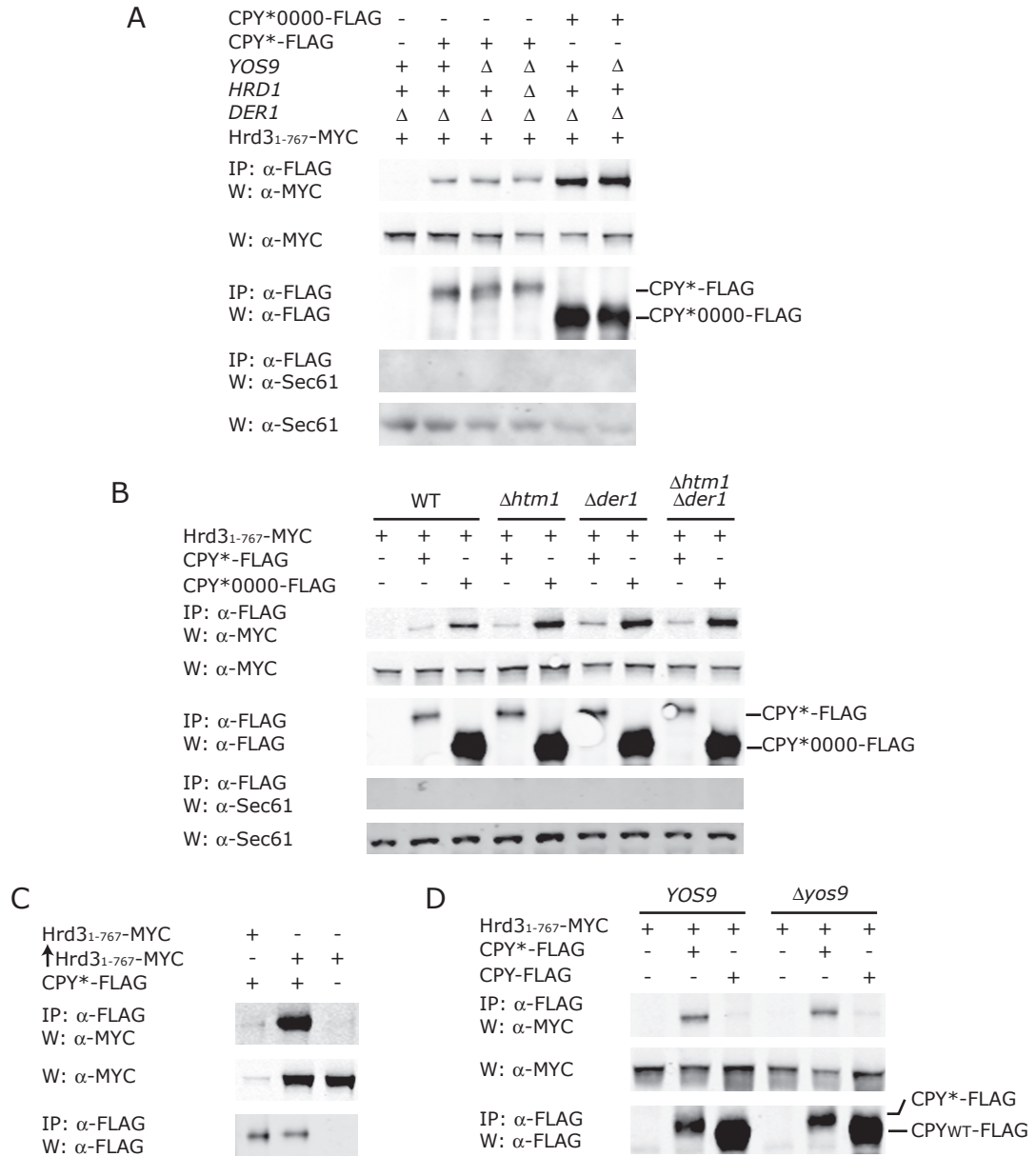


Figure 5. Hrd3p interacts specifically with CPY* and CPY*0000 but not wild type CPY in a YOS9-independent manner

(A) *Δder1YOS9HRD1*, *Δder1Δyos9HRD1*, or *Δder1Δyos9Δhrd1* cells expressing Hrd3₁₋₇₆₇-MYC were transformed with an empty vector or a vector expressing CPY* or CPY*0000, as indicated, and subjected to immunoprecipitation as in Figure 1D.

(B) The indicated strains expressing Hrd3₁₋₇₆₇-MYC were transformed with an empty vector or a vector expressing CPY* or CPY*0000 as shown and subjected to immunoprecipitation as in Figure 1D.

(C) Strains expressing endogenous or over-expressing tagged versions of Hrd3₁₋₇₆₇-MYC were transformed with empty vector or a vector expressing CPY* and subjected to immunoprecipitation as in Figure 1D. Upward arrow indicates TDH3 promoter driven expression.

(D) *Δder1Δerv29YOS9* or *Δder1Δerv29Δyos9* cells expressing Hrd3₁₋₇₆₇-MYC were transformed with an empty vector or a vector expressing CPY* or wild type CPY, as indicated, and subjected to immunoprecipitation as described in Figure 1D.

Substrate engagement with the multi-protein Hrd1p ligase complex is sugar-independent

The observation that the Yos9p lectin mutant (R200A) interacted with both substrates (Figure 4) and downstream ERAD components (Figure 2D) suggests that recognition and commitment to degradation are mechanistically separable events. To test this idea further, we made use of a recently identified ERAD-L component (Carvalho et al., 2006) Usa1p. As expected based on Usa1p's association with Yos9p and Hrd3p (Carvalho et al., 2006), we show that Usa1p can be co-immunoprecipitated with CPY* in a Hrd3p-dependent manner (Figure 6). Notably, despite the fact that CPY*0000 cannot be degraded by the ERAD-L system, it nonetheless is part of a multiprotein complex including Usa1p (Figure 6, Supplementary Figure S8). These data suggest that substrate recruitment to the ERAD core machinery can be mechanistically distinguished from a subsequent commitment to degradation. It is this commitment step in the ERAD process which confers dependence on substrate glycosylation and Yos9p's sugar-binding site.

Hrd1p gating by Yos9p/Hrd3p prevents promiscuous degradation

Our finding that Hrd3p plays a key role in bringing Yos9p to the ubiquitin degradation machinery and independently recognizing substrates seems at odds with previously published reports indicating that the strong substrate degradation defect in a $\Delta hrd3$ mutant is bypassed by over-expression of Hrd1p (Gardner et al., 2000; Plemper et al., 1999). To explore this apparent discrepancy, we first recapitulated the phenomenon by placing Hrd1p under the control of a strong (*TDH3*) promoter (Gardner et al., 2000) and

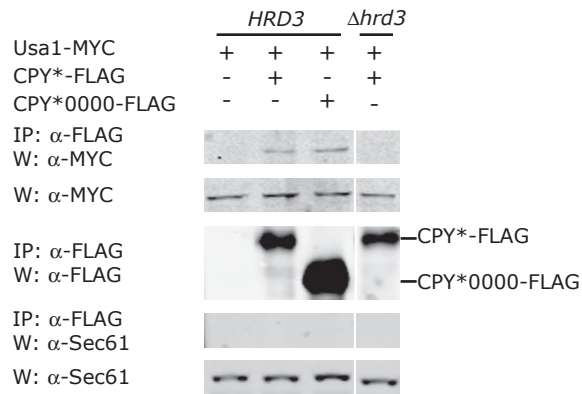


Figure 6. Sugar-independent association of misfolded carboxypeptidase Y with Usa1p

Wild type or Δ *hrd3* cells expressing C-terminally tagged Usa1-MYC were transformed with an empty vector or a vector expressing CPY* or CPY*0000, as indicated, and subjected to immunoprecipitated as in Figure 1D.

confirmed that CPY* stabilization in a *hrd3* delete is in fact partially alleviated by over-expression of Hrd1p (Figure 7A). Next, we examined the contribution of Yos9p to substrate recognition in the context of Hrd1p over-expression and found that deleting *YOS9* had no effect on Hrd1p's ability to stimulate CPY* degradation (Figure 7A). This is in marked contrast to the strong CPY* stabilizing effect of deleting *YOS9* in strains with regulated Hrd1p function (Bhamidipati et al., 2005; Buschhorn et al., 2004; Kim et al., 2005; Szathmary et al., 2005) Supplementary Figure S1). In light of the above suggestion that the sugar-binding site of Yos9p acts at a commitment step that is downstream of substrate recruitment to the complex, we wanted to reinvestigate the requirement for glycosylation in this Hrd1p over-expression bypass regime. We first confirmed that the removal of substrate sugars leads to a dramatic stabilization of CPY*, comparable to that observed when *HRD3* or *YOS9* are deleted. Strikingly, under conditions of Hrd1p over-expression in a *hrd3* deletion mutant, we saw significant degradation of CPY*0000, such that its degradation was now similar to that of CPY* (Figure 7B). This promiscuous destruction of an otherwise stable protein could account for our observation that over-expression of Hrd1p causes S288C yeast strains to grow at a reduced rate (Figure 7C). In order to confirm that this effect was indeed due to deregulated ubiquitin ligase activity, we deleted *CUE1*, the ER membrane anchor for the Ubc7p E2 enzyme (Biederer et al., 1997), and observed suppression of both the promiscuous degradation (Figure 7D and Supplementary Figure S9) and the growth phenotype (Figure 7C). Taken together, these data suggest that uncensored Hrd1p activity caused by the disruption of the Hrd3p/Yos9p gating mechanism results in the destruction

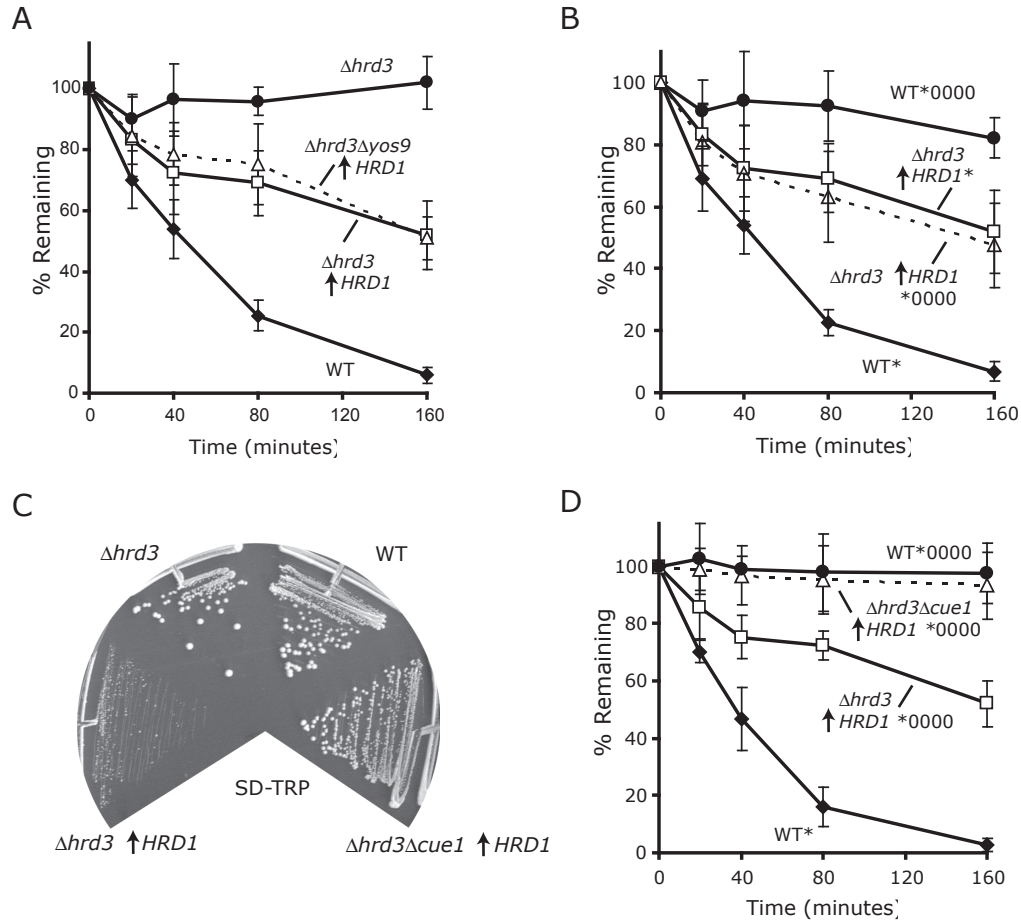


Figure 7. Over-expression of Hrd1p in a $\Delta hrd3$ background results in increased degradation of CPY* and CPY*0000 in a YOS9-independent manner

(A) Degradation of CPY* in (♦) wild type (WT), (□) $\Delta hrd3 \uparrow HRD1$ (upward arrow indicates *TDH3* promoter driven expression), (Δ) $\Delta hrd3 \Delta yos9 \uparrow HRD1$, and (●) $\Delta hrd3$ backgrounds was monitored by the cycloheximide chase degradation assay. Equal amounts of cells were removed at the indicated timepoints following addition of cycloheximide and subjected to SDS-PAGE followed by Western blotting with anti-HA and anti-hexokinase antibodies. Each timepoint represents the average and standard deviation of 4 measurements (2 independent experiments done in duplicate) normalized to a loading control.

(B) Degradation of CPY* in (♦) wild type (WT), (□) $\Delta hrd3 \uparrow HRD1$ (upward arrow indicates *TDH3* promoter driven expression) cells, or CPY*0000 in (●) wild type, (Δ) $\Delta hrd3 \uparrow HRD1$ was monitored as in Figure 7A.

(C) *Acue1* and $\Delta hrd3 \uparrow HRD1$ were crossed and sporulated. Wild type (WT), $\Delta hrd3$, $\Delta hrd3 \uparrow HRD1$ (upward arrow indicates *TDH3* promoter driven expression), and *Acue1* $\Delta hrd3 \uparrow HRD1$ cells were grown on minimal media lacking tryptophan.

(D) Degradation of CPY* in (♦) wild type (WT), or CPY*0000 in (●) wild type, (□) $\Delta hrd3 \uparrow HRD1$ (upward arrow indicates *TDH3* promoter driven expression) cells, or (Δ) *Acue1* $\Delta hrd3 \uparrow HRD1$ was monitored as in Figure 7A.

of proteins normally spared by the rules and restrictions of ERAD-L recognition, thus leading to impaired cellular viability.

Discussion

The ER must specifically identify terminally misfolded proteins in an environment dominated by structurally similar on-pathway folding intermediates. Compounding the complexity of this substrate selection problem is the fact that surveillance has to be enforced on three topological fronts (luminal, membrane, and cytosolic). Accordingly, the ER-associated degradation system comprises multiple converging pathways (Romisch, 2005; Sayeed and Ng, 2005). At the top of this arborized organization is a multiplicity of recognition factors in charge of initiating substrates down increasingly narrow paths that culminate in their degradation by the cytosolic proteasome machinery. While there have been substantial advances in understanding how in mammalian cells viruses target for destruction specific folded endogenous proteins such as class I MHC heavy chains (Lilley and Ploegh, 2004; Lilley and Ploegh, 2005; Ye et al., 2005; Ye et al., 2004), it remains poorly understood how recognition of terminally misfolded proteins is accomplished and coupled to shared downstream ERAD components.

In the present study we address this substrate selectivity issue for ERAD-L, a major conserved pathway responsible for the degradation of luminal misfolded glycoproteins (Vashist and Ng, 2004). In order to focus on a single, coherent branch of the ERAD system, we started with a top-down approach centered on Yos9p, a luminal lectin thought to act early in the pathway. This led to the identification of a Yos9p/Kar2p/Hrd3p surveillance complex that brings ERAD-L substrates into contact with the downstream Hrd1p ubiquitin ligase and the accompanying Ubx2p-recruited Cdc48p. Remarkably, both Yos9p/Kar2p and Hrd3p can individually recognize the

prototypical ERAD-L substrate CPY* in a manner that depends on the folding status but not the glycosylation state of the substrate. The above recruitment step tethers putative substrates to the ubiquitination/extraction machinery on the other side of the membrane by way of the Hrd3p/Hrd1p interaction. Substrate degradation requires a distinct commitment step which is dependent on both the substrate sugars and an intact Yos9p sugar-binding site. The mechanism by which this commitment step allows substrates to proceed down the ERAD-L pathway remains unclear. One intriguing possibility is that Yos9p, possibly together with Htm1p, queries the sugar status of the substrate and, for glycoproteins judged to be legitimate ERAD substrates, allows for the participation of Der1p in the subsequent retrotranslocation step. Interestingly, recent studies suggest physical interaction between glycosylated ERAD substrates and Der1p/Derlin (Gauss et al., 2006b; Oda et al., 2006) arguing for the possible existence of distinct substrate recognition events that are not mediated by the Yos9p/Hrd3p recruitment complex. It remains to be established how this multiplicity of recognition events are coordinated to bring about the substrate commitment to degradation.

Why has such a baroque mechanism evolved for selection of ERAD substrates? While the exact structural and kinetic features of misfolded proteins that lead to their recognition by the ERAD machinery are not well delineated, it now appears that recognition does not simply involve assessment of a protein's thermodynamic stability (Sekijima et al., 2005). The cooperation of two interacting complexes (Hrd3p and Yos9p/Kar2p), each of which are individually capable of binding misfolded forms, could allow for a more sophisticated probing of the biophysical properties of non-native proteins. For example, dual binding would be expected to favor recognition of substrates

with extended or multiple non-native epitopes. On a more speculative note, the use of a two step process (i.e., recruitment and commitment) could allow for enhanced specificity by a kinetic proofreading mechanism especially if the two steps are separated by an irreversible process (Hopfield, 1974) such as, for example, sugar trimming (Hirao et al., 2006b) or ATP hydrolysis by Kar2p. Additionally, there may be proofreading steps upstream and/or downstream of the Yos9p/Hrd3p recruitment process studied here.

More concretely, we demonstrate that the Yos9p/Kar2p/Hrd3p surveillance complex promotes specificity by acting as a gatekeeper of the Hrd1p ubiquitin ligase, ensuring that only legitimate substrates are degraded. It acts to enhance the delivery and degradation of bona fide ERAD-L substrates, while on the other hand repressing indiscriminate degradation of ER proteins. The significance of suppressing the basal degradation activity is illustrated by the slow growth phenotype that results when upstream recognition is bypassed in a *hrd3* deletion mutant over-expressing Hrd1p. Such deleterious effects are elegantly avoided in wild type cells by the fact that Hrd1p has a built in auto-destruction mechanism when it is not complexed with Hrd3p (Gardner et al., 2000; Plemper et al., 1999). This reduced specificity for retrotranslocation caused by Hrd1p over-expression is reminiscent of bacterial translocon mutants that are able to promiscuously export polypeptides in a signal sequence-independent manner (Flower et al., 1994).

More practically, manipulating the specificity of the ERAD system could yield an attractive therapeutic strategy (e.g. for supporting degradation of a mutant allele). However, such efforts are hampered by the broad protective role of the ERAD systems and the fact that many ERAD components are shared with other biological processes

(Adams, 2002). Because the ERAD-L surveillance complex is dedicated to channeling only a subset of ERAD substrates for degradation, a better understanding of this targeting step may aid in the development of future pharmacological approaches with enhanced selectivity for specific disease processes.

Experimental Procedures

Plasmid and Strain Construction

See Supplemental Experimental Procedures.

Antibodies

Sec61p and Kar2p antisera were a gift from Randy Schekman (University of California, Berkeley) and Peter Walter (University of California, San Francisco). HA epitope was detected using 12CA5 monoclonal antibody (Roche). In Figure 4B, HA epitope was detected using polyclonal Y11 HA-probe (Santa Cruz Biotechnology). Anti-CBP TEV-N Peptide, anti-FLAG M2 monoclonal antibody, anti-hexokinase and anti-CPY mouse monoclonal 10A5 were purchased from Bethyl Laboratories Inc, Sigma, US Biologicals, and Molecular Probes, Inc, respectively. MYC tag was detected by 9E10 monoclonal antibody(Roche). Secondary Antibodies labeled with IR800 dye and Alexa Fluor 680 were purchased from Rockland Immunochemicals and Molecular Probes, Inc, respectively.

Native Immunoprecipitations (large scale)

ER derived microsomes were prepared from late mid-log phase yeast cells (~2800 OD₆₀₀ units) grown in YPD (The strains in Figure 2C were grown in selective media) and harvested by centrifugation. The cells were washed with water, resuspended in 50ml of 100mM Tris-HCL [9.4] buffer containing 10mM DTT and incubated for 5 minutes at room temperature. The cells were pelleted and resuspended in 20ml lyticase buffer

(50mM Tris-HCL [7.8], 1M sorbitol, 5mM β Me, 100mM NaCl). 3ml of lyticase made using a plasmid that was a gift from Randy Schekman (University of California, Berkeley) was added and the cells were incubated at 30 degrees until at least 80% spheroplasting efficiency was achieved. The spheroplasts were pelleted at 3000g for 4 minutes at 4°C and washed with lyticase buffer before being resuspended in 25ml of cold lysis buffer (25mM HEPES-KOH[6.8], 10mM NaCl, 200mM sorbitol, 1mM $MgCl_2$, 1mM $CaCl_2$, protease inhibitors). The cells were then incubated for 15 minutes on ice and lysed by douncing. The lysates were cleared twice at 1000g for 8 minutes and the resulting supernatant was subjected to a high speed spin at 50,000g. The microsome pellet was washed once before being solubilized in 5ml HEPES IP buffer (50mM HEPES-KOH [6.8], 150mM KOAc, 2mM $MgOAc$, 1mM $CaCl_2$, protease inhibitors) plus 1% Triton X-100 for 1hr at 4°C. The solubilized microsomes were spun for 22 minutes at 50,000g. 120-150 μ l pre-equilibrated anti-FLAG resin (Sigma) was added to the supernatant and incubated at 4°C for 3hr. The immunoprecipates were washed with 4x5ml of IP buffer plus 1% Triton X-100. The bound protein was eluted with 60-75 μ l of 3X FLAG peptide (Sigma) resuspended in IP buffer plus 1% Triton X-100 to a final concentration of 1mg/ml and mixing on ice for 30 minutes. SDS loading buffer was added to half of the eluate and run on 4-12% SDS PAGE gels followed by staining overnight with Colloidal Blue stain (Invitrogen), referred to as Coomassie blue in the text.

For Figure 1A, protein bands were excised from the gel and analyzed by Arnie Falick, David King and Sharleen Zhou at the Howard Hughes Medical Institute Mass Spectrometry Laboratory, University of California, Berkeley. Gel slices were trypsinized

(Promega) and mass spectra were acquired on a Bruker Reflex III MALDI-TOF mass spectrometer. Proteins were identified by searching NCBI database using MS-Fit program on Protein Prospector (UCSF, <http://prospector.ucsf.edu>) (Jimenez et al., 1998).

Native Immunoprecipitations (small scale)

Yeast Cells (40-80 OD₆₀₀ units depending on experiment) were grown to late mid-log phase in selective media. After being washed in water, cells were lysed by bead beating in 0.5ml HEPES IP buffer containing 0.1% Triton X-100. The detergent concentration was then raised to 1% in a final volume of 1ml. The crude lysate was solubilized for 30 minutes at 4°C and then spun at 100,000g for 45 minutes (except for Figure 3B which was done at 21,000g for 10 minutes). The cleared supernatant was added to 25μL of equilibrated affinity resin and incubated at 4°C for 1-3 hours. The immunoprecipitates were washed 4x1ml with HEPES IP buffer plus 1% Triton X-100. Bound material was eluted by boiling in SDS loading buffer and subjected to SDS-PAGE followed by western blotting and detection using the LI-COR Odyssey system.

An alternative lysis protocol was used for Figures 4A, 4B, and S6. Here the cells were first spheroplasted (Bhamidipati et al, 2005) before being lysed by bead beating in HEPES IP buffer containing 0.2M sorbitol (without detergent). The lysate was spun at 21,000g for 10 minutes and the resulting crude membrane fraction solubilized in 1ml of HEPES IP buffer plus 1% Triton X-100 for 30 minutes at 4°C. The resulting solubilized membranes were cleared and processed exactly as indicated above.

EndoH treatment was performed as described (Bhamidipati et al., 2005).

Cycloheximide Chase Degradation Assay

Cycloheximide chase degradation assays were performed as previously described (Bhamidipati et al, 2005). In brief, log phase cells were treated with 200ug/ml cycloheximide to terminate protein synthesis. Timepoints were aliquoted into cold YEP (to facilitate subsequent pelleting) and 10mM NaF/NaN₃ followed by pelleting and flash freezing in liquid nitrogen. The cells were then lysed with boiling SDS loading buffer, subjected to SDS PAGE and immunoblotted as described above. Bands were visualized using the LI-COR Odyssey system (which allows for two color detection) and subsequently quantitated with LI-COR Odyssey software. Following normalization to the hexokinase loading control, the values were plotted as averages \pm standard deviation of 4 measurements (2 independent experiments done in duplicate) with timepoint 0 set to 100%.

Acknowledgments

We thank M. Bassik for experimental assistance; A. Falick, D. King and S. Zhou for mass spectrometry analysis; T. Rapoport for communicating results prior to publication; J. Brodsky, R. Hampton, D. Ng, R. Schekman and P. Walter for reagents; A. Bhamidipati, D. Breslow, J. Brodsky, J. Christianson, R. Hampton, J. Hollien, R. Kopito, and K. Tipton for helpful discussion; B. Toyama for help with graphics. We are grateful for the support from the National Science Foundation (E.Q.) and the Howard Hughes Medical Institute.

Received 22 February 2006; revised 20 April 2006; accepted 10 May 2006.

Published: July 27, 2006.

Available online 27 July 2006.

Supplemental Data

A Luminal Surveillance Complex that Selects Misfolded Glycoproteins for ER-Associated Degradation

Vladimir Denic, Erin M. Quan and Jonathan S. Weissman

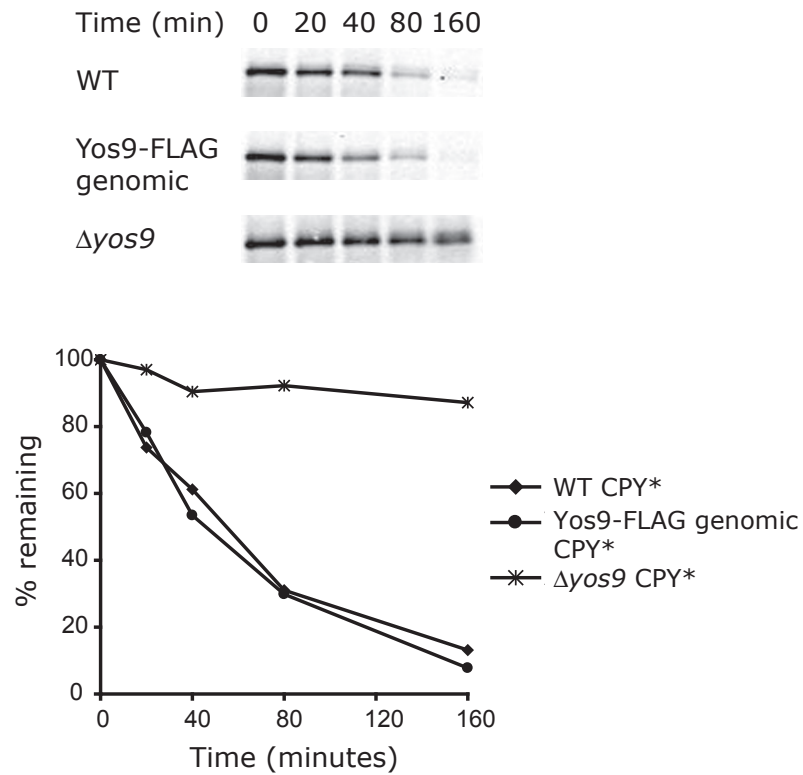


Figure S1. Yos9-FLAG genomic is functional for ERAD-L

Western blots and quantification of CPY* degradation in isogenic (◆) wild-type, (●) Yos9-FLAG, (✱) $\Delta yos9::MET15$ (Bhamidipati et al., 2005) backgrounds at the specified timepoints after addition of cycloheximide.

Protein Identified	# of Peptides Identified	% Coverage
Cdc48	35	51
Hrd3	25	31
Usa1	19	29
Kar2	11	23
	6	10
	9	21
Yos9	7	16
	17	30
Ubx2	5	8
Hrd1	12	21
Emp47	7	17

Figure S2. Mass Spectrometry Statistics

Yos9-FLAG associated proteins were separated by SDS-PAGE, excised, trypsinized and mass spectra were acquired on a Bruker Reflex III MALDI-TOF mass spectrometer. Proteins were identified by searching NCBI database using the MS-Fit program on Protein Prospector (Jimenez et. al., 1998). The multiple statistics for Kar2p and Yos9p arise from their presence in multiple, contiguous gel slices.

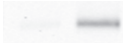

Hrd1-TAP	+	+
Yos9-FLAG	-	+
IP: α -FLAG		
W: α -CBP		
IP: α -FLAG		
W: α -FLAG		

Figure S3. Yos9p associates with Hrd1p

HRD1-TAP::HIS3MX6 cells were transformed with either empty vector, or pRS425-Yos9-FLAG and immunoprecipitated with anti-FLAG as described in Figure 1D.

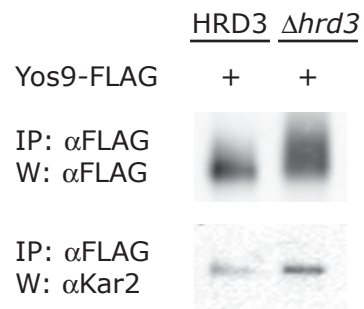


Figure S4. Yos9p/Kar2p association is independent of Hrd3p

Yos9-FLAG cells were immunoprecipitated as in 1A except that the SDS-PAGE gel was followed by Western blot analysis with the indicated antibodies.

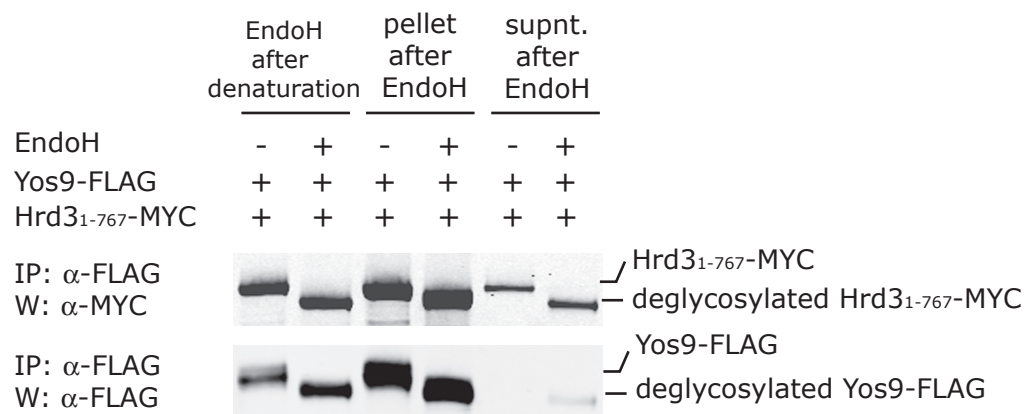


Figure S5. Deglycosylated Yos9p interacts with deglycosylated Hrd3p

A strain overexpressing Yos9p-FLAG and Hrd3₁₋₇₆₇-MYC was subjected to immunoprecipitation with anti-FLAG resin as described in Figure 1D. Following IP washes, immune-complexes were split in two. One was denatured by boiling in SDS loading buffer before being subjected to deglycosylation by EndoH while the other was subjected to native deglycosylation on the resin. Following treatment, the resin was spun out and the supernatant removed. The resin was then washed before the immunocomplexes were eluted by boiling in SDS loading buffer. The native deglycosylation samples contain ~4x as many IP equivalents as the denatured samples.

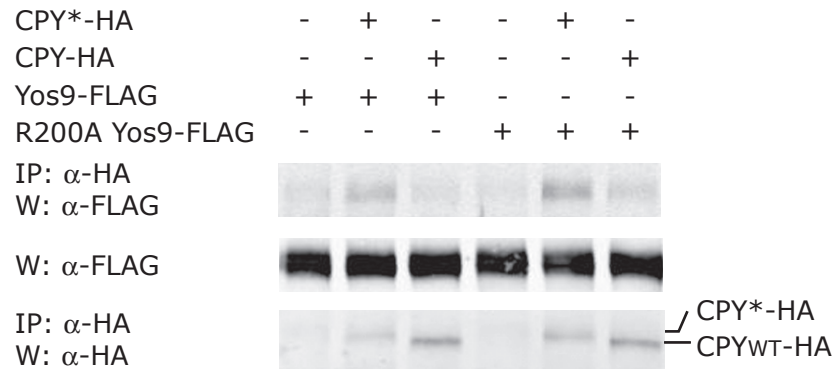


Figure S6. Yos9p and R200A Yos9p interact with CPY* but not CPY wild type

Δder1Δerv29Δyos9 cells were transformed with pRS425-Yos9-FLAG or pRS425-R200AYos9-FLAG, together with an empty vector or a vector expressing either CPY* or CPY wildtype, as indicated. Spheroplasting and immunoprecipitation with anti-HA were performed as in Figure 4.

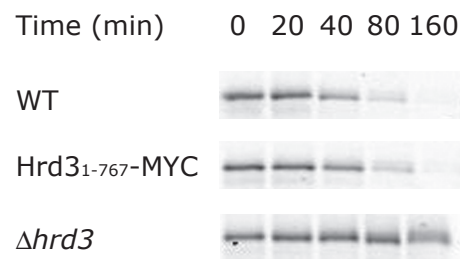


Figure S7. Hrd3₁₋₇₆₇-MYC is functional for CPY* degradation

Western blots from a cycloheximide chase degradation assay showing the degradation of CPY* in isogenic wild type, Hrd3₁₋₇₆₇-MYC and $\Delta hrd3$ strains.

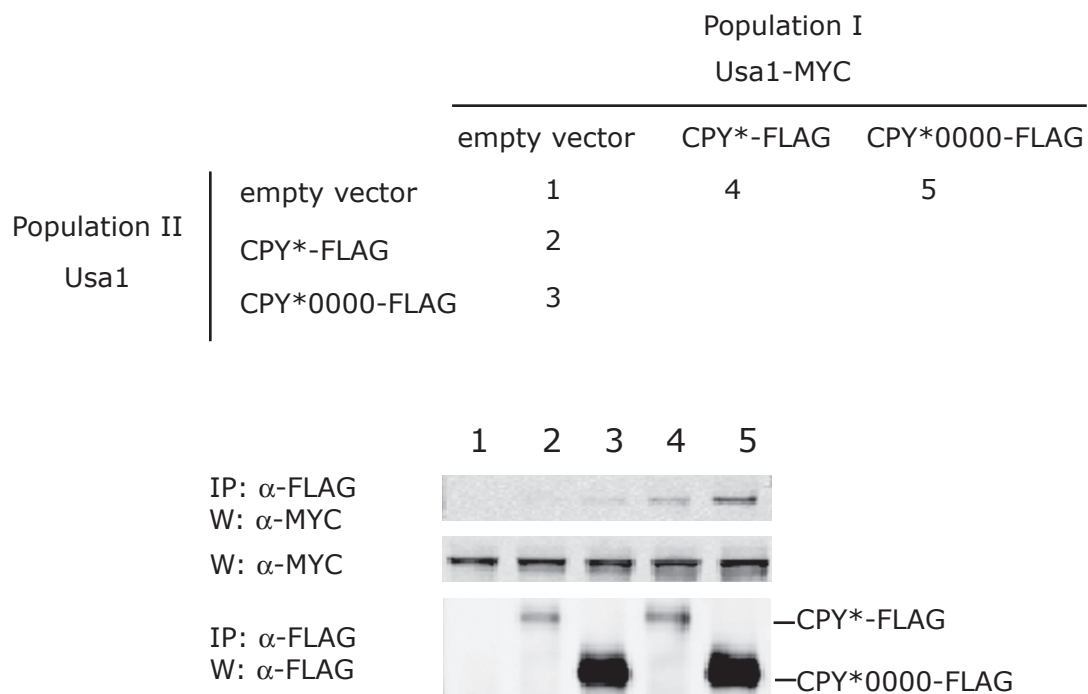


Figure S8. Usa1p is in a multiprotein complex containing misfolded carboxypeptidase Y prior to cell lysis

Wild type or Usa1-MYC expressing strains were transformed with empty vector, CPY*, or CPY*0000. Prior to lysis the indicated combinations of two populations (I and II) were mixed together. This was followed by bead beating and immunoprecipitation with anti-FLAG as described in Figure 1D.

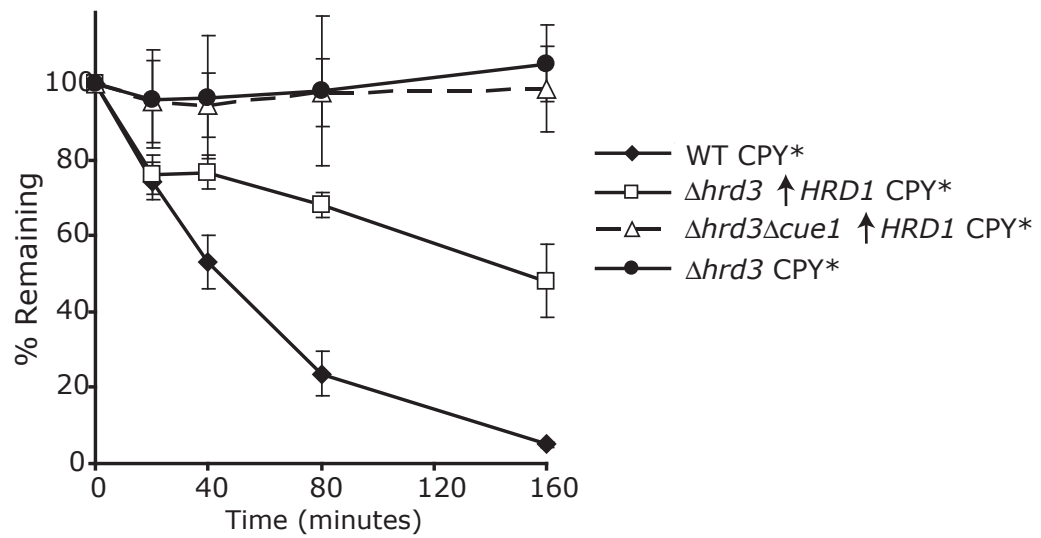


Figure S9: Degradation of CPY* when Hrd1p is overexpressed in a $\Delta hrd3$ background is suppressed by $\Delta cue1$

Degradation of CPY* in (◆) wild type (WT), (□) $\Delta hrd3 \uparrow HRD1$ CPY*, (△) $\Delta hrd3 \Delta cue1 \uparrow HRD1$, (●) $\Delta hrd3$ CPY* cells was monitored as in Figure 7A. Each timepoint represents the average and standard deviation of four measurements (two independent experiments done in duplicate) normalized to a loading control.

Supplemental Experimental Procedures

Plasmid Construction

Plasmids pRS425-YOS9-FLAG3, and pRS425-R200AYOS9-FLAG3 were constructed as previously described (Bhamidipati et al., 2005)

The CEN/ARS plasmids expressing CPY* from its native promoter and its variants were generated in the following manner: pRS316-BIPss-CPY*-HA3 was constructed as described (Bhamidipati et al., 2005). pRS316-CPYwt-HA3 was generated by PCR amplification of the *PRC1* gene plus its endogenous promoter (~500 base pairs upstream of the start codon) and terminator (~300 base pairs downstream of the stop codon). The PCR fragment was subcloned into the *KpnI* and *EcoRI* sites of pRS316 (Sikorski and Hieter, 1989). The HA3 tag was introduced as described previously (Bhamidipati et al., 2005). pRS316-CPY*abcd-HA (pES150, (Spear and Ng, 2005) was a gift from Davis Ng (National University of Singapore). The region of pES150 containing the glycosylation site mutations was subcloned into pRS316-BIPss-CPY*-HA3 using *SexAI* and *AflIII* to yield pRS316-BIPss-CPY*0000-HA3.

The 3xFLAG tag variants of CPY* were assembled as follows: p416-BIPss-CPY*-FLAG3 was made by first introducing annealed oligos bearing 3xFLAG sequence with a stop codon into the *XmaI/ClaI* sites of p416 MET25 (Mumberg et al., 1994). Next, CPY* was amplified from pRS-BIPss-316CPY*-HA3 with approximately 500 basepairs of its promoter and subcloned into the *SacI/XmaI* sites of p416-MET25-FLAG3 (in the process eliminating the MET25 promoter) resulting in an in-frame C-terminal fusion with the 3xFLAG tag. p416-CPY*0000-FLAG3 was constructed by subcloning the *SacI/MscI*

fragment from pES150 into p416-BIPss-CPY*-FLAG3. p416-CPYwt-FLAG3 was generated by PCR amplification of the PRC1 gene and its promoter from pRS316-CPYwt-HA3 and subcloning it into the *SacI/XmaI* sites in p416-BIPss-CPY*-FLAG3.

Strains

The YOS9-FLAG3 genomic strain was generated by first replacing the endogenous copy of *YOS9* in BY4741 (S288C, MATa *his3Δ1 leu2Δ0 met15Δ0 ura3Δ0*), with the *Kluyveromyces lactis* prototrophic marker *URA3*, using standard PCR-based gene replacement methods (Delneri et al., 1999). The resulting strain, *Δyos9::URA3*, was then transformed with the *XmaI/SacI* fragment from pRS425-YOS9-FLAG3 (Bhamidipati et al., 2005). Following recovery, transformants were selected on 5FOA. To facilitate detection of the *Yos9*-FLAG locus in subsequent crosses, we transformed in a kanamycin resistance cassette ~500 basepairs downstream of the *YOS9* stop codon using standard methods (Longtine et al., 1998)

The parent strains of *Δcue1*, *Δyos9*, *Δder1*, *Δhrd3*, and *Δhrd1* are BY4741 or Y3656 (Mat α *can1Δ::MFA1pr-His3-MFalpha1pr-Leu2 his3Δ1 leu2Δ0 met15Δ0 ura3Δ0 lys2Δ0*). Deletions made in the BY4741 background using the kanamycin resistance cassette were generated by the *Saccharomyces cerevisiae* deletion consortium (Winzeler et al., 1999). Deletions in the Y3656 background were generated using the pFA6-NAT-MX3 cassette using standard methods (Goldstein and McCusker, 1999; Schuldiner et al., 2005). *Δerv29* strains were made by replacing the endogenous copy of *ERV29* with the *Candida glabrata HIS3* prototrophic marker using standard methods in the specified

genetic backgrounds (Sakumoto et al., 1999). They were checked by Western blotting using anti-CPY for increased levels of the ER form of CPY.

Figure 1D *KAR2* and *kar2-1* strains were made in the W303 (MAT a *leu2-3,112 trp1-1 ura3-1 can1-100 ade2-1 his3-11,15*) background. *Kar2p* was deleted with the *Candida glabrata HIS3* prototrophic marker while the strain was covered by a *KAR2* plasmid. The *KAR2* plasmid was chased out and replaced by pMR713 *KAR2* or pMR713 *kar2-51* (CEN4, LEU2) (Kabani et al., 2003) which were a gift from Jeff Brodsky (University of Pittsburgh).

UBX2-TAP::HIS3 was generated as described (Ghaemmaghami et al., 2003). The *HRD3-MYC13* strains were made by tagging the genomic *HRD3* with the 13MYC cassette from pFA6a-13MYC-HIS3MX6 in the indicated genetic backgrounds after amino acid positions 390, 767 or the stop codon (Longtine et al., 1998). *USA1-MYC13::HIS3* was analogously made by inserting the 13MYC before the stop codon of the genomic *USA1*

The plasmid overexpressing *HRD1* from the *TDH3* promoter (pRH808, (Bays et al., 2001) was a gift from Randy Hampton (University of California, San Diego). pRH808 was cut with *HincII* and recombined into the *HRD1* genomic locus of BY4741, *Δhrd3::kan* and *Δhrd3::kanΔyos9::nat* strains. *TRP1* was first deleted in BY4741 with the *Candida glabrata HIS3* prototrophic marker using standard methods (Sakumoto et al., 1999) in order to allow for selection of recombinants on SD-TRP selective media.

The over-expressing *Yos9-FLAG* and *Hrd3₁₋₇₆₇-MYC* strains were made by using PCR-based gene insertion methods to knock in the *TDH3* promoter (687 base pairs from -691 to -4) with a pFA6a-NATMX6/KANMX6-based vector (Longtine et al., 1998) into

Yos9-FLAG and Hrd3₁₋₇₆₇-MYC strains. The strains were subsequently mated as indicated.

Strains with multiple deletions or genomically integrated proteins tags were made by crossing opposite mating types using standard yeast techniques except where noted (Guthrie and Fink, 1991). All strains altered by genomic deletions or protein tags were checked by colony PCR. The primer sequences used for gene deletions/taggings are available upon request.

CHAPTER 4

Defining the Glycan Destruction Signal for Endoplasmic Reticulum-Associated Degradation

Defining the Glycan Destruction Signal for Endoplasmic Reticulum-Associated Degradation

Erin M. Quan¹, Yukiko Kamiya^{2,3}, Daiki Kamiya², Vladimir Denic^{1,4}, Jimena Weibezahn¹, Koichi Kato^{2,3} and Jonathan S. Weissman¹

¹Hughes Medical Institute, Department of Cellular and Molecular Pharmacology, University of California-San Francisco, San Francisco, CA 94143-2542, USA

²Graduate School of Pharmaceutical Sciences, Nagoya City University, Tanabe-dori 3-1, Mizuho-ku, Nagoya 467-8603, Japan

³Okazaki Institute for Integrative Bioscience, National Institutes of Natural Sciences, 5-1 Higashiyama, Myodaiji, Okazaki 444-8787, Japan

⁴ Present address: Molecular and Cellular Biology, Harvard University, Cambridge MA, 02138, USA

Correspondence:

Jonathan S. Weissman

415-502-7642 (phone)

415-514-2073 (fax)

weissman@cmp.ucsf.edu

Koichi Kato

+81-52-836-3447 (phone and fax)

kkato@phar.nagoya-cu.ac.jp

[Reprinted from Molecular Cell, Vol. 32, Quan, E.M., Kamiya, Y., Kamiya, D., Denic, V., Weibezahn, J., Kato, K., Weissman J.S., Defining the Glycan Destruction Signal for Endoplasmic Reticulum-Associated Degradation, 870-877, Copyright (2008), with permission from Elsevier.]

Summary

The endoplasmic reticulum (ER) must target potentially toxic misfolded proteins for retrotranslocation and proteasomal degradation while avoiding the destruction of productive folding intermediates. For luminal proteins, this discrimination typically depends not only on the folding status of a polypeptide, but also on its glycosylation state. Two putative sugar binding proteins, Htm1p and Yos9p, are required for degradation of misfolded glycoproteins, but the nature of the glycan degradation signal and how such signals are generated and decoded remains unclear. Here we characterize Yos9p's oligosaccharide-binding specificity and find that it recognizes glycans containing terminal α 1,6-linked mannose residues. We also provide evidence in vivo that a terminal α 1,6-linked mannose-containing oligosaccharide is required for degradation and that Htm1p acts upstream of Yos9p to mediate the generation of such sugars. This strategy of marking potential substrates by Htm1p and decoding the signal by Yos9p is well suited to provide a proofreading mechanism that enhances substrate specificity.

Introduction

The endoplasmic reticulum (ER) contains sophisticated quality control systems that monitor protein folding to ensure that only properly folded and oligomerized forms are transported forward through the secretory pathway (Anelli and Sitia, 2008; Fewell, 2001). Despite the highly specialized folding environment of the ER, inevitably some fraction of newly made polypeptides misfolds (Casagrande et al., 2000; Friedlander et al., 2000; Helenius and Aebi, 2001; Jensen et al., 1995; Travers et al., 2000; Ward et al., 1995). Such terminally misfolded forms are cleared from the ER through ER-Associated Degradation (ERAD) pathways in which they are first recognized and then retrotranslocated into the cytosol for destruction by the ubiquitin-proteasome degradation system (Nakatsukasa and Brodsky, 2008; Romisch, 2005).

The cell must maintain a balance between overly promiscuous destruction of inherently slow-folding proteins or potentially functional mutants, while at the same time preventing the escape of toxic forms from the ER (Drumm et al., 1991; Sekijima et al., 2005). In order to achieve this balance, the ERAD machinery must accurately distinguish terminally misfolded proteins from abundant folding intermediates (Hebert and Molinari, 2007; Helenius and Aebi, 2001). The ERAD-L pathway, which degrades proteins that contain misfolded domains within the ER lumen (Huyer et al., 2004; Vashist and Ng, 2004), uses a bipartite recognition mechanism that interrogates both the glycosylation and the folding state of potential substrates (Denic et al., 2006; Gauss et al., 2006a; Knop et al., 1996b; Spear and Ng, 2005). This process is carried out by a large multi-protein complex that includes the E3 ubiquitin ligase Hrd1p (Bays et al., 2001; Deak and Wolf,

2001) and several transmembrane and cytosolic factors involved in extraction and ubiquitination of substrates (Carvalho et al., 2006; Denic et al., 2006; Gauss et al., 2006b). The luminal side of the complex contains a putative lectin, Yos9p, (Bhamidipati et al., 2005; Buschhorn et al., 2004; Kim et al., 2005; Szathmary et al., 2005) as well as Hrd3p (Gardner et al., 2000; Plemper et al., 1999), which recruits substrates based on the presence of misfolded domains. It has been recently shown that the disruption of the Yos9p sugar-binding domain or elimination of the sugar modification sites from the model ERAD-L substrate CPY* (CPY*0000) results in substrate stabilization (Finger et al., 1993; Knop et al., 1996b; Kostova and Wolf, 2005; Spear and Ng, 2005), however, CPY*0000 still efficiently interacts with Hrd3p in a manner that is dependent on folding status but not the glycosylation state of the substrate (Denic et al., 2006; Gauss et al., 2006a). These results suggest that recognition occurs as a multi-step process including the recruitment of misfolded proteins to the complex and a distinct commitment step where the presence of the glycans conveys information that is critical for substrate retrotranslocation and degradation (Denic et al., 2006; Gauss et al., 2006a).

Although it is clear that the identification of misfolded forms critically depends on the glycosylation status of the misfolded protein, the nature of the glycan species that triggers destruction and how it contributes to specificity remains unclear. Previously, it has been shown that the processing of the pre-assembled Glc₃Man₉GlcNAc₂ oligosaccharide that is initially transferred to proteins at N-X-S/T sites is involved in ERAD recognition. This initial glycan is trimmed through the sequential action of two glucosidases and a mannosidase (Mns1p) to yield a Man₈GlcNAc₂ species (Hebert et al., 2005; Helenius and Aebi, 2004). These trimming steps are required for ERAD-L, and it

has been suggested that the period of time it takes to reach a certain glycan structure provides proteins a period of time to fold without risk of being degraded (Helenius, 1994; Hitt and Wolf, 2004b; Jakob et al., 1998a; Knop et al., 1996b; Wu et al., 2003). However, recent studies in yeast suggest that the above trimming steps occur rapidly on the scale of synthesis and degradation and thus are not well suited to increase specificity (Szathmary et al., 2005). Here we reveal that Yos9p recognizes trimmed glycans that expose a terminal α 1,6-linked mannose and provide evidence that suggests that Htm1p, a mannosidase-like protein whose critical role in ERAD has been largely uncharacterized (Jakob et al., 2001; Nakatsukasa et al., 2001), is required to generate such sugars. Our results suggest a model where Htm1p “marks” misfolded glycoproteins by revealing a terminal α 1,6-linked mannose that is recognized by Yos9p as the signal for degradation. This dual checking mechanism could provide increased specificity during ERAD.

Results

Yos9p structure and function does not depend on its N-linked glycans

A hallmark of Yos9p and its mammalian homologues is the presence of a mannose 6-phosphate receptor homology (MRH) domain (Munro, 2001). Mutations in this domain (e.g. R200A) that ablate the putative sugar-binding pocket disrupt Yos9p's ability to support ERAD of glycoproteins suggesting that Yos9p acts as a lectin during substrate recognition (Bhamidipati et al., 2005; Szathmary et al., 2005). In order to explore Yos9p's role as a lectin, we sought to produce biochemical amounts of Yos9p and directly evaluate its sugar-binding specificity.

Recombinant production of suitable quantities of Yos9p posed a technical challenge as Yos9 is glycosylated and contains many disulfide bonds. First, we mutated all the N-linked glycosylation consensus sites on Yos9p and found that glycosylation of Yos9p is not required for function, as the mutant protein fully supported ERAD of CPY* in vivo (Figure 1A). Attempts to produce native protein in *E. coli* yielded soluble disulfide cross-linked aggregates (Figure S1). We therefore developed an alternate expression strategy in which Yos9p was isolated under denaturing conditions from *E.coli* inclusion bodies, refolded under optimized conditions, and purified to apparent homogeneity (Figure 1B, S2). The refolded material appeared well-ordered by circular dichroism spectroscopy (Figure 1D), contained minimal intermolecular disulfide crosslinks (Figure 1B) and migrated as a single peak by gel filtration that is consistent with it being a trimer (Figure 1C). Using the same protocol, we also produced the R200A Yos9p MRH mutant. The R200A mutation did not disturb the folding or structure of

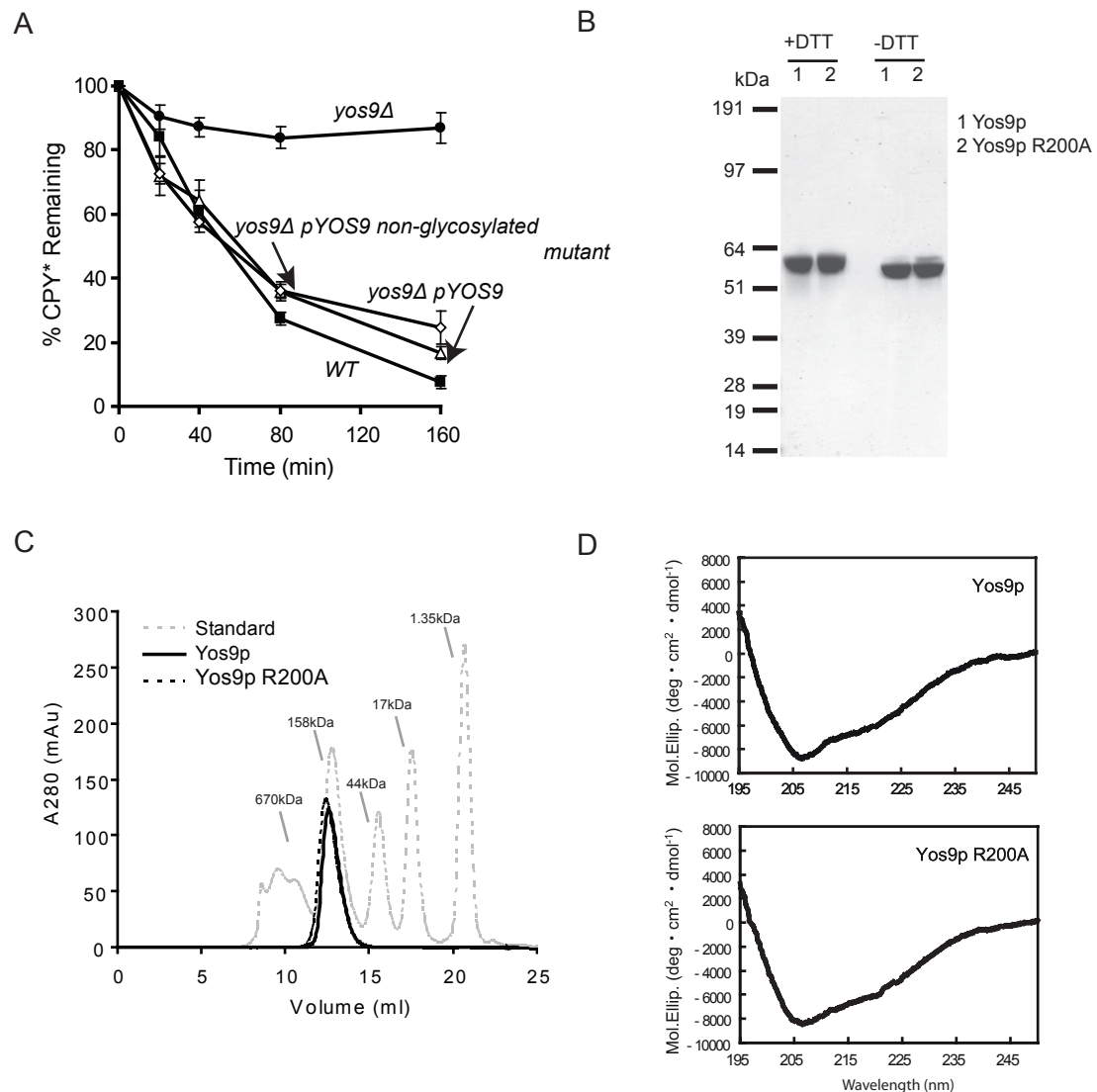


Figure 1. Purification of biochemical amounts of Yos9p from *E. coli*.

(A) Degradation of CPY* in (■) wild-type (WT), and (●) a *yos9Δ* strain harboring an empty vector, and *yos9Δ* strain covered with a plasmid expressing YOS9-flag (△) or a Yos9p variant that is missing glycosylation sites (◇) was monitored by cycloheximide chase. Equal amounts of log phase cells were removed at the indicated times following addition of cycloheximide. Samples were resolved by SDS-PAGE and detected by Western analysis using anti-HA and anti-hexokinase antibodies. Each time point represents the average and \pm standard error of the mean (SEM) of 4 measurements (two independent experiments done in duplicate) and normalized to the hexokinase loading control.

(B) Refolded recombinantly expressed Yos9p (1) and Yos9p R200A (2) was purified and analyzed by SDS-PAGE with sample buffer containing either DTT or N-ethylmaleimide (-DTT) and stained with Coomassie.

(C) Gel Filtration analysis of Yos9p (—), Yos9p R200A (- - -) and molecular size standards (gray).

(D) Circular Dichroism spectra were acquired of Yos9p (top) and Yos9p R200A (bottom) as described in the experimental procedures.

Yos9p which is consistent with the proposal that this mutation interferes with ERAD function specifically by preventing sugar-binding rather than causing global unfolding (Figure 1D) (Bhamidipati et al., 2005; Szathmary et al., 2005).

Yos9p recognizes a terminal α 1,6-linked mannose

We next determined the sugar-binding specificity of our recombinant Yos9p using frontal affinity chromatography (FAC), which provides a quantitative way to evaluate lectin-oligosaccharide interactions in solution. In this approach, protein is immobilized on a matrix and oligosaccharides, which are fluorescently labeled by pyridylation (PA), are applied to the column of immobilized protein. The degree of retardation of the sugar, relative to a control sugar that is not recognized by the immobilized protein, provides a quantitative equilibrium measure of the binding affinity, with longer delays corresponding to tighter binding constants (See Figure 2 and Experimental Procedures) (Hirabayashi et al., 2003).

The FAC analysis revealed that Yos9p has a specificity for oligosaccharides containing a terminal α 1,6-linked mannose which is not present in the initial N-linked glycan (see Figure 2A, 2B for schematics of high mannose sugars). Importantly, Yos9p's sugar specificity is dependent on an intact MRH domain, as the R200A lectin mutant shows no affinity for any of the glycans tested (Figure 2D). Yos9p has little affinity for the final trimming product of the two glucosidases (M9.1) or for the trimming product of Mns1p (M8.1) (Figure 2B)(Helenius and Aebi, 2004). In contrast, Yos9p recognizes species with the final mannose on the C branch removed to reveal a terminal α 1,6-linked mannose. A comparison between M8.1 and M8.2 highlights the critical role of the α 1,6-

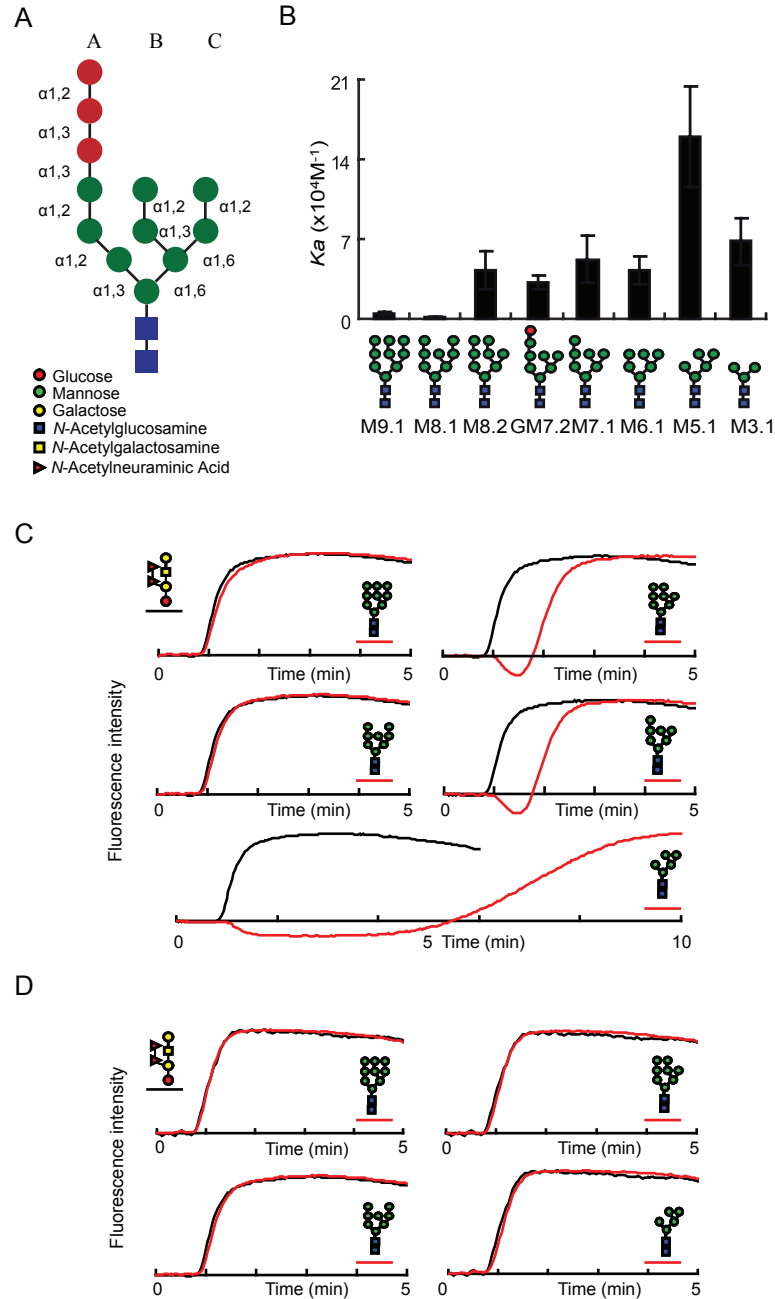


Figure 2. Yos9 recognizes glycans containing a terminal $\alpha 1,6$ -linked mannose

(A) A schematic representation of the initial $\text{Glc}_3\text{Man}_9\text{GlcNAc}_2$ N-linked sugar and the legend for each sugar moiety represented.

(B) FAC analysis of Yos9p sugar binding specificity. Indicated PA-oligosaccharides were tested for binding to Yos9p by FAC analysis. K_a values were determined as described in the supplemental experimental procedures and are mean \pm S.D. of three independent experiments. Each glycan structure is detailed and given a code name beneath the chart.

(C-D) Elution profiles over time of fluorescently labeled (PA)-oligosaccharides applied over immobilized histidine tagged Yos9p (C, red) or R200A mutant (D, red) in comparison to a negative control sugar (black) PA-glycans are schematically represented next to the corresponding elution profile.

linked mannose, as both have eight mannoses arranged into three branches but only M8.2, which has the terminal α 1,6-linked mannose, interacts with Yos9p. The α 1,6-linked mannose seems to be necessary and largely sufficient for recognition by Yos9p because sugars containing this signal show significant affinity for Yos9p. The other residues seem to have relatively small effects on Yos9p binding with one prominent exception being the M5.1 species which has a higher affinity. How and if this species is generated under physiological conditions is unclear (see discussion).

Terminal α 1,6-linked mannose containing N-linked glycans serve as the ERAD-L degradation signal

We next tested the functional significance of the terminal α 1,6-linked mannose as an ERAD signal in vivo focusing on M7.1 because it is most likely to serve as a degradation signal as it requires minimal modification to the Mns1p produced M8.1 sugar (Herscovics, 2001). To test the role of M7.1, we took advantage of the previous observation by Aeby and coworkers that the M7.1 sugar could be produced in vivo using a series of genetic mutations in the asparagine-linked glycosylation (ALG) biosynthesis pathway (Figure 3A top). Specifically, by simultaneously deleting *ALG9*, which leads to accumulation of M6.2 sugars, and then artificially bypassing the next step by over-expression of the *ALG12* mannosyltransferase, similar levels of M6.2 sugars and M7.1 sugars which contains a terminal α 1,6-linked mannose are transferred to proteins (Figure 3A bottom) (Burda et al., 1999).

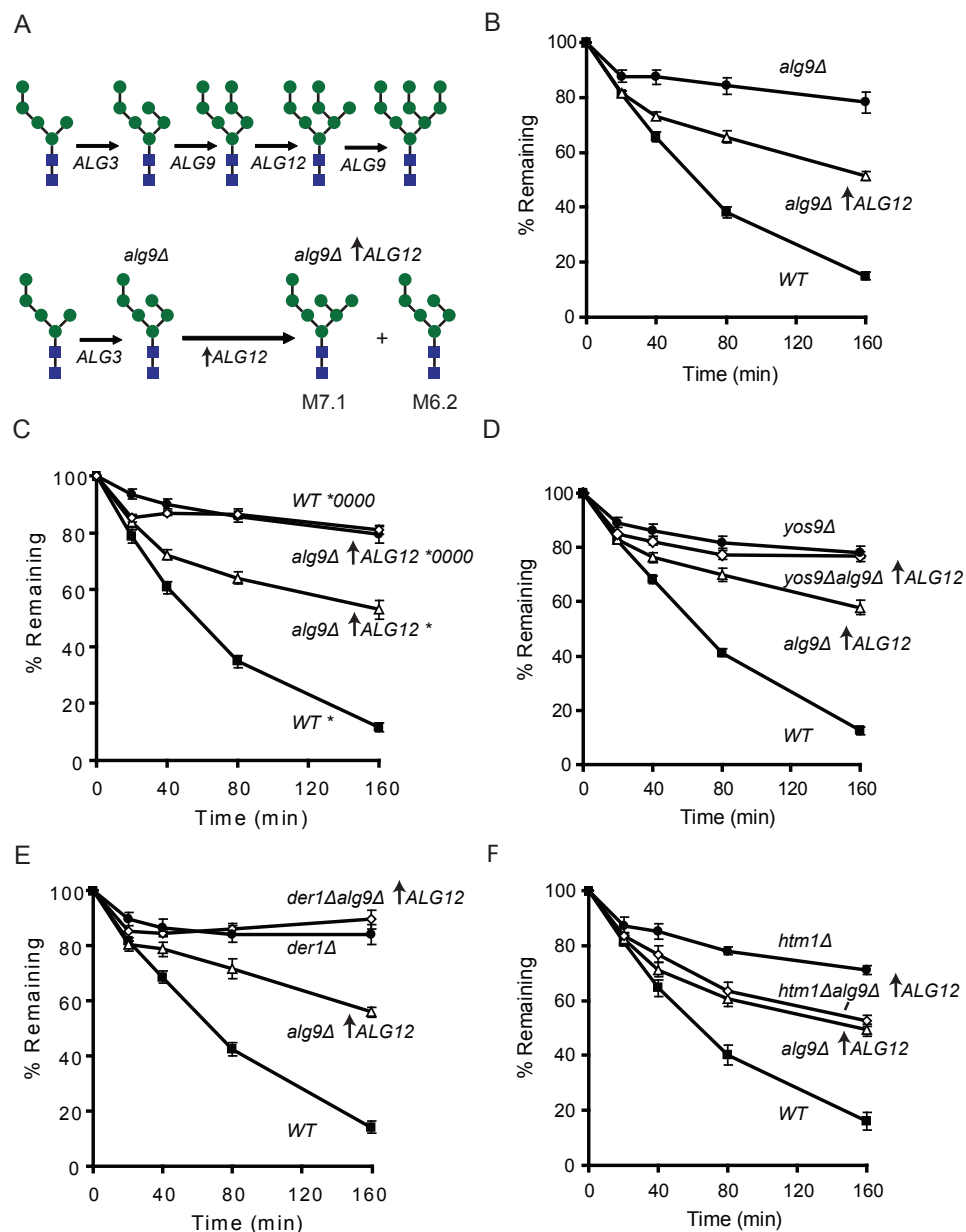


Figure 3. Production of Man₇GlcNAc₂ sugars in vivo results in ERAD dependent degradation and bypass of *HTM1*

(A) Schematic representation of a portion of the asparagine linked glycosylation (ALG) pathway. Shown are the glycans produced in the wild-type (top) pathway and an *alg9Δ* over-expressing *ALG12* (upward arrow indicates TDH3 driven expression) strain (bottom). Mannose residues are represented as blue circles and N-acetylglucosamine is represented by blue squares.

(B) Degradation of CPY* in a (■) wild-type (WT), (△) *alg9Δ*↑*ALG12*Δ, and (●) *alg9Δ* strains in this and the following panels were monitored as in Figure 1A except that each time point represents the average and +/- SEM of at least 8 measurements (4 independent experiments done in duplicate).

(C) Degradation of CPY* in (■) wild-type (WT) and (△) *alg9Δ*↑*ALG12* (upward arrow represents TDH3 driven expression), or CPY*0000 in (●) wild-type (WT) and (◇) *alg9Δ*↑*ALG12* cells. CPY* is represented as a * and non-glycosylatable CPY* is represented as *0000.

(D) Degradation of CPY* in (■) wild-type (WT), (△) *alg9Δ*↑*ALG12*, (◇) *yos9Δ* *alg9Δ*↑*ALG12* and (●) *yos9Δ* cells.

(E) Degradation of CPY* in (■) wild-type (WT), (△) *alg9Δ*↑*ALG12*, (◇) *der1Δ* *alg9Δ*↑*ALG12* and (●) *der1Δ* cells.

(F) Degradation of CPY* in (■) wild-type (WT), (△) *alg9Δ*↑*ALG12*, (◇) *htm1Δ* *alg9Δ*↑*ALG12* and (●) *htm1Δ* cells.

Analysis of ERAD-L in the *alg9Δ /ALG12* over-expression strain strongly supports the proposal that Man7.1 is productively recognized by Yos9p. As seen previously, deletion of *alg9* which produces M6.2 sugars that lack a terminal α 1,6-linked mannose, results in stabilization of CPY* (Figure 3B and S3) (Jakob et al., 1998a). By contrast, deletion of *alg9* together with over-expression of *ALG12* results in degradation of approximately fifty percent of CPY* (Figure 3B and S3). This result is consistent with the ratio of M6.2 and M7.1 sugars produced in the cell strongly suggesting that proteins with M7.1 are being subject to ERAD-L. Importantly, CPY* degradation in the *alg9Δ/ALG12* over-expression strain is dependent on presence of substrate glycans (Figure 3C), Yos9p (Figure 3D), and Der1p, another member of the Hrd1p complex (Figure 3E) (Gauss et al., 2006b; Knop et al., 1996a), indicating that degradation in this background goes through the classic ERAD-L pathway (Huyer et al., 2004; Kanehara et al., 2007; Kostova and Wolf, 2005; Spear and Ng, 2005; Vashist and Ng, 2004). Strikingly, in contrast to wild-type cells, we found that in the *alg9Δ/ALG12* over-expression background, Htm1p is dispensable for degradation (Figure 3F). An exposed α 1,6-linked mannose on a second ERAD-L substrate, KHN, (Vashist et al., 2001; Vashist and Ng, 2004) also bypasses the need for Htm1p (Figure S4). Thus the presence of the M7.1 signal circumvents the requirement for Htm1p without bypassing the need for later-acting components like Yos9p and Der1p that are involved in reading out the signal and the ensuing steps leading to substrate degradation.

Discussion

Here we revealed the sugar-binding specificity of Yos9p, which together with functional studies, supports a model in which two key lectins, Htm1p and Yos9p, cooperate to enhance the specificity of the ERAD-L degradation system (Figure 4). This model builds on the previous observation that degradation by the Hrd1/Hrd3/Yos9 ubiquitin ligase complex requires a bipartite recognition of substrates involving both recognition of misfolded domains and glycans (Denic et al., 2006; Gauss et al., 2006a). Specifically, Hrd3p recruits potential substrates to the Hrd1p ligase complex based on the presence of misfolded domains. Yos9p then queries the glycans for what we have determined to be Yos9p's preferred oligosaccharide binding specificity, a terminal α 1,6-linked mannose, through the action of Htm1p. Upon identification of an appropriate glycan signal, Yos9p commits the substrate for degradation. This model also provides an explanation for the previously enigmatic observation that ERAD-L occurs in *alg3 Δ* strains even though several *ALG* mutants with less severe defects in the biosynthesis of N-linked glycans abrogate ERAD-L (Jakob et al., 1998a), as the Man₅GlcNAc₂ sugar produced in an *alg3 Δ* strain also contains a terminal α 1,6-linked mannose. Consistent with this, degradation of CPY* in the *alg3 Δ* background does not require Htm1p (Clerc et al., 2009)(Figure S4).

Although the enzymatic activity of Htm1p has not been directly examined, several observations suggest that Htm1p is required for generating the Man₇GlcNAc₂ signal (either as an enzyme or as a cofactor) that is recognized by Yos9p. Jakob and colleagues reported that deletion of Htm1p results in reduced CPY*-Yos9p interaction (Szathmary et al., 2005). Htm1p is homologous to α 1,2-mannosidases but lacks conserved cysteine

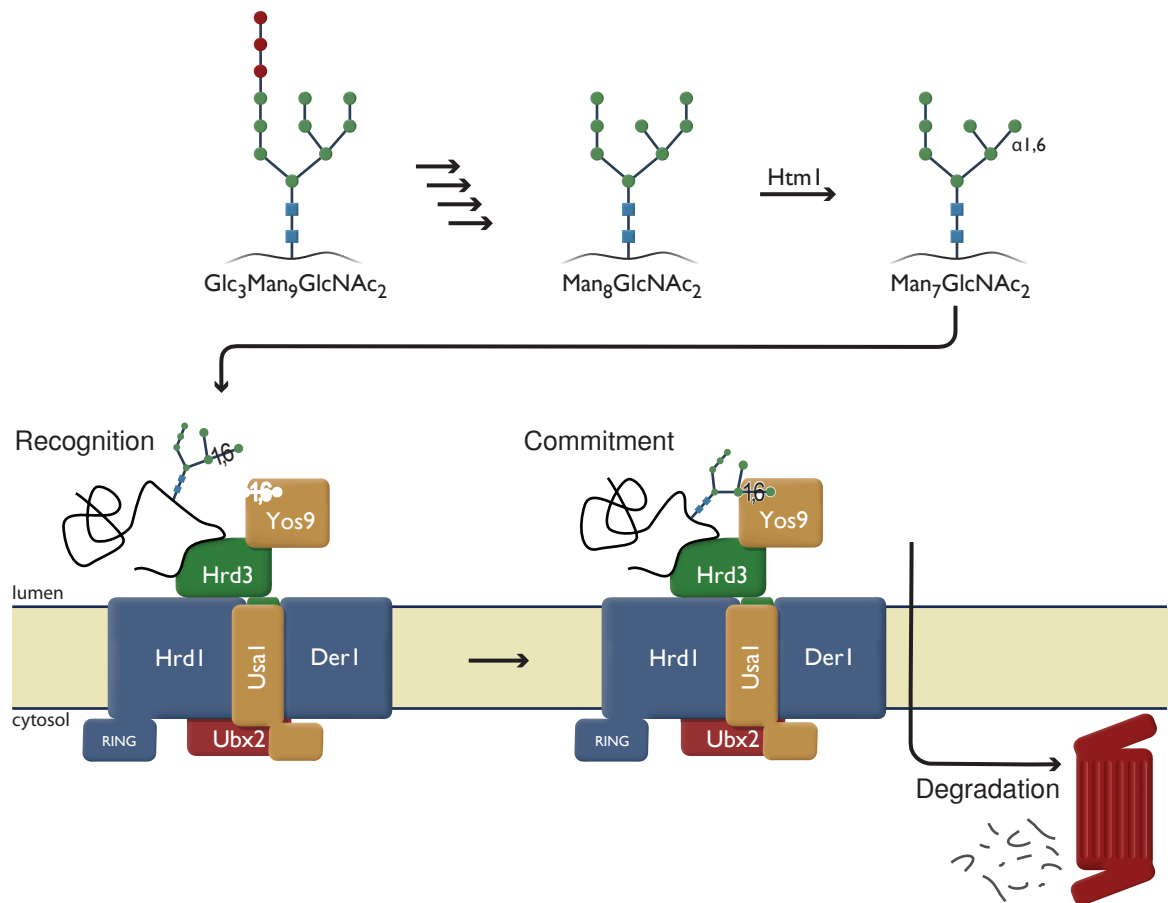


Figure 4. Model of dual recognition of substrates by ERAD.

Glycan processing from the initial N-linked $\text{Glc}_3\text{Man}_9\text{GlcNAc}_2$ to $\text{Man}_8\text{GlcNAc}_2$ occurs by Glucosidase I, II and Manosidase I, respectively. Htm1p marks potential substrates by playing a role in the generation of $\text{Man}_7\text{GlcNAc}_2$ (upper panel). Misfolded proteins are recruited to the Hrd1p complex by recognition of misfolded domains by Hrd3p. Yos9p queries the N-linked glycan and substrates are committed for degradation after Yos9p has identified the presence of a terminal $\alpha 1,6$ -linked mannose. Note: Whether Htm1p is an enzyme or cofactor remains to be determined.

residues that potentially contribute to enzymatic activity (Jakob et al., 2001; Lipari and Herscovics, 1996; Nakatsukasa et al., 2001). However, over-expression of the human Htm1p homologues, EDEM 1 and EDEM3, which also do not contain the cysteine residues, leads to demannosylation suggesting that they are active mannosidases (Hirao et al., 2006a; Olivari et al., 2006). Additionally, Aebi and coworkers (Clerc et al., 2009) find that overexpression of Htm1p results in increased production of protein-bound Man₇GlcNAc₂ oligosaccharide. Finally, we show that a yeast strain engineered to produce Man₇GlcNAc₂ glycans as the starting sugar bypasses the requirement for Htm1p in Yos9p-mediated degradation of CPY*.

How might the requirement for the generation and recognition of a specific degradation glycan increase ERAD-L specificity? One possibility is that Htm1p acts as “timer,” which acts independently of folding status of its substrate thereby providing all polypeptides with a protected window of time in which they can fold without risk of destruction (Helenius, 1994; Jakob et al., 1998a; Wu et al., 2003). It is also possible that Htm1p is more sophisticated and that the presence of specific misfolded structures determines whether a substrate is marked by Htm1p. A precedent for such a mechanism is provided by the mammalian UDP-Glc:glycoprotein glucosyltransferase, which adds a glucose only to glycans proximal to a misfolded domain (Ritter and Helenius, 2000; Ritter et al., 2005; Trombetta and Helenius, 2000; Trombetta et al., 1991). Htm1p is also in a complex with Pdi1p whose chaperone activity could confer specificity based on substrate structure (Collins et al., 2007; Krogan et al., 2006). Either way, this modification of sugars adds another level of surveillance to the bipartate recognition of misfolded domains and sugar status by Hrd3p/Yos9p (Denic et al., 2006; Gauss et al.,

2006a). The use of multiple query steps separated by irreversible steps would allow for a kinetic proofreading mechanism (Hopfield, 1974) ensuring enhanced specificity in the recruitment of misfolded proteins. In light of this model, it is intriguing that Yos9p shows its highest affinity for a specific $\text{Man}_5\text{GlcNAc}_2$ species that is missing the two A-branch mannose residues, as this species has been observed in mammals (Avezov et al., 2008; Frenkel et al., 2003; Hosokawa et al., 2003; Kitzmuller et al., 2003; Lederkremer and Glickman, 2005). While it remains to be seen how or even if this species can be generated through additional sugar trimming in yeast, the enhanced affinity of Yos9p for the $\text{Man}_5\text{GlcNAc}_2$ (M5.1) sugar species could provide a mechanism for preferentially degrading a subset of potential substrates.

On a practical note, a more sophisticated understanding of what constitutes a good ERAD substrate should enable a range of biochemical and structural studies to elucidate substrate recognition. In light of the multi-step nature of marking and decoding of ERAD-L substrates, it is perhaps not surprising that in vitro reconstitution of this process has proven so challenging. The discovery that substrate glycans containing a terminal $\alpha 1,6$ -linked mannose such as $\text{Man}_7\text{GlcNAc}_2$ are recognized by Yos9p should facilitate efforts to create a synthetic substrate with the correct glycan signal attached, thus bypassing the complicated upstream trimming steps. Furthermore, it should now be possible to monitor the specific recognition steps of ERAD-L in vitro. Several immediate questions emerge: How is Htm1p selecting its substrates? Are Yos9p and Hrd3p querying distinct structural features or are they simply double checking Htm1p's decisions? What is the mechanism of the commitment step once Yos9p confirms that the glycan is correct?

Addressing these and related issues will provide a detailed molecular understanding of how and when the cell decides to commit ER proteins for destruction.

Experimental Procedures

Yeast Strains and Plasmids

All yeast strains are derivatives of S288c. Gene deletions, epitope taggings and promoter insertions were done using standard PCR based techniques. Details are available in the Supplemental Data section.

Cycloheximide Degradation Assays

Cycloheximide chase degradation assays were performed as previously described (Denic et al., 2006) with the exception that bands were visualized and quantitated using the LI-COR Odyssey system using an area of the blot with no specific signal as background. Following normalization to the hexokinase loading control, the values were plotted as averages \pm standard error of the mean (SEM) with timepoint 0 set to 100%.

Yos9p Purification and Refolding

HIS-tagged Yos9p or Yos9 R200A was purified from Rosetta (DE3) pLysS inclusion bodies, solubilized in 8M urea and purified over a Ni-NTA agarose and a Source Q column. The protein was then refolded into 100mM Tris-HCL (pH 8.5) 150mM NaCl, 1mM CaCl₂, 0.5M L-arginine, 5mM GSH, and 0.5mM GSSG at 4°C for 24 hours and subsequently purified over a Resource Q column before being buffer exchanged into 10mM HEPES, 1mM Cacl₂, 10% glycerol, and 150mM NaCl (pH 7.4). Further details are given in the Supplemental Data.

Frontal Affinity Chromatography

FAC analyses were carried out as previously described (Kamiya et al., 2008; Kamiya et al., 2005; Kasai, 1986).

Briefly, Yos9p and its R200A mutant were immobilized on a Ni²⁺-sepharose high performance column by their histidine-tag following the manufacturer's instructions (GE healthcare). After immobilization, the sepharose beads were packed into a stainless steel column (4.0 × 10 mm, GL Sciences).

The PA-oligosaccharide library was constructed as described previously (Kamiya et al., 2008). PA-oligosaccharides were dissolved at a concentration of 10 nM in 10 mM HEPES (pH 7.4) containing 150 mM NaCl and 1 mM CaCl₂, and applied onto the column at a flow rate of 0.25 ml/min at 20 °C. The elution profile was monitored by the fluorescence intensity at 400 nm (excitation at 320 nm). The retardation compared with control oligosaccharide was computed using the difference of each elution volume, V_f . The dissociation constant, K_d ($=1 / K_a$), of the lectins for GlcMan₇GlcNAc₂-PA (GM7.2) was determined by the concentration-dependent analysis using the Equation 1.

$$[A]_0 \cdot (V_f - V_0) = B_t - K_d \cdot (V_f - V_0) \text{ (Eq. 1)}$$

where $[A]_0$, V_0 , and B_t , are initial concentration of the PA-oligosaccharide, the elution volume of the control sugar, and the total amount of immobilized lectins in the column, respectively. The elution profile was monitored by UV absorption at 300 nm to avoid possible quenching caused by the relatively high concentration of the PA-sugar. For the determination of V_0 , 50 μM *p*-nitrophenyl-β-D-galactopyranoside was used. K_d was calculated based on the retardation $V_f - V_0$ measured at concentrations of 2-16 μM GM7.2.

The relative affinity of each oligosaccharide was calculated under conditions where $[A]_0$ is negligibly small compared with K_d , using Equation 2.

$$V_f - V_0 = B_t / K_d \text{ (Eq. 2)}$$

To determine V_0 , Gal β 1-3GalNAc β 1-4(Neu5Ac α 2-8Neu5Ac α 2-3)Gal β 1-4Glc-PA (PA-GD1b-hexasaccharide) was used as control sugar for the analyses of Yos9p. K_a values are mean \pm S.D. of three independent experiments.

Circular Dichroism Spectroscopy

Circular dichroism (CD) measurements were conducted on a Jasco J-725 spectropolarimeter (Jasco Inc., Japan) at room temperature using samples containing 0.05 mg/ml of Yos9p or its R200A mutant in 0.1 M sodium phosphate, at pH 7.4. Each spectrum was recorded as the average of four scans over the range 195 -250 nm with a step size of 0.1 nm and a bandwidth of 1.0 nm.

Acknowledgments

We thank V. Van Voorhis for help with the initial observations of the M7.1 glycan CPY* degradation; C. Chu for help with the protein production strategy; M. Bassik, D. Breslow, and N. Ingolia for helpful discussions and critical reading of the manuscript; M. Aebi, D. Ng, and K. Nagata for communicating results prior to publication; D. Ng for reagents; B. Toyama for help with graphics. We are grateful for support from the National Science Foundation (EQ), an EMBO long-term fellowship (1201-2006) (JW), an HFSP long-term fellowship (LT00821/2007-L) (JW), the Howard Hughes Medical Institute (JSW) and Grant-in-aid for Scientific Research from Ministry of Education, Culture, Sports, Science, and Technology of Japan (KK).

Received 7 August 2008; revised 31 October 2008; accepted 24 November 2008.

Published: December 24, 2008.

Available online 24 December 2008.

Supplemental Data

Defining the Glycan Destruction Signal for Endoplasmic Reticulum-Associated Degradation

Erin M. Quan, Yukiko Kamiya, Daiki Kamiya, Vladimir Denic, Jimena Weibezahn, Koichi Kato and Jonathan S. Weissman

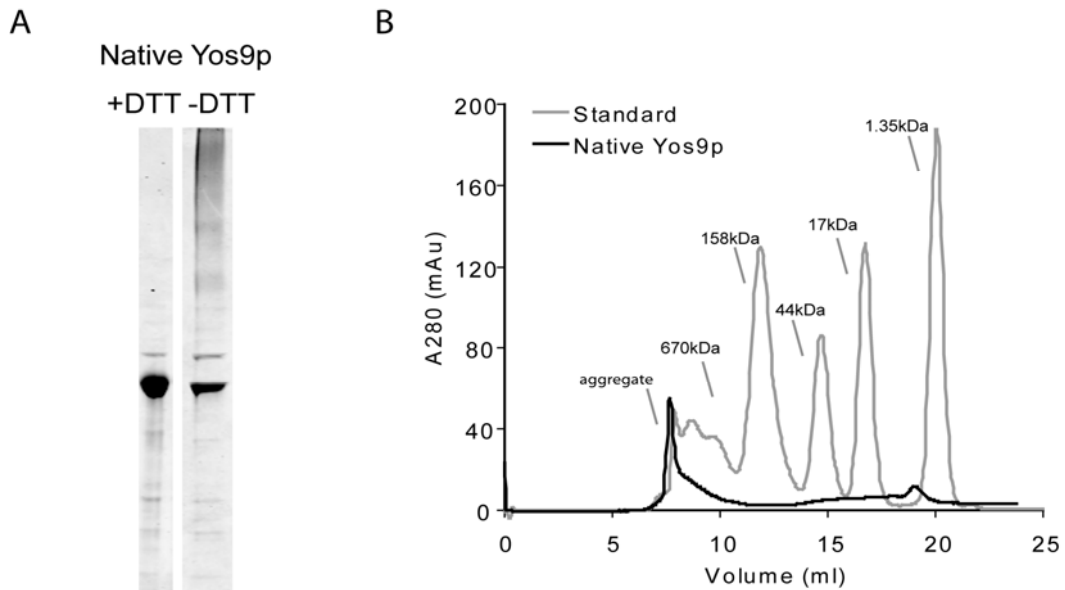
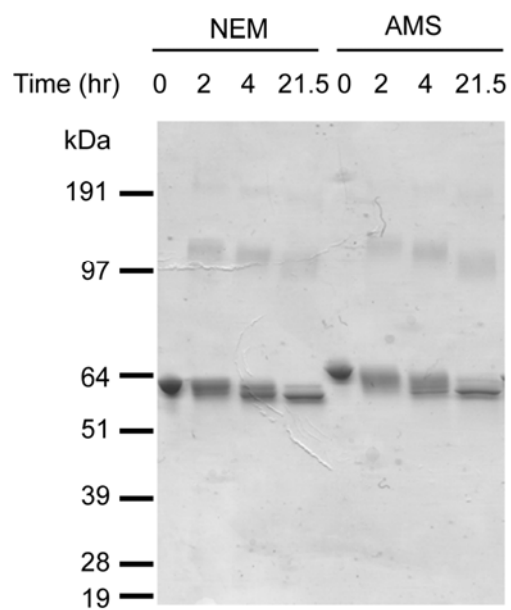


Figure S1. Native Yos9p forms disulfide-crosslinked aggregates

(A) Soluble Yos9p purified under non-denaturing conditions from *E. coli* was analyzed by SDS-PAGE with sample buffer containing either DTT or N-ethylmaleimide (-DTT).

(B) Elution profile for Yos9p purified natively from *E. coli* (black) and standards (gray) run on a gel filtration column in 20mM Tris-HCl (7.9), 150mM NaCl, 10% glycerol, 5mM GSH, and 1mM EDTA.



Figures S2. Refolding process of denatured Yos9p

Refolding of denatured Yos9p. To block free cysteines, 4-acetamido-4'-maleimidylstilbene-2,2'- disulfonic acid (AMS) or N-ethylmaleimide (NEM) were added to protein samples taken over time, resolved by SDS-PAGE and Coomassie stained. Note the time dependent shift of the protein. The protein was further purified to remove the higher molecular weight oligomers.

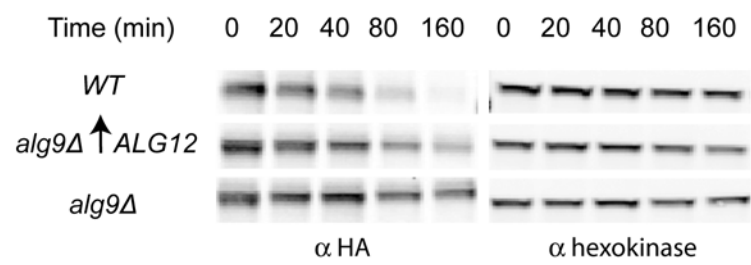


Figure S3. Production of $\text{Man}_7\text{GlcNAc}_2$ sugars results in degradation of CPY*
 Degradation of CPY* in the indicated strain backgrounds were monitored and processed as in Figure 3B. A representative western blot is shown. Quantitation of the experiment is shown in Figure 3B.

Further Evidence that an exposed α 1,6-linked mannose allows for Htm1p-independent ERAD of misfolded glycoproteins.

We tested a second ERAD-L glycoprotein substrate, KHN, to see if like CPY*, the Htm1p dependence could be bypassed by genetic manipulations that produced sugars containing an exposed α 1,6-linked mannose. Because of the limited dynamic range of the *alg9 Δ /ALG12* over-expression system, we used an *alg3 Δ* to produce Man5.2 sugars with a terminal α 1,6-linked mannose (Figure S4A)(Jakob et al., 1998b). In agreement with observations from Aebi and coworkers (personal communication), we find that the loss of *ALG3* removes the requirement for Htm1p for the degradation of CPY* (Aebi and coworkers, personal communication and Figure S4B). Similarly, we find that deletion of *ALG3*, eliminates the need for Htm1p in the degradation of KHN (Figure S4C). This is consistent with the hypothesis that a terminal α 1,6-linked mannose is sufficient to allow for productive recognition by Yos9p although we have not directly tested Yos9p's ability to bind to M5.2 *in vitro*.

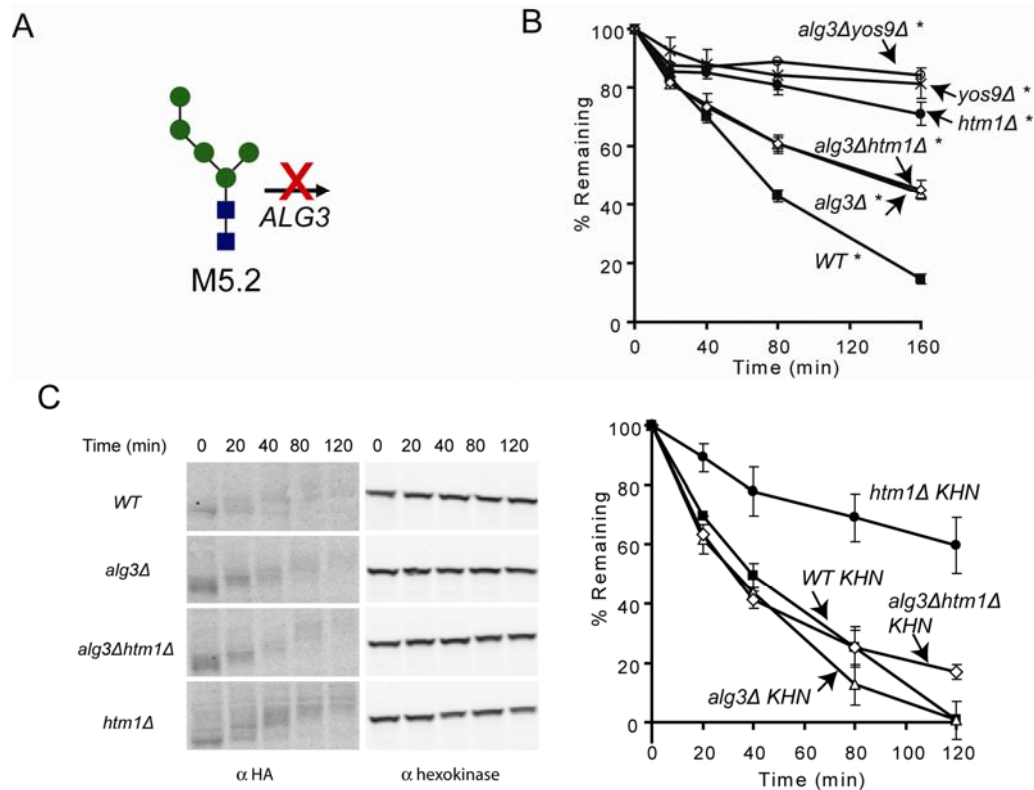


Figure S4. An exposed α 1,6-linked mannose on CPY* or KHN results in bypass of *HTM1*

(A) A schematic representation of M5.2, a probably non-natural sugar produced by an *alg3 Δ* strain. Mannose residues are represented as green circles and N-acetylglucosamine is represented by blue squares. (B) Degradation of CPY* (depicted as a *) in (■) wild-type (WT), (△) *alg3 Δ* , (◇) *htm1 Δ alg3 Δ* and (●) *htm1 Δ* cells, (○) *yos9 Δ alg3 Δ* and (×) *yos9 Δ* cells was monitored and processed as in Figure 1A. (C) Degradation of KHN in (■) wild-type (WT), (△) *alg3 Δ* , (◇) *htm1 Δ alg3 Δ* and (●) *htm1 Δ* cells was monitored and processed as in Figure 3B. Representative gel shown (left).

Supplemental Experimental Procedures

Plasmids

Yos9p without glycans (Figure 1A) was expressed from a CEN/ARS plasmid made by using QuikChange mutagenesis (Stratagene) to change N to Q in the four N-X-S/T sites in the coding region of a C-terminal 3FLAG-tagged Yos9p expressed from its endogenous promoter (Denic et al., 2006).

For cycloheximide degradation assays, CEN/ARS CPY* and CPY*0000 plasmids were constructed with ~700 base pairs of the endogenous *PRCI* promoter, signal sequence, and the CPY* or CPY*0000 (made from pES150, a gift from Davis Ng, National University of Singapore) gene. CPY*/CPY*0000 was tagged with 3HA between the end of the coding region and the *PRCI* terminator as previously described (Bhamidipati et al., 2005). KHN (pSM70) was a gift from Davis Ng, National University of Singapore. For Figure 1A p316-BIPss-CPY*-3HA (Bhamidipati et al., 2005) was used.

C-terminally *HIS* tagged Yos9p was expressed in bacteria using pet23b-Yos9-6HIS (Figure 2B) constructed by amplifying the *YOS9* coding sequence without the signal sequence and inserting it into the *NdeI/XhoI* sites in pet23b. pet23b-Yos9 R200A-6HIS (Figure 2D) was made by subcloning the R200A mutation from pRS315-Yos9 R200A-FLAG3 (Denic et al., 2006) into pet23b-Yos9-6HIS using *NcoI/PacI*. Pet23b-Yos9-8HIS (Figure 2C) was constructed by replacing the 6HIS with a GGS GGS linker and 8HIS tag.

All PCR derived inserts were checked by sequencing. The sequences of the plasmids are available upon request.

Strains

yos9Δ::MET was constructed as previously described (Bhamidipati et al., 2005). *yos9Δ::MET* and BY4741 (S288C, *MATa his3Δ1 leu2Δ0 met15Δ0 ura3Δ0*) were transformed with CPY* and either an empty vector or pRS315-YOS9-FLAG3 (Denic et al., 2006) with or without the glycosylation consensus sites to test whether the glycans on Yos9p are necessary for function (Figure 1A).

Strains for Figure 3 were made by crossing BY4741 with BY4742 (Brachmann et al., 1998) and subsequently deleting *ALG9* with the *Candida glabrata* *HIS3* prototrophic marker (Sakumoto et al., 1999), inserting the *TDH3* promoter in front of *ALG12* using a pFA6a-NATMX4-pTDH3 plasmid (a gift from D. Breslow, based on plasmids from (Longtine et al., 1998)) and deleting either *YOS9*, *DER1* or *HTM1* with the *Candida glabrata* *LEU2* gene using standard PCR-mediated methods at the genomic level. The diploid was then sporulated to obtain haploids that carried the desired combination of markers in the background of *Mat alpha his3Δ1 leu2Δ0 ura3Δ0 +/-lys2Δ0*. Strains for Figure S4 were made by taking the wild-type and single ERAD deletions from the above sporulation and deleting *ALG3* with the *Candida glabrata* *HIS3* prototrophic marker (Sakumoto et al., 1999). All strains altered by genomic insertions or deletions were checked by PCR.

Antibodies

The HA epitope was detected using 12CA5 monoclonal antibody (Roche) or HA.11 (Covance). Anti-hexokinase antibody was purchased from US Biologicals. Secondary

antibodies labeled with IR800 dye and Alex Fluor 680 were purchased from Rockland Immunochemicals and Molecular Probes, Inc, respectively.

Protein Purification

Yos9p protein was expressed in Rosetta (DE3) pLysS cells (Novagen) from pet23b-Yos9-6HIS, Yos9-8HIS, or Yos9 R200A-6HIS. Expression was checked by Coomassie staining and Western analysis using an anti-His antibody (Santa Cruz Biotechnology). Cells were harvested, washed in 10mM Tris-HCL (pH 7.9), resuspended in 50mM Tris-HCL (pH7.9), 1mM EDTA, 150mM NaCl, protease inhibitors and lysed with 100µg/ml lysozyme on ice for 30 minutes plus sonication. Inclusion bodies were pelleted and washed twice with 50mM Tris-HCL (pH 7.9), 1mM EDTA, 2% Triton X-100, and protease inhibitors, and once with 50mM Tris-HCL (pH 7.9), 0.5mM EDTA, and protease inhibitors. The inclusion bodies were then dissolved in Buffer U (25mM Tris-HCL, 8mM 2-mercaptoethanol, 8M urea, protease inhibitors (pH 8.1)), incubate for 1hour and then centrifuged. The supernatant was filtered and bound in batch to Ni-NTA agarose (Qiagen). Bound protein was washed over a column with Buffer U with 0.8M NaCl, followed by a no salt wash and elution with 200mM Imidazole. Pooled fractions containing Yos9p were applied to a Source Q column and eluted using 25mM Tris-HCL, 10mM DTT, 1mM EDTA, 7M Urea, and a gradient of 0-400mM NaCL at pH 8.1. Fractions with protein were pooled, concentrated, and buffer exchanged using a PD-10 column (GE Healthcare) to remove DTT and EDTA. The protein was then refolded by dilution from 5mg/ml into 100mM Tris-HCL (pH 8.5) 150mM NaCl, 1mM CaCl₂, 0.5M L-arginine, 5mM GSH, and 0.5mM GSSG at 4°C over the course of 1.5 hours for a final

concentration of 100 μ g/ml (Lilie et al., 1998; Rudolph and Lilie, 1996). Refolding was monitored by running a SDS-PAGE gel of timepoints treated with 10mM 4-acetamido-4'-maleimidylstilbene-2,2'- disulfonic acid (AMS) or N-ethylmaleimide (NEM). After 24 hours, the protein was concentrated and diluted with 50mM Tris-HCL and 1mM CaCl₂ (pH 8.1) to lower the salt concentration before being applied to a Resource Q column (GE Healthcare) and eluted using 10mM HEPES, 1mM CaCl₂, 10% glycerol, and a 0-400mM NaCl gradient at pH 7.4. Clean fractions were then combined, and buffer exchanged into 10mM HEPES, 1mM CaCl₂, 10% glycerol, and 150mM NaCl (pH 7.4). Final protein was checked for presence of aggregates by gel filtration on a Superdex 200 10/300 GL column (GE Healthcare) and a non-reducing SDS-PAGE gel.

CHAPTER 5

Conclusions

CONCLUSIONS

At the time these studies began, genetic screens and co-immunoprecipitation experiments had implicated a large number of genes to be involved in ERAD but there was limited understanding of what functions each performed and how these activities were coordinated. Furthermore, although progress was being made on the cytosolic ERAD events, the mechanism of the upstream steps of recognition and targeting to the ubiquitination machinery were poorly understood. Biochemical experiments with Yos9p revealed how ERAD factors involved in many distinct aspects of the pathway are assembled into a molecular machine that is capable of carrying out the complicated multistep process of ERAD. These results also shed light on an important role for Hrd3p in the recognition step and led to a model where a bipartite substrate interaction with the Yos9p/Kar2p/Hrd3p surveillance complex promotes specificity by targeting only terminally misfolded proteins to Hrd1p for ubiquitination and degradation. At this point, it became clear that an *in vitro* approach would be valuable. Purified Yos9p provided further insight into the substrate recognition step by showing that Yos9p recognizes a novel class of sugar species that contain a terminal α 1,6-linked mannose residue. *In vivo* experiments then provided evidence for a new role for Htm1p in generating this terminal α 1,6-linked mannose residue after years of limited progress in understanding Htm1p's role in ERAD. Collectively, my studies support the following model: Kar2p-bound potential substrates (either terminally misfolded proteins or folding intermediates) are brought to the Hrd1p ligase complex presumably through interaction of substrate disordered segments with Hrd3p. Yos9p then queries the glycan for the presence of a

terminal α 1,6-linked mannose residue generated by Htm1p. If both signals are present, then the substrate is degraded. Glycoproteins with the wrong glycan signal are released and allowed to continue to fold. Collectively, my findings have provided key insights into Yos9p's role in ERAD and helped define a more comprehensive, mechanistic model for glycoprotein ERAD recognition.

Parallel and subsequent studies have supported different aspects of my research. The Rapoport laboratory co-published complementary data to my finding that ERAD components involved in recognition, ubiquitination and extraction from a core multi-protein complex when they showed that the Hrd1p and Doa10p E3 ubiquitin ligases coordinate distinct complexes that participate in the different ERAD pathways. Additionally, they identified and characterized a new ERAD protein, Usa1p, which we also found when we immunoprecipitated Yos9p (Carvalho et al., 2006). In parallel, using co-immunoprecipitation experiments, Sommer and colleagues also found that Hrd3p and Yos9p are binding partners that complex with Hrd1p. They also showed that Hrd3p interacts with misfolded substrates independent of substrate sugars. In fact, Hrd3p seems to interact more strongly with a non-glycosylatable version of CPY* than with CPY* with its glycans present, which was proposed to be due to the absence of carbohydrates rendering the protein more hydrophobic (Gauss et al., 2006a; Gauss et al., 2006b). As my findings suggested, Aeby and co-workers find that over-expression of Htm1p results in increased production of protein-bound Man₇GlcNAc₂ indicating that Htm1p has mannosidase activity in vivo (Clerc et al., 2009). These data correlates with previous reports that showing that over-expression of EDEM1 and EDEM3 in mammalian cells results in demannosylation, indicating that they are active mannosidases

despite also lacking the conserved cysteine residues thought to potentially be important for enzymatic activity (Hirao et al., 2006b; Olivari et al., 2006). Furthermore, Htm1p was shown to interact with the chaperone PDI (Collins et al., 2007; Krogan et al., 2006), which perhaps hints at how Htm1p selects substrates. Also, it was shown by Ng and colleagues that correctly folded CPY is not degraded even when modified with glycans that have an exposed terminal α 1,6-linked mannose residues, thus reinforcing the requirement for a bipartite signal in ERAD recognition (Xie et al., 2009).

My results also raise new questions and set the stage for future work. How do the mammalian Yos9p homologs function? As with Yos9p, the refolded MRH domain of a Yos9p homolog, OS-9, has been shown to have an affinity for glycans with an exposed terminal α 1,6-linked mannose residue (Hosokawa et al., 2009). Additionally, both OS-9 and another Yos9p homolog, XTP3, interact with the mammalian Hrd3p homolog, SEL1, and ERAD substrates independent of their sugars (Bernasconi et al., 2008; Christianson et al., 2008; Hosokawa et al., 2008). However, these initial studies reveal some differences between the yeast and mammalian homologs, suggesting that further studies are needed to understand the roles of OS-9 and XTP3 in mammalian ERAD.

Other directions for future work include understanding further mechanistic details of how Htm1p, Hrd3p, and Yos9p recognize and commit substrates for degradation. First, can Htm1p α -mannosidase activity be shown in vitro? How does Htm1p recognize its substrates? Is it purely a “timer” or does it act specifically on substrates that are non-native? Secondly, how do Yos9p and Hrd3p work with each other? Do Hrd3p and Yos9p have chaperone-like qualities to prevent aggregation? Do they detect different determinants than those that are potentially recognized Htm1p? If non-ERAD substrates

are recruited to the complex by Hrd3p and escape degradation because they do not have a bipartite signal, is there a specific mechanism for release? What happens after Yos9p recognizes substrates for degradation? Specifically, is Der1p or another factor recruited into the complex or is there a change in oligomerization state? The answer to many of these questions may require structural studies of these components as well as probing the recognition steps in vitro. An ideal system of in vitro reconstitution of the degradation of an ERAD-L substrate would be a powerful technique to address these questions but has so far not been attainable perhaps due to the complexity of the upstream glycan trimming steps. However, with many key components of the ERAD machinery known and improved characterization of the basic features of substrate recognition, especially by Yos9p, generation of a synthetic substrate with a specific glycan will be an important tool for vitro recognition studies and also a good starting point for reconstitution of degradation.

APPENDIX A

Unpublished Data

APPENDIX A

This appendix reports some of the unpublished work done in parallel with Chapter 4. Once we worked out the Yos9p/Hrd3p bipartite model of recognition which indicated that Hrd3p recruited misfolded proteins to the ERAD complex and Yos9p was needed for a second sugar dependent commitment step (Chapter 3), I felt that the next step toward understanding this mechanism, necessitated in vitro experiments with better resolution to add to the standard co-immunoprecipitation experiments. Thus, I started a series of preliminary experiments to inform us about how to make the pieces to put together an in vitro recognition system consisting of Hrd3p, Yos9p, and a peptide substrate. The Yos9p purification and characterization is published and presented in Chapter 4.

Similar to Yos9p, producing biochemical amounts of Hrd3p presents a technical challenge as Hrd3p has five glycan consensus sites and many disulfide bonds. First, I mutated the N-linked glycosylation sites individually or all together to check for functionality by the cycloheximide degradation assay (Figure 1). Unfortunately, while Hrd3p with its transmembrane domain removed and C-terminally tagged (Hrd3₁₋₇₆₇myc) is functional when modified in the genome (Denic et al., 2006), the CEN/ARS plasmid expressing Hrd3₁₋₇₆₇myc is only partially functional (Figure 1A). The presence of a tag on the plasmid does not affect the outcome, as the untagged version shows a similar defect (Figure 1A). Expression from a 2 μ m plasmid makes the defect worse (data not shown). Since there is still a dynamic range between the wild-type Hrd3p plasmid and a deletion of Hrd3p, we decided to analyze the Hrd3p sugar mutants using the plasmid. No single glycosylation mutant affects the function in comparison to the wild-type plasmid

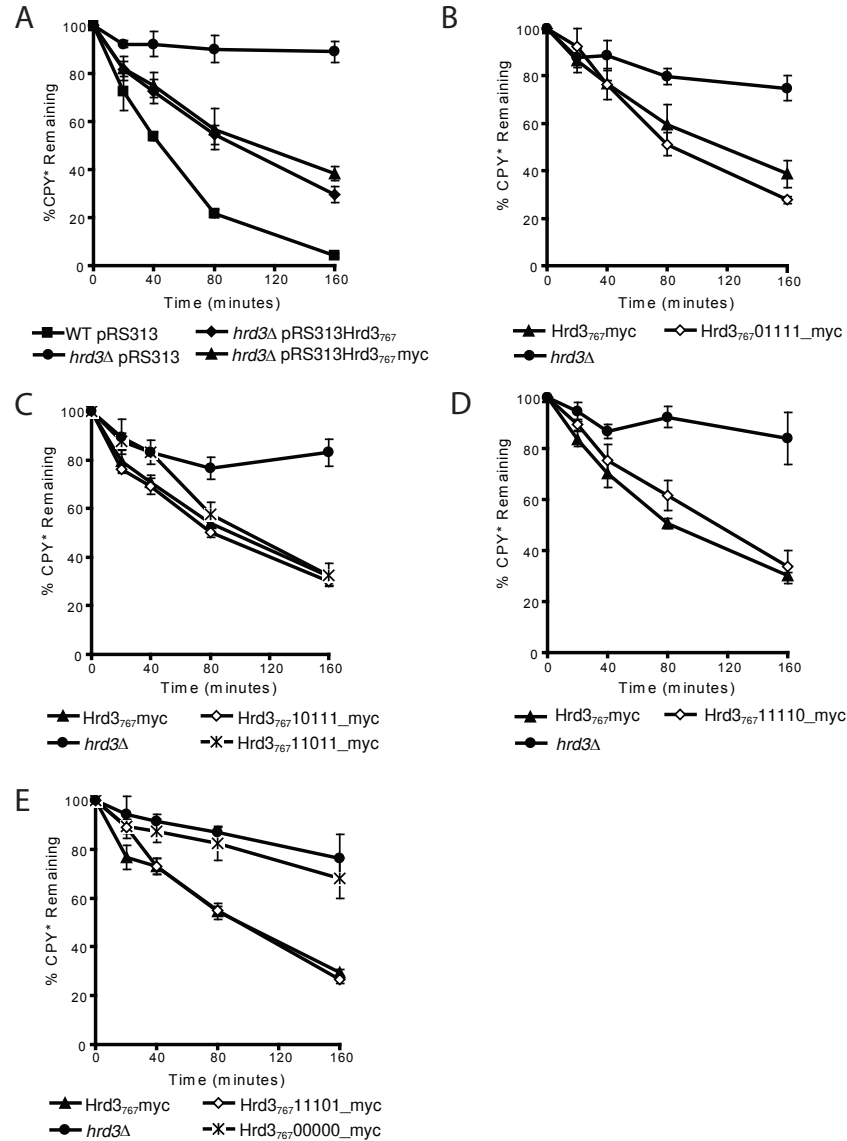


Figure 1. Hrd3p requires its glycans to function in ERAD

(A) Degradation of CPY* in wild-type (WT; ■) and *hrd3Δ* strain (●) harboring a empty vector, and *hrd3Δ* covered by a plasmid expressing Hrd3₁₋₇₆₇13myc (▲) or Hrd3₁₋₇₆₇ (◆) were monitored by cycloheximide chase. Equal amounts of log phase cells were removed at the indicated times following addition of cycloheximide. Samples were resolved by SDS-PAGE and detected by Western analysis using anti-HA and anti-hexokinase antibodies. Each time point represents the average and +/- standard error of the mean (SEM) of 4 measurements (two independent experiments done in duplicate) and normalized to the hexokinase loading control.

(B) Degradation of CPY* in *hrd3Δ* strain covered by an empty vector (●) or a plasmid expressing Hrd3₁₋₇₆₇13myc (▲) or Hrd3₁₋₇₆₇13myc with the first glycan consensus site mutated (01111; ◇). “0” represents the mutated glycan consensus site and “1” represents the native glycan consensus site.

(C) Degradation of CPY* in *hrd3Δ* strain covered by an empty vector (●) or a plasmid expressing Hrd3₁₋₇₆₇13myc (▲) or Hrd3₁₋₇₆₇13myc with the second glycan consensus site mutated (10111; ◇) or Hrd3₁₋₇₆₇13myc with the third glycan consensus site mutated (11011; *).

(D) Degradation of CPY* in *hrd3Δ* strain covered by an empty vector (●) or a plasmid expressing Hrd3₁₋₇₆₇13myc (▲) or Hrd3₁₋₇₆₇13myc with the fifth glycan consensus site mutated (11110; ◇).

(E) Degradation of CPY* in *hrd3Δ* strain covered by an empty vector (●) or a plasmid expressing Hrd3₁₋₇₆₇13myc (▲) or Hrd3₁₋₇₆₇13myc with the fourth glycan consensus site mutated (11101; ◇) or all the glycan consensus sites mutated (00000; *).

(Figure 1), however, mutation of all five consensus sites results in a defect equivalent to the absence of *HRD3* (Figure 1E). It is unclear why having the glycans present are necessary for Hrd3p function. In light of the fact that the non-glycosylatable version of Hrd3p results in a decrease in protein levels (data not shown), a likely possibility is that the sugars are necessary to help with the folding of the protein and thus losing all five makes the protein fold incorrectly, whereas the other four glycans can make up for the loss of one. Another possibility is that the sugars on Hrd3p are playing a signaling role in ERAD and that some combination of them is necessary. Experiments with these mutants integrated in the genome should make future experiments to distinguish between these options easier. In any case, these results indicated that it is necessary to make Hrd3p from a eukaryotic source. Initial attempts at expressing and purifying Hrd3₁₋₇₆₇ with a 3HA-TEV-8HIS tag from a 2µm plasmid with a galactose inducible promoter in *Saccharomyces cerevisiae* as described previously (Tu et al., 2000) yielded much of the Hrd3p in the insoluble fraction.

In addition to Yos9p and Hr3p, a substrate is necessary to set up an in vitro recognition system. To determine a minimal substrate determinant that binds to Hrd3p in hopes of both trying to classify what Hrd3p is recognizing as well as a to find a small peptide for purification, I constructed a soluble domain (DHFR) attached to different CPY*0000 pieces. Because sugars not necessary for interaction, I used pieces of the non-glycosylatable version of CPY*, with the idea that if I identified a region containing a sugar consensus site, I would revert to the native sequence and assay for the ability of the peptide to be degraded or confer degradation. First, in the absence of *YOS9*, *DER1*, and *HRD1*, I assayed the full length CPY* (A), CPY*0000 (B), the N-terminal half of

CPY*0000 (C), the C-terminal half of CPY*0000 (D) and the C-terminal quarter of CPY*0000 (E). All these constructs interacted with Hrd3₁₋₇₆₇myc to differing degrees, indicating that there might be more than one interaction epitope (Figure 2A). We decided to focus on the C-terminal quarter of CPY*0000 because the Asn-368-linked glycan, the most C-terminal glycan is necessary and sufficient for degradation of CPY* is located in that region (Kostova and Wolf, 2005; Spear and Ng, 2005). Cutting in by approximately 18 amino acids on both ends of the C-terminal quarter of CPY*0000 yielded 8 constructs (F-L) that all interacted with Hrd3₁₋₇₆₇myc to differing degrees (Figure 2B). Construct “E”, “F” and “J” reproducibly interacted more strongly with Hrd3₁₋₇₆₇myc. Further work is necessary to show whether these pieces are degraded in the presence of the glycan. Unexpectedly, the DHFR-CPY*0000 constructs were expressed as doublets. Previous experiments with Kar2 signal sequence attached to DHFR-CPY* (Bhamidipati et al., 2005) showed that this was sufficient to insert the construct into the ER. EndoH analysis (Figure C) revealed that surprisingly, the constructs seem to be glycosylated as EndoH causes the doublet to collapse into a single band for all the constructs containing a CPY*0000 piece. However, sequencing confirms the lack of a consensus glycan sequence making this result puzzling.

The differential affinity of CPY*0000 piece “J” and “K” with Hrd3_{p1-767}-myc made them good candidates to purify from *E. coli*. Expression and purification of full length and the “J” and “K” CPY*0000 pieces using a N-terminal maltose binding protein (MBP) resulted in soluble protein although the smaller pieces are considerably more soluble than the full length versions (Figure 3). Rosetta (DE3) pLysS cells shown in Figure 3 yielded more soluble protein than BL21 (DE3) cells. Like the aforementioned

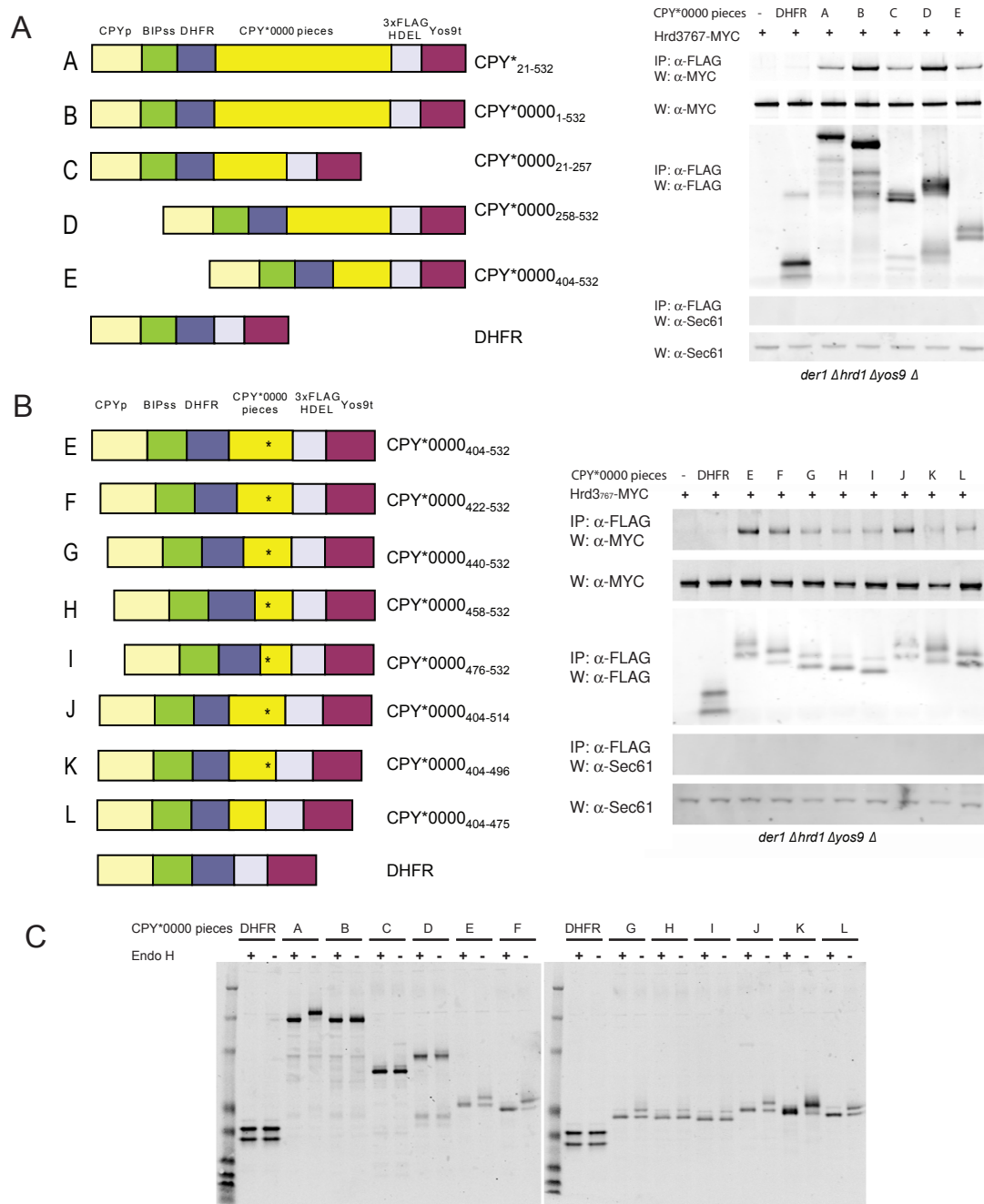


Figure 2. Hrd3p interaction with non-glycosylatable DHFR-CPY* pieces

(A) *der1Δ yos9Δ hrd1Δ* cells expressing Hrd3₁₋₇₆₇13myc were transformed with an empty vector or a vector expressing the indicated piece of DHFR-CPY*0000 and subjected to immunoprecipitation. Total cell lysates were solubilized with 1% Triton X-100, cleared and immunoprecipitated with anti-FLAG resin. Bound proteins were eluted by boiling in SDS loading buffer and along with total cell lysates were resolved by SDS-PAGE followed by Western blot analysis. (B) *der1Δ yos9Δ hrd1Δ* cells expressing Hrd3₁₋₇₆₇13myc were transformed with an empty vector or a vector expressing the indicated piece of DHFR-CPY*0000 and subjected to immunoprecipitation as in Figure 2A. * indicates the location of Asn368.

(C) *der1Δ yos9Δ hrd1Δ* cells expressing Hrd3₁₋₇₆₇13myc were transformed with an empty vector or a vector expressing the indicated piece of DHFR-CPY*0000 was lysed by SDS loading buffer before being subjected to deglycosylation by EndoH. Equal amounts were analyzed by SDS-PAGE followed by Western analysis.

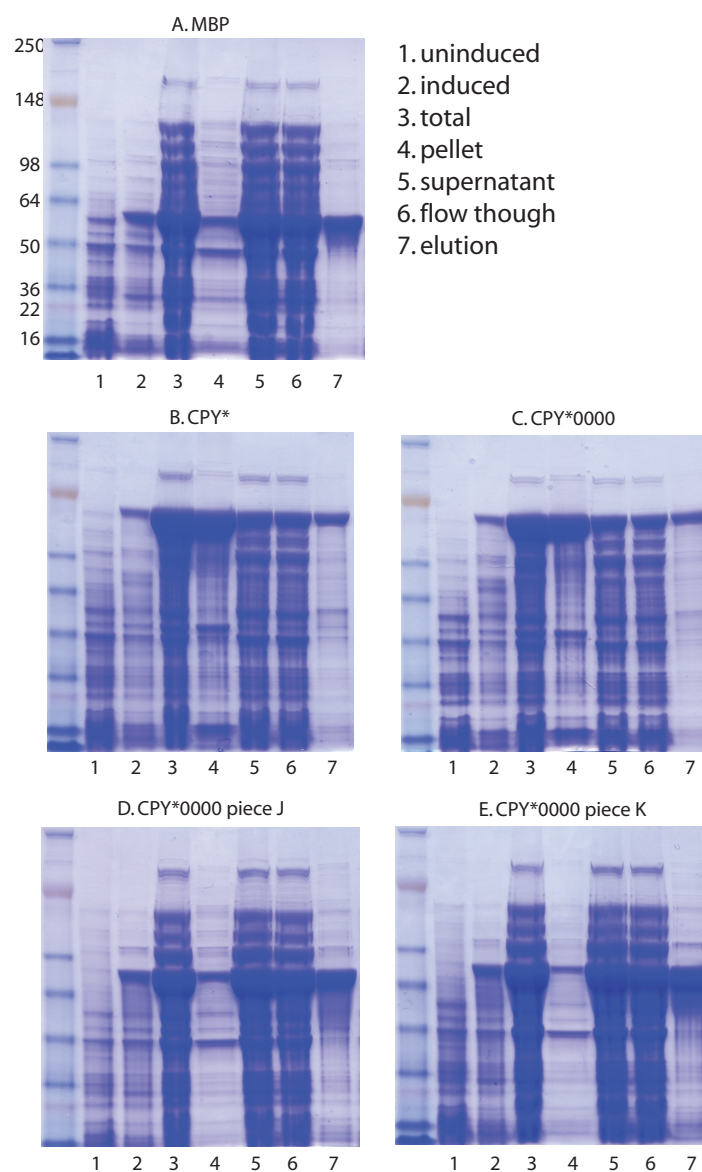


Figure 3. Bacterial expression of MBP-CPY* variants

(A) Maltose binding protein (MBP) expressed in Rosetta pLysS cells (induced) were lysed (total), spun at 10,000g (supernatant and pellet), and then affinity purified by amylose resin (flow through) and the eluted with SDS PAGE loading buffer (elution) and analyzed by SDS-PAGE followed by Coomassie staining.

(B) MBP-CPY* was analyzed as in Figure 3A.

(C) MBP-CPY*0000 (non-glycosylatable CPY*) was analyzed as in Figure 3A.

(D) MBP-CPY*0000₄₀₄₋₅₁₄ (non-glycosylatable CPY* piece J as indicated in Figure 2B) was analyzed as in Figure 3A.

(E) MBP-CPY*0000₄₀₄₋₄₉₆ (non-glycosylatable CPY* piece K as indicated in Figure 2B) was analyzed as in Figure 3A.

experiments, these results provide a basis for further study but follow-up and improvement of these tools is necessary.

Experimental Procedures

Plasmid construction

Hrd3p with the glycan consensus sites mutated (Figure 1) was made by using QuikChange mutagenesis (Stratagene) to change N to Q in the indicated N-X-S/T sites in the coding region of a C-terminal 13MYC-tagged Hrd3₁₋₇₆₇p expressed from its endogenous promoter on a CEN/ARS plasmid. Hrd3p promoter length dictated by the 3' end of the gene located 5' of it. For cycloheximide degradation assays, CEN/ARS CPY*-HA was made as described in Chapter 4 (Quan et al., 2008). The Kar2ss-DHFR-3xFLAG plasmid was made by inserting the fusion PCR product of the promoter, signal sequence and DHFR from the DHFR-CPY*-HA plasmid described in Chapter 2 (Bhamidipati et al., 2005) with the 3xFLAG and Yos9p terminator from the pRS315-Yos9-3XFLAG plasmid described in Chapter 3 (Denic et al., 2006) into a CEN/ARS backbone. DHFR-CPY* pieces (Figure 2) generated by PCR from CPY*/CPY*0000 plasmids (Denic et al., 2006) were inserted in frame with the DHFR and 3xFLAG in the Kar2ss-DHFR-3xFLAG plasmid. The MPB constructs were generated by inserting the indicated pieces into a pMal-c2x plasmid (NEB) modified by the Lim lab to include a TEV site instead of Factor Xa site.

Strains

Hrd3₁₋₇₆₇-13MYC Δ yos9 Δ der1 Δ hard1 and Δ hrd3 strains were described in Chapter 3 (Denic et al., 2006). MBP constructs were expressed in Rosetta (DE3) pLysS cells or BL21 (DE3) cells (Novagen).

Cycloheximide Degradation Assay and Native immunoprecipitations - small scale

Cycloheximide degradation assays and native immunoprecipitation assays were performed as previously described (Denic et al., 2006).

MBP affinity purification

Bacterial pellets were resuspended in 20mM HEPES pH 7.4, 200mM NaCl, 1mM EDTA, 5% glycerol and 1mM PMSF and treated with lysozyme before sonication. The lysate was centrifuged at 10,000g for 20 minutes and amylose resin was added to the supernatant for an half an hour at 4 degrees followed by washes with the above buffer. Bound protein was eluted from the beads with SDS-PAGE loading buffer and subjected to SDS-PAGE followed by Coomassie staining. Expression and elution was confirmed by Western analysis with an anti-MBP antibody (NEB).

APPENDIX B

References

Adams, J. (2002). Preclinical and clinical evaluation of proteasome inhibitor PS-341 for the treatment of cancer. *Curr Opin Chem Biol* 6, 493-500.

Ahner, A., and Brodsky, J. L. (2004). Checkpoints in ER-associated degradation: excuse me, which way to the proteasome? *Trends Cell Biol* 14, 474-478.

Anelli, T., and Sitia, R. (2008). Protein quality control in the early secretory pathway. *Embo J* 27, 315-327.

Anfinsen, C. B. (1973). Principles that govern the folding of protein chains. *Science* 181, 223-230.

Avezov, E., Frenkel, Z., Ehrlich, M., Herscovics, A., and Lederkremer, G. Z. (2008). Endoplasmic Reticulum (ER) Mannosidase I Is Compartmentalized and Required for N-Glycan Trimming to Man5 6GlcNAc2 in Glycoprotein ER-associated Degradation. *Mol Biol Cell* 19, 216-225.

Baek, J. H., Mahon, P. C., Oh, J., Kelly, B., Krishnamachary, B., Pearson, M., Chan, D. A., Giaccia, A. J., and Semenza, G. L. (2005). OS-9 Interacts with Hypoxia-Inducible Factor 1alpha and Prolyl Hydroxylases to Promote Oxygen-Dependent Degradation of HIF-1alpha. *Mol Cell* 17, 503-512.

Bays, N. W., Gardner, R. G., Seelig, L. P., Joazeiro, C. A., and Hampton, R. Y. (2001). Hrd1p/Der3p is a membrane-anchored ubiquitin ligase required for ER-associated degradation. *Nat Cell Biol* 3, 24-29.

Belden, W. J., and Barlowe, C. (2001). Role of Erv29p in collecting soluble secretory proteins into ER-derived transport vesicles. *Science* 294, 1528-1531.

Bernasconi, R., Pertel, T., Luban, J., and Molinari, M. (2008). A dual task for the Xbp1-responsive OS-9 variants in the mammalian endoplasmic reticulum: inhibiting secretion of misfolded protein conformers and enhancing their disposal. *J Biol Chem* 283, 16446-16454.

Bhamidipati, A., Denic, V., Quan, E. M., and Weissman, J. S. (2005). Exploration of the topological requirements of ERAD identifies Yos9p as a lectin sensor of misfolded glycoproteins in the ER lumen. *Mol Cell* 19, 741-751.

Biederer, T., Volkwein, C., and Sommer, T. (1997). Role of Cue1p in ubiquitination and degradation at the ER surface. *Science* 278, 1806-1809.

Blobel, G., and Dobberstein, B. (1975). Transfer to proteins across membranes. II. Reconstitution of functional rough microsomes from heterologous components. *J Cell Biol* 67, 852-862.

Bonifacino, J. S., Suzuki, C. K., and Klausner, R. D. (1990). A peptide sequence confers retention and rapid degradation in the endoplasmic reticulum. *Science* 247, 79-82.

Bordallo, J., Plemper, R. K., Finger, A., and Wolf, D. H. (1998). Der3p/Hrd1p is required for endoplasmic reticulum-associated degradation of misfolded luminal and integral membrane proteins. *Molecular Biology of the Cell* 9, 209-222.

Brachmann, C. B., Davies, A., Cost, G. J., Caputo, E., Li, J., Hieter, P., and Boeke, J. D. (1998). Designer deletion strains derived from *Saccharomyces cerevisiae* S288C: a useful set of strains and plasmids for PCR-mediated gene disruption and other applications. *Yeast* 14, 115-132.

Brodsky, J. L., Hamamoto, S., Feldheim, D., and Schekman, R. (1993). Reconstitution of protein translocation from solubilized yeast membranes reveals topologically distinct roles for BiP and cytosolic Hsc70. *J Cell Biol* 120, 95-102.

Burda, P., Jakob, C. A., Beinhauer, J., Hegemann, J. H., and Aebl, M. (1999). Ordered assembly of the asymmetrically branched lipid-linked oligosaccharide in the endoplasmic reticulum is ensured by the substrate specificity of the individual glycosyltransferases. *Glycobiology* 9, 617-625.

Buschhorn, B. A., Kostova, Z., Medicherla, B., and Wolf, D. H. (2004). A genome-wide screen identifies Yos9p as essential for ER-associated degradation of glycoproteins. *FEBS Lett* 577, 422-426.

Byrd, J. C., Tarentino, A. L., Maley, F., Atkinson, P. H., and Trimble, R. B. (1982). Glycoprotein synthesis in yeast. Identification of Man8GlcNAc2 as an essential intermediate in oligosaccharide processing. *J Biol Chem* 257, 14657-14666.

Caramelo, J. J., and Parodi, A. J. (2007). How sugars convey information on protein conformation in the endoplasmic reticulum. *Semin Cell Dev Biol* 18, 732-742.

Carvalho, P., Goder, V., and Rapoport, T. A. (2006). Distinct ubiquitin-ligase complexes define convergent pathways for the degradation of ER proteins. *Cell* 126, 361-373.

Casagrande, R., Stern, P., Diehn, M., Shamu, C., Osario, M., Zuniga, M., Brown, P. O., and Ploegh, H. (2000). Degradation of proteins from the ER of *S. cerevisiae* requires an intact unfolded protein response pathway. *Mol Cell* 5, 729-735.

Christianson, J. C., Shaler, T. A., Tyler, R. E., and Kopito, R. R. (2008). OS-9 and GRP94 deliver mutant alpha1-antitrypsin to the Hrd1-SEL1L ubiquitin ligase complex for ERAD. *Nat Cell Biol* 10, 272-282.

Clerc, S., Hirsch, C., Oggier, D. M., Deprez, P., Jakob, C., Sommer, T., and Aebl, M. (2009). Htm1 protein generates the N-glycan signal for glycoprotein degradation in the endoplasmic reticulum. *J Cell Biol* 184, 159-172.

Collins, S. R., Miller, K. M., Maas, N. L., Roguev, A., Fillingham, J., Chu, C. S., Schuldiner, M., Gebbia, M., Recht, J., Shales, M., *et al.* (2007). Functional dissection of protein complexes involved in yeast chromosome biology using a genetic interaction map. *Nature* 446, 806-810.

Craven, R. A., Egerton, M., and Stirling, C. J. (1996). A novel Hsp70 of the yeast ER lumen is required for the efficient translocation of a number of protein precursors. *Embo Journal* 15, 2640-2650.

Deak, P. M., and Wolf, D. H. (2001). Membrane topology and function of Der3/Hrd1p as an ubiquitin-ligase (E3) involved in endoplasmic reticulum degradation. *J Biol Chem* 276, 10663-10669.

Delneri, D., Gardner, D. C., Bruschi, C. V., and Oliver, S. G. (1999). Disruption of seven hypothetical aryl alcohol dehydrogenase genes from *Saccharomyces cerevisiae* and construction of a multiple knock-out strain. *Yeast* 15, 1681-1689.

Denic, V., Quan, E. M., and Weissman, J. S. (2006). A luminal surveillance complex that selects misfolded glycoproteins for ER-associated degradation. *Cell* 126, 349-359.

Drumm, M. L., Wilkinson, D. J., Smit, L. S., Worrell, R. T., Strong, T. V., Frizzell, R. A., Dawson, D. C., and Collins, F. S. (1991). Chloride conductance expressed by delta F508 and other mutant CFTRs in *Xenopus* oocytes. *Science* 254, 1797-1799.

Eilers, M., and Schatz, G. (1986). Binding of a specific ligand inhibits import of a purified precursor protein into mitochondria. *Nature* 322, 228-232.

Ellgaard, L., and Helenius, A. (2003). Quality control in the endoplasmic reticulum. *Nat Rev Mol Cell Biol* 4, 181-191.

Fewell, S. W., Travers, K. J., Weissman, J. S., and Brodsky, J. L. (2001). The action of molecular chaperones in the early secretory pathway. *Annu Rev Genet* 35, 149-191.

Fewell, S. W., Travers, K. J., Weissman, J. S., and Brodsky, J. L. (2001). The action of molecular chaperones in the early secretory pathway. *Annual Review of Genetics* 35.

Fiebigler, E., Story, C., Ploegh, H. L., and Tortorella, D. (2002). Visualization of the ER-to-cytosol dislocation reaction of a type I membrane protein. *Embo J* 21, 1041-1053.

Finger, A., Knop, M., and Wolf, D. H. (1993). Analysis of two mutated vacuolar proteins reveals a degradation pathway in the endoplasmic reticulum or a related compartment of yeast. *Eur J Biochem* 218, 565-574.

Flower, A. M., Doebele, R. C., and Silhavy, T. J. (1994). PrlA and PrlG suppressors reduce the requirement for signal sequence recognition. *J Bacteriol* 176, 5607-5614.

Flynn, G. C., Pohl, J., Flocco, M. T., and Rothman, J. E. (1991). Peptide-binding specificity of the molecular chaperone BiP. *Nature* 353, 726-730.

Frenkel, Z., Gregory, W., Kornfeld, S., and Lederkremer, G. Z. (2003). Endoplasmic reticulum-associated degradation of mammalian glycoproteins involves sugar chain trimming to Man6-5GlcNAc2. *J Biol Chem* 278, 34119-34124.

Friedlander, R., Jarosch, E., Urban, J., Volkwein, C., and Sommer, T. (2000). A regulatory link between ER-associated protein degradation and the unfolded-protein response. *Nat Cell Biol* 2, 379-384.

Friedmann, E., Salzberg, Y., Weinberger, A., Shaltiel, S., and Gerst, J. E. (2002). YOS9, the putative yeast homolog of a gene amplified in osteosarcomas, is involved in the endoplasmic reticulum (ER)-Golgi transport of GPI-anchored proteins. *J Biol Chem* 277, 35274-35281.

Gardner, R. G., Shearer, A. G., and Hampton, R. Y. (2001). In vivo action of the HRD ubiquitin ligase complex: mechanisms of endoplasmic reticulum quality control and sterol regulation. *Mol Cell Biol* 21, 4276-4291.

Gardner, R. G., Swarbrick, G. M., Bays, N. W., Cronin, S. R., Wilhovsky, S., Seelig, L., Kim, C., and Hampton, R. Y. (2000). Endoplasmic reticulum degradation requires lumen to cytosol signaling. Transmembrane control of Hrd1p by Hrd3p. *J Cell Biol* 151, 69-82.

Gauss, R., Jarosch, E., Sommer, T., and Hirsch, C. (2006a). A complex of Yos9p and the HRD ligase integrates endoplasmic reticulum quality control into the degradation machinery. *Nat Cell Biol* 8, 849-854.

Gauss, R., Sommer, T., and Jarosch, E. (2006b). The Hrd1p ligase complex forms a linchpin between ER-luminal substrate selection and Cdc48p recruitment. *Embo J* 25, 1827-1835.

Ghaemmaghami, S., Huh, W. K., Bower, K., Howson, R. W., Belle, A., Dephoure, N., O'Shea, E. K., and Weissman, J. S. (2003). Global analysis of protein expression in yeast. *Nature* 425, 737-741.

Ghosh, P., Dahms, N. M., and Kornfeld, S. (2003). Mannose 6-phosphate receptors: new twists in the tale. *Nat Rev Mol Cell Biol* 4, 202-212.

Goldberger, R. F., Epstein, C. J., and Anfinsen, C. B. (1963). Purification and properties of a microsomal enzyme system catalyzing the reactivation of reduced ribonuclease and lysozyme. *J Biol Chem* 238, 1406-1410.

Goldstein, A. L., and McCusker, J. H. (1999). Three new dominant drug resistance cassettes for gene disruption in *Saccharomyces cerevisiae*. *Yeast* 15, 1541-1553.

Guthrie, C., and Fink, G. (1991). Guide to Yeast Genetics and Molecular Biology. *Methods in Enzymology* 194, 933.

Hampton, R. Y., and Bhakta, H. (1997). Ubiquitin-mediated regulation of 3-hydroxy-3-methylglutaryl-CoA reductase. *Proceedings of the National Academy of Sciences of the United States of America* 94, 12944-12948.

Hampton, R. Y., Gardner, R. G., and Rine, J. (1996). Role of 26S proteasome and HRD genes in the degradation of 3-hydroxy-3-methylglutaryl-CoA reductase, an integral endoplasmic reticulum membrane protein. *Mol Biol Cell* 7, 2029-2044.

Hancock, M. K., Haskins, D. J., Sun, G., and Dahms, N. M. (2002). Identification of residues essential for carbohydrate recognition by the insulin-like growth factor II/mannose 6-phosphate receptor. *J Biol Chem* 277, 11255-11264.

Hartl, F. U., and Hayer-Hartl, M. (2009). Converging concepts of protein folding in vitro and in vivo. *Nat Struct Mol Biol* 16, 574-581.

Hebert, D. N., Garman, S. C., and Molinari, M. (2005). The glycan code of the endoplasmic reticulum: asparagine-linked carbohydrates as protein maturation and quality-control tags. *Trends Cell Biol* 15, 364-370.

Hebert, D. N., and Molinari, M. (2007). In and out of the ER: protein folding, quality control, degradation, and related human diseases. *Physiol Rev* 87, 1377-1408.

Helenius, A. (1994). How N-linked oligosaccharides affect glycoprotein folding in the endoplasmic reticulum. *Mol Biol Cell* 5, 253-265.

Helenius, A., and Aebi, M. (2001). Intracellular functions of N-linked glycans. *Science* 291, 2364-2369.

Helenius, A., and Aebi, M. (2004). Roles of N-linked glycans in the endoplasmic reticulum. *Annu Rev Biochem* 73, 1019-1049.

Herscovics, A. (2001). Structure and function of Class I alpha 1,2-mannosidases involved in glycoprotein synthesis and endoplasmic reticulum quality control. *Biochimie* 83, 757-762.

Hiller, M. M., Finger, A., Schweiger, M., and Wolf, D. H. (1996). ER degradation of a misfolded luminal protein by the cytosolic ubiquitin-proteasome pathway. *Science* 273, 1725-1728.

Hirabayashi, J., Arata, Y., and Kasai, K. (2003). Frontal affinity chromatography as a tool for elucidation of sugar recognition properties of lectins. *Methods Enzymol* 362, 353-368.

Hirao, K., Natsuka, Y., Tamura, T., Wada, I., Morito, D., Natsuka, S., Romero, P., Sleno, B., Tremblay, L. O., Herscovics, A., *et al.* (2006a). EDEM3, a soluble EDEM homolog, enhances glycoprotein endoplasmic reticulum-associated degradation and mannose trimming. *J Biol Chem* 281, 9650-9658.

Hirao, K., Natsuka, Y., Tamura, T., Wada, I., Morito, D., Natsuka, S., Romero, P., Sleno, B., Tremblay, L. O., Herscovics, A., *et al.* (2006b). EDEM3, a soluble EDEM homolog, enhances glycoprotein ERAD and mannose trimming. *J Biol Chem*.

Hirsch, C., Jarosch, E., Sommer, T., and Wolf, D. H. (2004). Endoplasmic reticulum-associated protein degradation--one model fits all? *Biochim Biophys Acta* 1695, 215-223.

Hitt, R., and Wolf, D. H. (2004a). Der1p, a protein required for degradation of malformed soluble proteins of the endoplasmic reticulum: topology and Der1-like proteins. *FEMS Yeast Res* 4, 721-729.

Hitt, R., and Wolf, D. H. (2004b). DER7, encoding alpha-glucosidase I is essential for degradation of malformed glycoproteins of the endoplasmic reticulum. *FEMS Yeast Res* 4, 815-820.

Hopfield, J. J. (1974). Kinetic proofreading: a new mechanism for reducing errors in biosynthetic processes requiring high specificity. *Proc Natl Acad Sci U S A* 71, 4135-4139.

Hosokawa, N., Kamiya, Y., Kamiya, D., Kato, K., and Nagata, K. (2009). Human OS-9, a lectin required for glycoprotein endoplasmic reticulum-associated degradation, recognizes mannose-trimmed N-glycans. *J Biol Chem* 284, 17061-17068.

Hosokawa, N., Tremblay, L. O., You, Z., Herscovics, A., Wada, I., and Nagata, K. (2003). Enhancement of endoplasmic reticulum (ER) degradation of misfolded Null Hong Kong alpha1-antitrypsin by human ER mannosidase I. *J Biol Chem* 278, 26287-26294.

Hosokawa, N., Wada, I., Hasegawa, K., Yorihuzi, T., Tremblay, L. O., Herscovics, A., and Nagata, K. (2001). A novel ER alpha-mannosidase-like protein accelerates ER-associated degradation. *EMBO Rep* 2, 415-422.

Hosokawa, N., Wada, I., Nagasawa, K., Moriyama, T., Okawa, K., and Nagata, K. (2008). Human XTP3-B forms an endoplasmic reticulum quality control scaffold with the HRD1-SEL1L ubiquitin ligase complex and BiP. *J Biol Chem* 283, 20914-20924.

Huh, W. K., Falvo, J. V., Gerke, L. C., Carroll, A. S., Howson, R. W., Weissman, J. S., and O'Shea, E. K. (2003). Global analysis of protein localization in budding yeast. *Nature* 425, 686-691.

Huyer, G., Piluek, W. F., Fansler, Z., Kreft, S. G., Hochstrasser, M., Brodsky, J. L., and Michaelis, S. (2004). Distinct machinery is required in *Saccharomyces cerevisiae* for the endoplasmic reticulum-associated degradation of a multispreading membrane protein and a soluble luminal protein. *J Biol Chem* 279, 38369-38378.

Jahn, T. R., and Radford, S. E. (2005). The Yin and Yang of protein folding. *Febs J* 272, 5962-5970.

Jakob, C. A., Bodmer, D., Spirig, U., Battig, P., Marcil, A., Dignard, D., Bergeron, J. J., Thomas, D. Y., and Aebi, M. (2001). Htm1p, a mannosidase-like protein, is involved in glycoprotein degradation in yeast. *EMBO Rep* 2, 423-430.

Jakob, C. A., Burda, P., Roth, J., and Aebi, M. (1998a). Degradation of mis-folded endoplasmic reticulum glycoproteins in *Saccharomyces cerevisiae* is determined by a specific oligosaccharide structure. *J Cell Biol* 142, 1223-1233.

Jakob, C. A., Burda, P., te Heesen, S., Aebi, M., and Roth, J. (1998b). Genetic tailoring of N-linked oligosaccharides: the role of glucose residues in glycoprotein processing of *Saccharomyces cerevisiae* in vivo. *Glycobiology* 8, 155-164.

Jarosch, E., Taxis, C., Volkwein, C., Bordallo, J., Finley, D., Wolf, D. H., and Sommer, T. (2002). Protein dislocation from the ER requires polyubiquitination and the AAA-ATPase Cdc48. *Nat Cell Biol* 4, 134-139.

Jensen, T. J., Loo, M. A., Pind, S., Williams, D. B., Goldberg, A. L., and Riordan, J. R. (1995). Multiple proteolytic systems, including the proteasome, contribute to CFTR processing. *Cell* 83, 129-135.

Jimenez, C. R., Huang, L., Qiu, Y., and Burlingame, A. L. (1998). In-Gel Digestion of Proteins for MALDI-MS Fingerprint Mapping. *Current Protocols in Protein Science* 16.4.1-16.4.5.

Johnson, A. E., and Haigh, N. G. (2000). The ER translocon and retrotranslocation: is the shift into reverse manual or automatic? *Cell* 102, 709-712.

Johnston, J. A., Johnson, E. S., Waller, P. R., and Varshavsky, A. (1995). Methotrexate inhibits proteolysis of dihydrofolate reductase by the N-end rule pathway. *Journal of Biological Chemistry* 270, 8172-8178.

Kabani, M., Beckerich, J. M., and Gaillardin, C. (2000). Sls1p stimulates the Sec63p-mediated activation of Kar2p in a conformation dependent manner in the yeast endoplasmic reticulum. *Mol Cell Biol* 20, 6923-6934.

Kabani, M., Kelley, S. S., Morrow, M. W., Montgomery, D. L., Sivendran, R., Rose, M. D., Gierasch, L. M., and Brodsky, J. L. (2003). Dependence of endoplasmic reticulum-associated degradation on the peptide binding domain and concentration of BiP. *Mol Biol Cell* 14, 3437-3448.

Kamiya, Y., Kamiya, D., Yamamoto, K., Nyfeler, B., Hauri, H. P., and Kato, K. (2008). Molecular basis of sugar recognition by the human L-type lectins ERGIC-53, VIPL, and VIP36. *J Biol Chem* 283, 1857-1861.

Kamiya, Y., Yamaguchi, Y., Takahashi, N., Arata, Y., Kasai, K., Ihara, Y., Matsuo, I., Ito, Y., Yamamoto, K., and Kato, K. (2005). Sugar-binding properties of VIP36, an intracellular animal lectin operating as a cargo receptor. *J Biol Chem* 280, 37178-37182.

Kanehara, K., Kawaguchi, S., and Ng, D. T. (2007). The EDEM and Yos9p families of lectin-like ERAD factors. *Semin Cell Dev Biol* 18, 743-750.

Kasai, K., Oda, Y., Nishikawa, M., and Ishii, S. (1986). Frontal affinity chromatography: theory for its application to studies on specofoc interactions of biomolecules. *J Chromatogr* 376, 33-47.

Kaufman, R. J. (2004). Regulation of mRNA translation by protein folding in the endoplasmic reticulum. *Trends Biochem Sci* 29, 152-158.

Kim, W., Spear, E. D., and Ng, D. T. (2005). Yos9p detects and targets misfolded glycoproteins for ER-associated degradation. *Mol Cell* 19, 753-764.

Kitzmuller, C., Caprini, A., Moore, S. E., Frenoy, J. P., Schwaiger, E., Kellermann, O., Ivessa, N. E., and Ermonval, M. (2003). Processing of N-linked glycans during endoplasmic-reticulum-associated degradation of a short-lived variant of ribophorin I. *Biochem J* 376, 687-696.

Knop, M., Finger, A., Braun, T., Hellmuth, K., and Wolf, D. H. (1996a). Der1, a novel protein specifically required for endoplasmic reticulum degradation in yeast. *Embo J* 15, 753-763.

Knop, M., Hauser, N., and Wolf, D. H. (1996b). N-Glycosylation affects endoplasmic reticulum degradation of a mutated derivative of carboxypeptidase yscY in yeast. *Yeast* 12, 1229-1238.

Kopito, R. R. (1999). Biosynthesis and degradation of CFTR. *Physiol Rev* 79, S167-173.

Kostova, Z., and Wolf, D. H. (2005). Importance of carbohydrate positioning in the recognition of mutated CPY for ER-associated degradation. *J Cell Sci* 118, 1485-1492.

Krogan, N. J., Cagney, G., Yu, H., Zhong, G., Guo, X., Ignatchenko, A., Li, J., Pu, S., Datta, N., Tikuisis, A. P., *et al.* (2006). Global landscape of protein complexes in the yeast *Saccharomyces cerevisiae*. *Nature* 440, 637-643.

Kumar, A., Agarwal, S., Heyman, J. A., Matson, S., Heidtman, M., Piccirillo, S., Umansky, L., Drawid, A., Jansen, R., Liu, Y., *et al.* (2002). Subcellular localization of the yeast proteome. *Genes Dev* 16, 707-719.

Lederkremer, G. Z., and Glickman, M. H. (2005). A window of opportunity: timing protein degradation by trimming of sugars and ubiquitins. *Trends Biochem Sci* 30, 297-303.

Lee, C., Schwartz, M. P., Prakash, S., Iwakura, M., and Matouschek, A. (2001). ATP-dependent proteases degrade their substrates by processively unraveling them from the degradation signal. *Mol Cell* 7, 627-637.

Lilie, H., Schwarz, E., and Rudolph, R. (1998). Advances in refolding of proteins produced in *E. coli*. *Curr Opin Biotechnol* 9, 497-501.

Lilley, B. N., and Ploegh, H. L. (2004). A membrane protein required for dislocation of misfolded proteins from the ER. *Nature* 429, 834-840.

Lilley, B. N., and Ploegh, H. L. (2005). Multiprotein complexes that link dislocation, ubiquitination, and extraction of misfolded proteins from the endoplasmic reticulum membrane. *Proc Natl Acad Sci U S A* 102, 14296-14301.

Lipari, F., and Herscovics, A. (1996). Role of the cysteine residues in the alpha1,2-mannosidase involved in N-glycan biosynthesis in *Saccharomyces cerevisiae*. The conserved Cys340 and Cys385 residues form an essential disulfide bond. *J Biol Chem* 271, 27615-27622.

Litovchick, L., Friedmann, E., and Shaltiel, S. (2002). A selective interaction between OS-9 and the carboxyl-terminal tail of meprin beta. *J Biol Chem* 277, 34413-34423.

Liu, Y., Choudhury, P., Cabral, C. M., and Sifers, R. N. (1999). Oligosaccharide modification in the early secretory pathway directs the selection of a misfolded glycoprotein for degradation by the proteasome. *J Biol Chem* 274, 5861-5867.

Longtine, M. S., McKenzie, A., 3rd, Demarini, D. J., Shah, N. G., Wach, A., Brachat, A., Philippsen, P., and Pringle, J. R. (1998). Additional modules for versatile and economical PCR-based gene deletion and modification in *Saccharomyces cerevisiae*. *Yeast* 14, 953-961.

Matlack, K. E., Mothes, W., and Rapoport, T. A. (1998). Protein translocation: tunnel vision. *Cell* 92, 381-390.

Matouschek, A., Azem, A., Ratliff, K., Glick, B. S., Schmid, K., and Schatz, G. (1997). Active unfolding of precursor proteins during mitochondrial protein import. *Embo J* 16, 6727-6736.

McClellan, A. J., Tam, S., Kaganovich, D., and Frydman, J. (2005). Protein quality control: chaperones culling corrupt conformations. *Nat Cell Biol* 7, 736-741.

Meusser, B., Hirsch, C., Jarosch, E., and Sommer, T. (2005). ERAD: the long road to destruction. *Nat Cell Biol* 7, 766-772.

Molinari, M., Calanca, V., Galli, C., Lucca, P., and Paganetti, P. (2003). Role of EDEM in the release of misfolded glycoproteins from the calnexin cycle. *Science* 299, 1397-1400.

Mumberg, D., Muller, R., and Funk, M. (1994). Regulatable promoters of *Saccharomyces cerevisiae*: comparison of transcriptional activity and their use for heterologous expression. *Nucleic Acids Res* 22, 5767-5768.

Munro, S. (2001). The MRH domain suggests a shared ancestry for the mannose 6-phosphate receptors and other N-glycan-recognising proteins. *Curr Biol* 11, R499-501.

Nakatsukasa, K., and Brodsky, J. L. (2008). The recognition and retrotranslocation of misfolded proteins from the endoplasmic reticulum. *Traffic* 9, 861-870.

Nakatsukasa, K., Nishikawa, S., Hosokawa, N., Nagata, K., and Endo, T. (2001). Mnl1p, an α -mannosidase-like protein in yeast *Saccharomyces cerevisiae*, is required for endoplasmic reticulum-associated degradation of glycoproteins. *J Biol Chem* 276, 8635-8638.

Neuber, O., Jarosch, E., Volkwein, C., Walter, J., and Sommer, T. (2005). Ubx2 links the Cdc48 complex to ER-associated protein degradation. *Nat Cell Biol* 7, 993-998.

Ng, D. T., Brown, J. D., and Walter, P. (1996). Signal sequences specify the targeting route to the endoplasmic reticulum membrane. *J Cell Biol* 134, 269-278.

Nishikawa, S., Brodsky, J. L., and Nakatsukasa, K. (2005). Roles of molecular chaperones in endoplasmic reticulum (ER) quality control and ER-associated degradation (ERAD). *J Biochem (Tokyo)* 137, 551-555.

Nishikawa, S., Fewell, S. W., Kato, Y., Brodsky, J. L., and Endo, T. (2001a). Molecular chaperones in the yeast ER maintain the solubility of proteins for retro-translocation and degradation. *J Cell Biol* 153, 1061-1069.

Nishikawa, S. I., Fewell, S. W., Kato, Y., Brodsky, J. L., and Endo, T. (2001b). Molecular chaperones in the yeast endoplasmic reticulum maintain the solubility of proteins for retrotranslocation and degradation. *J Cell Biol* 153, 1061-1070.

Oda, Y., Hosokawa, N., Wada, I., and Nagata, K. (2003). EDEM as an acceptor of terminally misfolded glycoproteins released from calnexin. *Science* 299, 1394-1397.

Oda, Y., Okada, T., Yoshida, H., Kaufman, R. J., Nagata, K., and Mori, K. (2006). Derlin-2 and Derlin-3 are regulated by the mammalian unfolded protein response and are required for ER-associated degradation. *J Cell Biol* 172, 383-393.

Olivari, S., Cali, T., Salo, K. E., Paganetti, P., Ruddock, L. W., and Molinari, M. (2006). EDEM1 regulates ER-associated degradation by accelerating de-mannosylation of folding-defective polypeptides and by inhibiting their covalent aggregation. *Biochem Biophys Res Commun* 349, 1278-1284.

Olson, L. J., Zhang, J., Lee, Y. C., Dahms, N. M., and Kim, J. J. (1999). Structural basis for recognition of phosphorylated high mannose oligosaccharides by the cation-dependent mannose 6-phosphate receptor. *J Biol Chem* 274, 29889-29896.

Onuchic, J. N., and Wolynes, P. G. (2004). Theory of protein folding. *Curr Opin Struct Biol* 14, 70-75.

Pelham, H. R., Hardwick, K. G., and Lewis, M. J. (1988). Sorting of soluble ER proteins in yeast. *Embo J* 7, 1757-1762.

Plempner, R. K., Bordallo, J., Deak, P. M., Taxis, C., Hitt, R., and Wolf, D. H. (1999). Genetic interactions of Hrd3p and Der3p/Hrd1p with Sec61p suggest a retro-translocation complex mediating protein transport for ER degradation. *J Cell Sci* 112 (Pt 22), 4123-4134.

Quan, E. M., Kamiya, Y., Kamiya, D., Denic, V., Weibezahn, J., Kato, K., and Weissman, J. S. (2008). Defining the glycan destruction signal for endoplasmic reticulum-associated degradation. *Mol Cell* 32, 870-877.

Richly, H., Rape, M., Braun, S., Rumpf, S., Hoege, C., and Jentsch, S. (2005). A series of ubiquitin binding factors connects CDC48/p97 to substrate multiubiquitylation and proteasomal targeting. *Cell* 120, 73-84.

Riordan, J. R. (2008). CFTR function and prospects for therapy. *Annu Rev Biochem* 77, 701-726.

- Ritter, C., and Helenius, A. (2000). Recognition of local glycoprotein misfolding by the ER folding sensor UDP-glucose:glycoprotein glucosyltransferase. *Nat Struct Biol* 7, 278-280.
- Ritter, C., Quirin, K., Kowarik, M., and Helenius, A. (2005). Minor folding defects trigger local modification of glycoproteins by the ER folding sensor GT. *Embo J* 24, 1730-1738.
- Romisch, K. (2005). Endoplasmic reticulum-associated degradation. *Annu Rev Cell Dev Biol* 21, 435-456.
- Rudolph, R., and Lilie, H. (1996). In vitro folding of inclusion body proteins. *Faseb J* 10, 49-56.
- Sakumoto, N., Mukai, Y., Uchida, K., Kouchi, T., Kuwajima, J., Nakagawa, Y., Sugioka, S., Yamamoto, E., Furuyama, T., Mizubuchi, H., *et al.* (1999). A series of protein phosphatase gene disruptants in *Saccharomyces cerevisiae*. *Yeast* 15, 1669-1679.
- Sayeed, A., and Ng, D. T. (2005). Search and destroy: ER quality control and ER-associated protein degradation. *Crit Rev Biochem Mol Biol* 40, 75-91.
- Schubert, U., Anton, L. C., Gibbs, J., Norbury, C. C., Yewdell, J. W., and Bennink, J. R. (2000). Rapid degradation of a large fraction of newly synthesized proteins by proteasomes. *Nature* 404, 770-774.
- Schuberth, C., and Buchberger, A. (2005). Membrane-bound Ubx2 recruits Cdc48 to ubiquitin ligases and their substrates to ensure efficient ER-associated protein degradation. *Nat Cell Biol* 7, 999-1006.
- Schuldiner, M., Collins, S. R., Thompson, N. J., Denic, V., Bhamidipati, A., Punna, T., Ihmels, J., Andrews, B., Boone, C., Greenblatt, J. F., *et al.* (2005). Exploration of the function and organization of the yeast early secretory pathway through an epistatic miniarray profile. *Cell* 123, 507-519.
- Sekijima, Y., Wiseman, R. L., Matteson, J., Hammarstrom, P., Miller, S. R., Sawkar, A. R., Balch, W. E., and Kelly, J. W. (2005). The biological and chemical basis for tissue-selective amyloid disease. *Cell* 121, 73-85.
- Sikorski, R. S., and Hieter, P. (1989). A system of shuttle vectors and yeast host strains designed for efficient manipulation of DNA in *Saccharomyces cerevisiae*. *Genetics* 122, 19-27.
- Simons, J. F., Ferro-Novick, S., Rose, M. D., and Helenius, A. (1995). BiP/Kar2p serves as a molecular chaperone during carboxypeptidase Y folding in yeast. *J Cell Biol* 130, 41-49.
- Solda, T., Galli, C., Kaufman, R. J., and Molinari, M. (2007). Substrate-specific requirements for UGT1-dependent release from calnexin. *Mol Cell* 27, 238-249.
- Spear, E. D., and Ng, D. T. (2005). Single, context-specific glycans can target misfolded glycoproteins for ER-associated degradation. *J Cell Biol* 169, 73-82.
- Spiro, R. G. (2004). Role of N-linked polymannose oligosaccharides in targeting glycoproteins for endoplasmic reticulum-associated degradation. *Cell Mol Life Sci* 61, 1025-1041.
- Stevens, F. J., and Argon, Y. (1999). Protein folding in the ER. *Semin Cell Dev Biol* 10, 443-454.
- Su, K., Stoller, T., Rocco, J., Zemsky, J., and Green, R. (1993). Pre-Golgi degradation of yeast prepro-alpha-factor expressed in a mammalian cell. Influence of cell type-specific oligosaccharide processing on intracellular fate. *J Biol Chem* 268, 14301-14309.

Su, Y. A., Hutter, C. M., Trent, J. M., and Meltzer, P. S. (1996). Complete sequence analysis of a gene (OS-9) ubiquitously expressed in human tissues and amplified in sarcomas. *Mol Carcinog* 15, 270-275.

Swanson, R., Locher, M., and Hochstrasser, M. (2001). A conserved ubiquitin ligase of the nuclear envelope/endoplasmic reticulum that functions in both ER-associated and Matalpha2 repressor degradation. *Genes Dev* 15, 2660-2674.

Szathmary, R., Biemann, R., Nita-Lazar, M., Burda, P., and Jakob, C. A. (2005). Yos9 protein is essential for degradation of misfolded glycoproteins and may function as lectin in ERAD. *Mol Cell* 19, 765-775.

Takahashi, R., and Imai, Y. (2003). Pael receptor, endoplasmic reticulum stress, and Parkinson's disease. *J Neurol* 250 Suppl 3, III25-29.

Taxis, C., Hitt, R., Park, S. H., Deak, P. M., Kostova, Z., and Wolf, D. H. (2003). Use of modular substrates demonstrates mechanistic diversity and reveals differences in chaperone requirement of ERAD. *J Biol Chem* 278, 35903-35913.

Tirosh, B., Furman, M. H., Tortorella, D., and Ploegh, H. L. (2003). Protein unfolding is not a prerequisite for endoplasmic reticulum-to-cytosol dislocation. *J Biol Chem* 278, 6664-6672.

Travers, K. J., Patil, C. K., Wodicka, L., Lockhart, D. J., Weissman, J. S., and Walter, P. (2000). Functional and genomic analyses reveal an essential coordination between the unfolded protein response and ER-associated degradation. *Cell* 101, 249-258.

Trombetta, E. S., and Helenius, A. (2000). Conformational requirements for glycoprotein reglucosylation in the endoplasmic reticulum. *J Cell Biol* 148, 1123-1129.

Trombetta, S. E., Ganan, S. A., and Parodi, A. J. (1991). The UDP-Glc:glycoprotein glucosyltransferase is a soluble protein of the endoplasmic reticulum. *Glycobiology* 1, 155-161.

Tsai, B., Ye, Y., and Rapoport, T. A. (2002). Retro-translocation of proteins from the endoplasmic reticulum into the cytosol. *Nat Rev Mol Cell Biol* 3, 246-255.

Tu, B. P., Ho-Schleyer, S. C., Travers, K. J., and Weissman, J. S. (2000). Biochemical basis of oxidative protein folding in the endoplasmic reticulum. *Science* 290, 1571-1574.

Vabulas, R. M., and Hartl, F. U. (2005). Protein synthesis upon acute nutrient restriction relies on proteasome function. *Science* 310, 1960-1963.

van Anken, E., and Braakman, I. (2005). Versatility of the endoplasmic reticulum protein folding factory. *Crit Rev Biochem Mol Biol* 40, 191-228.

Vashist, S., Kim, W., Belden, W. J., Spear, E. D., Barlowe, C., and Ng, D. T. (2001). Distinct retrieval and retention mechanisms are required for the quality control of endoplasmic reticulum protein folding. *J Cell Biol* 155, 355-368.

Vashist, S., and Ng, D. T. (2004). Misfolded proteins are sorted by a sequential checkpoint mechanism of ER quality control. *J Cell Biol* 165, 41-52.

Vembar, S. S., and Brodsky, J. L. (2008). One step at a time: endoplasmic reticulum-associated degradation. *Nat Rev Mol Cell Biol* 9, 944-957.

Ward, C. L., Omura, S., and Kopito, R. R. (1995). Degradation of CFTR by the ubiquitin-proteasome pathway. *Cell* 83, 121-127.

Winzeler, E. A., Shoemaker, D. D., Astromoff, A., Liang, H., Anderson, K., Andre, B., Bangham, R., Benito, R., Boeke, J. D., Bussey, H., *et al.* (1999). Functional characterization of the *S. cerevisiae* genome by gene deletion and parallel analysis. *Science* 285, 901-906.

- Wu, Y., Swulius, M. T., Moremen, K. W., and Sifers, R. N. (2003). Elucidation of the molecular logic by which misfolded alpha 1-antitrypsin is preferentially selected for degradation. *Proc Natl Acad Sci U S A* *100*, 8229-8234.
- Xie, W., Kanehara, K., Sayeed, A., and Ng, D. T. (2009). Intrinsic conformational determinants signal protein misfolding to the Hrd1/Htm1 endoplasmic reticulum-associated degradation system. *Mol Biol Cell* *20*, 3317-3329.
- Ye, Y., Meyer, H. H., and Rapoport, T. A. (2001). The AAA ATPase Cdc48/p97 and its partners transport proteins from the ER into the cytosol. *Nature* *414*, 652-656.
- Ye, Y., Shibata, Y., Kikkert, M., van Voorden, S., Wiertz, E., and Rapoport, T. A. (2005). Inaugural Article: Recruitment of the p97 ATPase and ubiquitin ligases to the site of retrotranslocation at the endoplasmic reticulum membrane. *Proc Natl Acad Sci U S A* *102*, 14132-14138.
- Ye, Y., Shibata, Y., Yun, C., Ron, D., and Rapoport, T. A. (2004). A membrane protein complex mediates retro-translocation from the ER lumen into the cytosol. *Nature* *429*, 841-847.
- Yoshida, Y., Chiba, T., Tokunaga, F., Kawasaki, H., Iwai, K., Suzuki, T., Ito, Y., Matsuoka, K., Yoshida, M., Tanaka, K., and Tai, T. (2002). E3 ubiquitin ligase that recognizes sugar chains. *Nature* *418*, 438-442.

Publishing Agreement

It is the policy of the University to encourage the distribution of all theses, dissertations, and manuscripts. Copies of all UCSF theses, dissertations, and manuscripts will be routed to the library via the Graduate Division. The library will make all theses, dissertations, and manuscripts accessible to the public and will preserve these to the best of their abilities, in perpetuity.

Please sign the following statement:

I hereby grant permission to the Graduate Division of the University of California, San Francisco to release copies of my thesis, dissertation, or manuscript to the Campus Library to provide access and preservation, in whole or in part, in perpetuity.

Elin Quan Tayama
Author Signature

9/3/09
Date